Aus dem Max-Delbrück-Centrum für Molekulare Medizin Berlin
Zelluläre Neurowissenschaften

DISSERTATION

New insights into TRPV1 function in the brain under physiological and pathological conditions

zur Erlangung des akademischen Grades
Doctor of Philosophy (PhD)
im Rahmen des
International Graduate Program Medical Neurosciences

vorgelegt der Medizinischen Fakultät
Charité – Universitätsmedizin Berlin

von

Kristin Stock

aus Brandenburg an der Havel

Gutachter/in: 1. Prof. Dr. H. Kettenmann

2. Prof. Dr. D. Hambardzumyan

3. Prof. Dr. F. A. Moreira

Datum der Promotion: 30. November 2012

Für meine Familie

I. Contents

II. List of figures

III. List of tables

IV. Abbreviations

°C	Degree Celsius
µl	Microliter
µm	Micrometer
µM	Micromolar
2-AG	2-arachidonoylglycerol
AEA	N-arachidonoyl-ethanolamide, anandamide
AMPA	2-amino-3-(5-methyl-3-oxo-1,2-oxazol-4-yl)propanoic acid
APCI	Atmospheric pressure chemical ionization
ATP	Adenosine-5'-triphosphate
BMP	Bone morphogenetic protein
bp	Base pair
BrdU	Bromodeoxyuridine
BSA	Bovine serum albumin
CA	*Cornu ammonis* area
CB	Cannabinoid receptor
cDNA	Complementary DNA
CE	Coefficient of error
cm	Centimeter
CM	Conditioned medium
CNS	Central nervous system
CO_2	Carbon dioxide
CZP	Capsazepine
d	Day
DAGL	Diacylglycerol lipase
DAPI	4,6-diamidino-2-phenylindole
Dcx	Doublecortin
DG	Dentate gyrus
DMEM	Dulbecco's modified eagles medium
DMSO	Dimethyl sulfoxide

DNA	Deoxyribonucleic acid
dNTPs	Deoxynucleosid-triphosphate mix
DRG	Dorsal root ganglia
EDTA	Ethylenediaminetetraacetic acid
EGF	Epidermal growth factor
ER	Endoplasmic reticulum
FAAH	Fatty acid amide hydrolase
FCS	Fetal calf serum
FGF-2	Fibroblast growth factor-2
Fig.	Figure
fw	Forward
g	Gram
GABA	Gamma-aminobutyric acid
GAPDH	Glyceraldehyde-3-phosphate dehydrogenase
GBM	Glioblastoma multiforme
GBM1, 2, 3	Human primary glioblastoma cells
GDNF	Glial cell-derived neurotrophic factor
GFAP	Glial fibrillary acidic protein
GFP	Green fluorescent protein
GL261	Murine high-grade astrocytoma cell line
h	Hour(s)
HBSS	Hank's buffered salt solution
HEPES	4-(2-hydroxyethyl)-1-piperazineethanesulfonic acid
HRP	Horseradish peroxidase
i.p.	Intraperitoneal
ko	Knockout
l	Liter
LC	Liquid chromatography
LTD	Long-term depression
LTP	Long-term potentiation
M	Molar

MAGL	Monoacylglycerol lipase
MCAO	Middle cerebral artery occlusion
mg	Milligram
min	Minute(s)
ml	Milliliter
mM	Millimolar
MRI	Magnetic resonance imaging
mRNA	Messenger ribonucleic acid
MS	Mass spectrometry
MWM	Morris water maze
NaCl	Sodium chloride
NADA	N-arachidonoyl-dopamine
NAPE-PLD	NAPE-specific phospholipase D
NeuN	Neuronal nuclei
ng	Nanogram
NG	Nodose ganglia
NGF	Nerve growth factor
nm	Nanometer
nM	Nanomolar
NMDA	N-methyl-D-aspartate
NPC	Neural stem and precursor cells
NPC-A, -B, -C	Human primary neural precursor cells
o/n	Over night
OEA	Oleoyl-ethanolamide
p	Postnatal day
PBS	Phosphate buffered saline
PCR	Polymerase chain reaction
PEA	Palmitoyl-ethanolamide
PET	Positron emission tomography
PFA	Paraformaldehyde
PIP2	Phosphatidylinositol 4,5-bisphosphate

PKA	Protein kinase A
PKC	Protein kinase C
PLC	Receptor-activated phospholipase C
PLL	Poly-L-lysine
PO	Poly-L-ornithine
qRT-PCR	Quantitative reverse transcription polymerase chain reaction
rev	Reverse
RMS	Rostral migratory stream
rpm	Revolutions per minute
RT	Reverse transcriptase
s	Second(s)
SGZ	Subgranular zone
Shh	Sonic hedgehog
SIM	Selected ion monitoring
Sox2	SRY (sex determining region Y)-box 2 transcription factor
SRM	Selected reaction monitoring
SVZ	Subventricular zone
T3	3,3′,5-triiodo-L-thyronine
TAE	Tris-acetate-EDTA buffer
TBS	Tris-buffered saline
TG	Trigeminal ganglia
THC	Delta9-tetrahydrocannabinol
Tris	Tris-(hydroxymethyl)-aminomethane
TRP	Transient receptor potential channels
TRPV1	Transient receptor potential vanilloid type 1
U	Units
UV	Ultraviolet
V	Volt
VEGF	Vascular endothelial growth factor
WHO	World Health Organization
wt	Wildtype

1. Introduction

1.1. The endocannabinoid / endovanilloid system

Cannabinoids are the active components of *cannabis sativa* (hemp) and their derivatives, which were first isolated in the 1960's [Lerner, 1963]. Besides these plant-derived phytocannabinoids, synthetic variants exist as well [Hardman et al., 1971]. However, cannabinoids are also generated endogenously in the body. These endocannabinoids are a family of lipids which are the endogenous ligands in contrast to the plant-derived or synthetic cannabinoids. The endocannabinoid system consists of three receptors, their

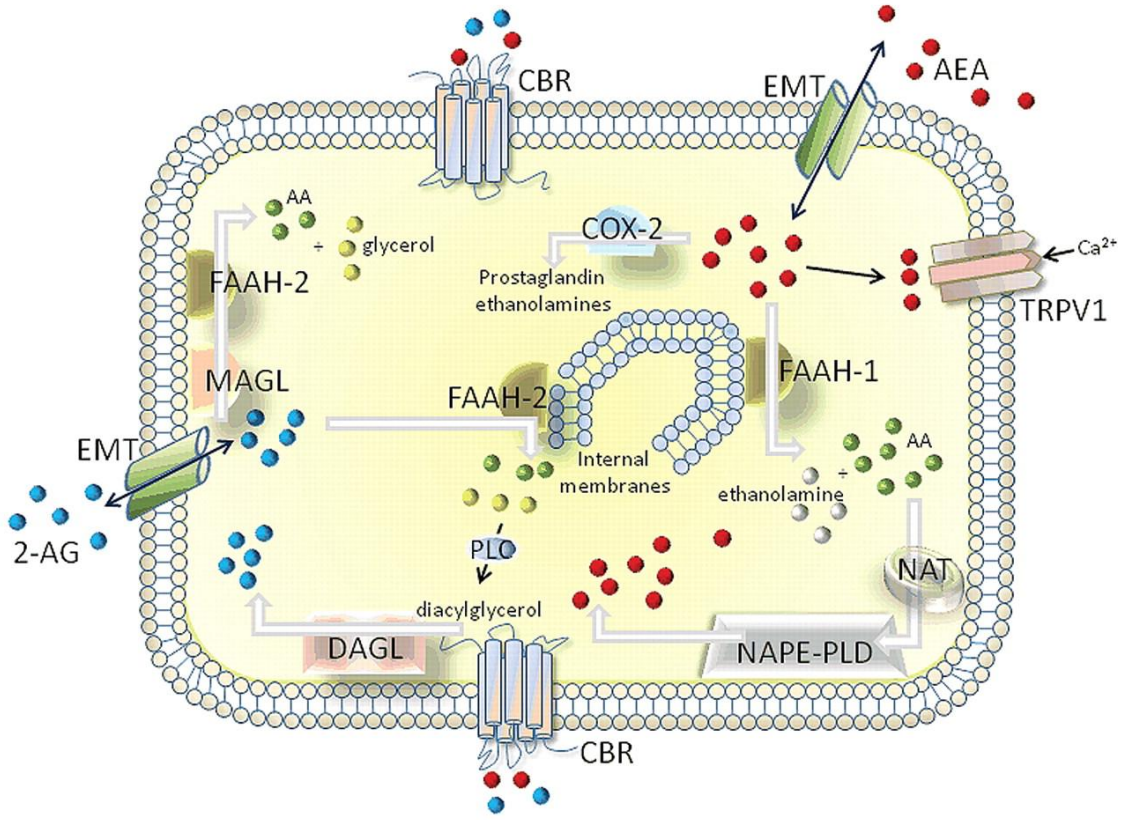

Fig. 1.1 The endocannabinoid / endovanilloid system

The endocannabinoid / endovannilloid system is composed of three receptors CB1, CB2 and TRPV1, the ligands AEA (N-arachidonoylethanolamine, anandamide, red) and 2-AG (2-Arachidonoylglycerol, blue) and the production and hydrolysis machinery. AEA is produced by the activity of a NAPE-specific phospholipase D (NAPE-PLD) and binds to all receptors. It is degraded by fatty acid amide hydrolase (FAAH). 2-AG is released from membrane lipids through the activity of diacylglycerol lipase (DAGL). It binds only to CB receptors and can be hydrolyzed by FAAH or monoacylglycerol lipase (MAGL). From [Karasu et al., 2011].

ligands and the production and hydrolysis machinery (Fig. 1.1). The receptors are the G-protein coupled cannabinoid receptors (CB1 and CB2) as well as the ionotropic vanilloid receptor TRPV1 (transient receptor potential vanilloid type 1). The endogenous ligands of these receptors are anandamide (N-arachidonoyl-ethanolamide, AEA) and 2-arachidonoylglycerol (2-AG), which are generated from arachidonic acid. Arachidonic acid is a non-essential fatty acid, which is a precursor for eicosanoids like the endocannabinoid / -vanilloid anandamide in neurons, glia and other cells [Freund et al., 2003]. Anandamide is synthesized by a NAPE-specific phospholipase D (NAPE-PLD) and 2-AG by the activity of diacylglycerol lipase (DAGL). The degradation occurs via fatty acid amide hydrolase (FAAH) and monoacylglycerol lipase (MAGL), respectively.

Endocannabinoids are known to modulate neurotransmitter release, thereby affecting many functions like cognitive processes and motor functions but also emotion and endocrine functions [Mackie, 2006]. Endocannabinoids are produced on demand which is locally and timely regulated, but also deactivated quickly by reuptake or degrading enzymes [Piomelli, 2003]. Furthermore, endocannabinoid levels as well as CB1 expression are regulated in development [Fernandez-Ruiz et al., 2000; Begbie et al., 2004]. Changes in the expression of components of the endocannabinoid system are also reported in pathological situations for example in human gliomas [Wu et al., 2012]. CB1 receptors are expressed in multiple areas of the brain, whereas CB2 expression is largely restricted to immune cells e.g. microglia in the brain [Piomelli, 2003]. Ligands on CB and TRPV1 receptors are shown in Fig. 1.2.

Endovanilloids on the other hand are defined as endogenous ligands of the vanilloid receptor TRPV1 (see 1.2.). Endocannabinoids like anandamide can also act on TRPV1 channels. In the beginning, the endovanilloid and endocannabinoid systems were thought to be independent systems, but recently the interaction has become evident. The endocannabinoid and endovanilloid systems share ligands and the receptors are often co-expressed, which might hint to a regulatory function. Functional cross-talk between CB1

and TRPV1 receptors of the same cell is shown for example in central dopaminergic neurons [Kim et al., 2005]. Moreover, Hong et al. have found reciprocal changes in TRPV1 and CB1 receptor expression in DRGs from stressed rats [Hong et al., 2009]. The interaction of both systems has been reported e.g. in neuropathic pain [Maione et al., 2006], osteoporosis [Rossi et al., 2011] and the control of anxiety-like behavior [Fogaça et al., 2012].

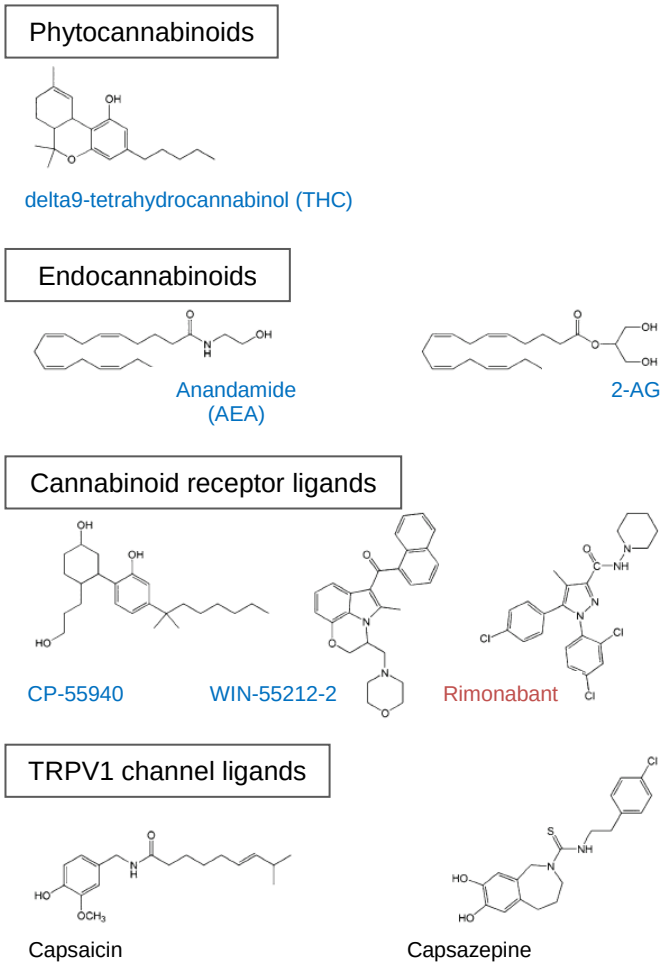

Fig. 1.2 Ligands of cannabinoid and vanilloid receptors

The structures of cannabinoid receptor and TRPV1 channel ligands is shown here. The phytocannabinoid delta9-tetrahydrocannabinol (THC), the endocannabinoids anandamide and 2-arachidonoylglycerol (2-AG) as well as the synthetic cannabinoids CP-55940 and WIN-55212-2 are agonists on CB receptors (blue). Rimonabant (SR141716A) on the other hand blocks CB receptors. In the lower panel, a TRPV1 agonist (capsaicin) and antagonist (capsazepine) are shown. Adapted from [Moreira and Wotjak, 2010].

1.2. Transient receptor potential vanilloid type 1 (TRPV1)

1.2.1. TRPV1 channel features

Transient receptor potential vanilloid type 1 (TRPV1) belongs to the superfamily of Transient receptor potential (TRP) channels (for review see [Montell, 2005]) and was originally isolated using a calcium imaging-based expression method [Caterina et al., 1997]. TRPV1 is activated by capsaicin (the pungent ingredient of hot peppers), vanilloid compounds, protons (low pH) and heat (> 43°C) [Caterina et al., 1997; Davis et al., 2000; Caterina and Julius, 2001; Tominaga and Tominaga, 2005; Siemens et al., 2006; Dhaka et al., 2009]. Furthermore, TRPV1 can be activated by a depolarization of the cell membrane [Voets et al., 2004; Matta and Ahern, 2007].

Suggested endogenous ligands are membrane-derived endovanilloids like anandamide, lipoxygenase derivatives of arachidonic acid and long-chain, linear fatty acid dopamines (e.g. N-arachidonoyl-dopamine (NADA) and N-oleoyl-dopamine) [Devane et al., 1992; Huang et al., 2002; Nagy et al., 2004; Tominaga and Caterina, 2004]. Anandamide, which regulates the activity of TRPV1 channels [Di Marzo et al., 2001], is also an endogenous CB receptor agonist [Devane et al., 1992]. Furthermore, it is known to modulate the cell death / survival decision of different neural cell types and regulates neural precursor proliferation and differentiation, acting as an instructive proliferative signal through CB1 [Galve-Roperh et al., 2006]. Synergistic TRPV1 activation by anandamide together with other fatty acid ethanolamides like oleoyl-ethanolamide (OEA) or palmitoyl-ethanolamide (PEA) is also observed [Szallasi et al., 2007; Toth et al., 2009].

TRPV1 is a nonselective cation channel with a limited selectivity for calcium. It consists of six transmembrane segments and is found mainly as a tetrameric homomer [Garcia-Sanz et al., 2004]. The receptor activity can be modulated by various intracellular signaling molecules, including protein kinase A (PKA), protein kinase C (PKC) and receptor-activated phospholipase C (PLC) (see review by [Ramsey et al., 2006]). TRPV1 is

sensitized by inflammatory mediators and proinflammatory cytokines (e.g. bradykinin, histamine, serotonin and prostaglandin E2) [Chuang et al., 2001; Moriyama et al., 2005]. Sustained agonist-sensitivity requires TRPV1 to be phosphorylated via an adenosine-5'-triphosphate (ATP)-dependent mechanism, accordingly the channel can be desensitized by agonists via dephosphorylation [Docherty et al., 1996; Szallasi and Blumberg, 1999].

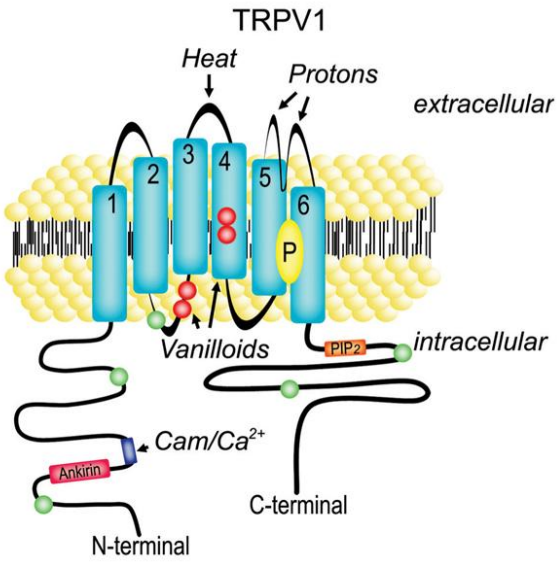

Fig. 1.3 Structure of TRPV1 channels

TRPV1 protein consists of six transmembrane segments. The pore region is formed by the fifth and sixth transmembrane domains (P, yellow). The N- and C-terminus are intracellular. The N-terminus contains three ankirin repeats (pink) and a calcium/calmodulin-interacting site (blue). An interacting site for phosphatidylinositol 4,5-bisphosphate (PIP2; orange) is found in the the C-terminus. The protein can be phosphorylated at several residues (green) by the protein kinases C and A (PKC and PKA). Ligand binding sites are shown by arrows. Heat and proton detection are mediated by specific residues located in extracellular protein loops. The vanilloid agonist sites (red) are located in intracellular loops and in the fourth transmembrane domain.
From [Leonelli et al., 2011].

1.2.2. TRPV1 expression and function

TRPV1 is highly expressed in small diameter primary afferent nociceptors of the dorsal root (DRG), trigeminal (TG) and nodose ganglia (NG), where it is important for the detection of noxious chemical and thermal stimuli [Szallasi et al., 1995; Caterina et al., 1997; Tominaga et al., 1998]. Activation of TRPV1 channels in sensory neurons leads to a release of pro-inflammatory cytokines, neuropeptides (Substance P and Calcitonin gene related peptide) and glutamate through calcium ion influx in the dorsal horn, which results in pain signal transduction from the periphery into the central nervous system (CNS) (for review see [Jara-Oseguera et al., 2008; Premkumar, 2010]).

In following studies the receptor was found in further neuronal and non-neuronal tissues (for review see [Caterina, 2003; Steenland et al., 2006]). TRPV1 expression at lower levels is found in epithelial cells [Birder et al., 2001; Denda et al., 2001; Inoue et al., 2002; Lazzeri et al., 2004; Lazzeri et al., 2005]; immune cells e.g. macrophages [Chen et al., 2003], neutrophil granulocytes [Heiner et al., 2003], mast cells [Stander et al., 2004]; smooth muscle cells [Birder et al., 2002] and fibroblasts [Birder et al., 2001].

Expression of TRPV1 in the CNS (brain and spinal cord) has been reported by several groups. In these studies diverse methods were used, e.g. RT-PCR [Sasamura et al., 1998; Mezey et al., 2000], Northern blot [Sanchez et al., 2001b], *in situ* hybridization [Mezey et al., 2000], radioligand binding [Acs et al., 1996; Roberts et al., 2004], immunohistochemistry [Mezey et al., 2000; Liapi and Wood, 2005; Toth et al., 2005; Cristino et al., 2006], pharmacological characterization [Steenland et al., 2006] and reporter systems [Cavanaugh et al., 2011]. Unfortunately, the expression patterns vary considerably between studies, due to differences in detection thresholds, methodologies, species investigated and developmental stages of the animals.

Additionally, knockout mice were investigated to reveal TRPV1 functions [Caterina et al., 2000]. These animals show normal responses to noxious mechanical stimuli but no vanilloid-evoked pain behavior. They are impaired in the detection of painful heat and

show little thermal hypersensitivity during inflammation [Caterina et al., 2000; Davis et al., 2000]. TRPV1 knockout mice exhibit changes in anxiety, conditioned fear and a decrease in hippocampal long-term potentiation (LTP) [Marsch et al., 2007]. Furthermore, an increased number of BrdU-labeled cells in the dentate gyrus is shown in adult mice [Jin et al., 2004]. In addition to its established role in the detection of noxious heat stimuli, TRPV1 has been proposed to have a more generalized function in the physiology of multiple brain areas, including the hippocampus and striatum [Gibson et al., 2008; Maccarrone et al., 2008].

Studies investigating TRPV1 in the brain found expression in regions which are known to be involved in the modulation or transmission of pain e.g. the periaqueductal gray [Mezey et al., 2000]. Furthermore, TRPV1 contributes to synaptic transmission by controlling glutamate release. When TRPV1 is activated glutamate release from nerve endings is increased in the peripheral [Caterina et al., 1997; Sikand and Premkumar, 2007] and central nervous system, e.g. in the basal ganglia, hypothalamus, periaqueductal gray and hippocampus [Marinelli et al., 2003; Li et al., 2004; Starowicz et al., 2007; Xing and Li, 2007; Gibson et al., 2008; Musella et al., 2009]. However, GABAergic synaptic transmission remains unaffected by TRPV1 stimulation [Yang et al., 1998; Marinelli et al., 2003; Li et al., 2004; Derbenev et al., 2006; Starowicz et al., 2007; Xing and Li, 2007; Musella et al., 2009]. In the hypothalamus, TRPV1 activation leads to glutamate release and an increase in the firing rate of neurons [Sasamura et al., 1998]. TRPV1 is involved in synaptic plasticity in the hippocampus, playing a role in learning and memory. This is shown by studies on hippocampal long-term potentiation (LTP) [Marsch et al., 2007] and depression (LTD) [Gibson et al., 2008]. Further investigations revealed a CB1- independent endocannabinoid modulation of synaptic plasticity via TRPV1. Synaptic transmission is reduced by promotion of the endocytosis of AMPA-type glutamate receptors [Chavez et al., 2010; Grueter et al., 2010]. A recent study shows, that TRPV1 is

also important in the human brain for the regulation of cortical excitability by modulation of synaptic transmission [Mori et al., 2012].

TRPV1 is not only expressed in neurons but also in astrocytes [Toth et al., 2005; Kim et al., 2006] and pericytes in the brain [Toth et al., 2005]. Further studies show TRPV1 expression in microglia in the spinal cord [Kim et al., 2006; Chen et al., 2009] and retina [Sappington and Calkins, 2008]. TRPV1 expression is not only associated with physiological conditions but also with severe pathophysiologies that show peripheral inflammatory pain e.g. inflammatory bowel diseases like Crohn disease and ulcerative colitis [Yiangou et al., 2001; White et al., 2010]. TRPV1 is also involved in migraine [Goadsby, 2007], autoimmune diabetes [Razavi et al., 2006] and obesity [Zhang et al., 2007].

TRPV1 expression is flexible and dependent on the presence or absence of growth factors. Especially nerve growth factor (NGF) and glial cell-derived neurotrophic factor (GDNF) differentially regulate TRPV1 expression in DRGs [Amaya et al., 2004]. Application of NGF increases TRPV1 expression on mRNA level, the trafficking to the plasma membrane and the sensitivity of the receptor to capsaicin in cultured DRG neurons [Winston et al., 2001; Galoyan et al., 2003; Zhang et al., 2005; Stein et al., 2006]. Additionally, NGF is involved in the upregulation of TRPV1 during inflammation [Ji et al., 2002; Amaya et al., 2004]. On the other hand, TRPV1 can be down-regulated by sciatic nerve axotomy, probably lacking trophic factors, which are important for TRPV1 expression [Michael and Priestley, 1999].

Due to its role in pain, there are multiple clinical studies applying TRPV1 agonists to desensitize or antagonists to block the receptor for pain relief [Szallasi et al., 2007; Wong and Gavva, 2009; Rowbotham et al., 2011]. The presence of TRPV1 in the brain is now well established but to avoid unnecessary side effects, the expression and role of TRPV1 needs to be further studied.

1.3. Neural stem cells and neurogenesis

1.3.1. Neural stem cells

Neural stem cells are somatic multipotent stem cells, which can self-renew and give rise to neural precursor cells. The latter can further differentiate into the neuronal or glial lineage (Fig. 1.4). Somatic stem cells differ from pluripotent embryonic stem cells mainly in two ways. They are tissue-specific and have only limited self-renewing capacities as well as a restricted differentiation potential. Neural stem cells continuously generate neurons, astrocytes and oligodendrocytes in the adult mammalian brain [Gage, 2000].

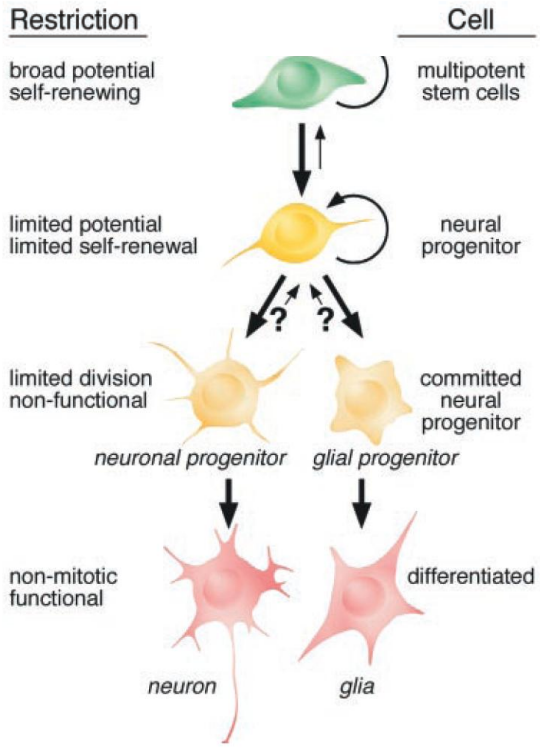

Fig. 1.4 Hierarchy of neural stem and precursor cells

Multipotent stem cells form the highest level of cells, which can self-renew and differentiate into neural precursor (or progenitor) cells. These precursors can further differentiate, thereby loosing their potential to self-renew and gaining differentiated cell properties. From [Gage, 2000].

1.3.2. Neural stem cell niches in the brain

Two stem cell niches have been identified in the CNS, the subventricular zone (SVZ) and the subgranular zone (SGZ) [Altman and Das, 1967; Reynolds and Weiss, 1992; Gage, 2000; Kempermann, 2006] (Fig. 1.5).

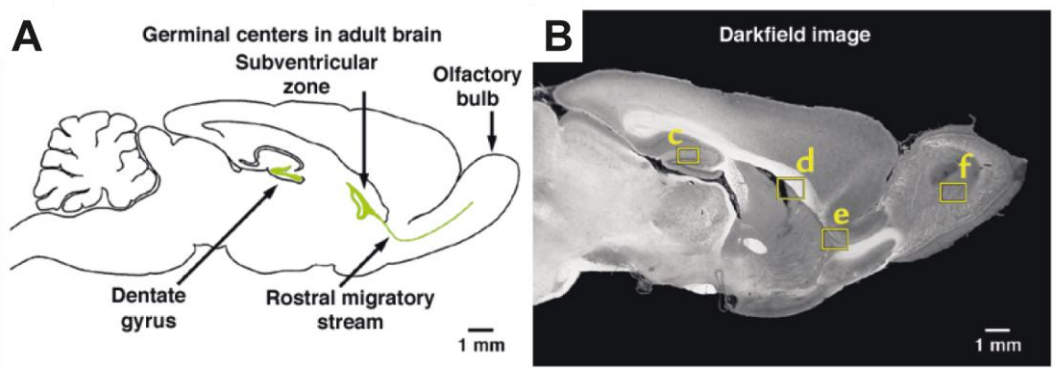

Fig. 1.5 Neural stem cell niches in the mouse brain

Neurogenesis in the adult brain is largely restricted to two neural stem cell niches: the subventricular zone lining the lateral ventricles and the hippocampal dentate gyrus. (A) shows a schematic drawing and (B) a sagital mouse brain section. From [Hallbergson et al., 2003].

1.3.2.1. The subventricular zone

The subventricular zone (SVZ) is a narrow band of cells lining the lateral ventricle. This neural stem and precursor cell (NPC) niche is organized in a specific way (Fig. 1.3). There are three different kinds of cells. The first type are B cells, which are the stem cells of the niche and give rise to type C cells. These are fast dividing, transit-amplifying cells which differentiate into neuroblasts (A cells) [Doetsch et al., 1997]. These three cell types form chains and create microenvironments (Fig. 1.6). Every cell type is characterized by a specific marker combination. Several factors are important for the regulation of the neurogenic niche, e.g. Noggin, Bone morphogenetic proteins (BMPs), Sonic hedgehog (Shh), Notch, TGFα, Eph/ephrins and Vascular endothelial growth factor (VEGF) [Alvarez-Buylla and Lim, 2004]. NPCs from the anterior part of the SVZ enter the rostral migratory

stream (RMS) and migrate to the olfactory bulb to generate new interneurons [Altman, 1969; Corotto et al., 1993; Luskin, 1993; Lois and Alvarez-Buylla, 1994]. This neurogenesis was shown by a series of studies in rodents and primates [Altman, 1969; Bayer, 1983; Kaplan, 1985; Kishi, 1987; Corotto et al., 1993; Lois and Alvarez-Buylla, 1994; Kornack and Rakic, 2001a, b].

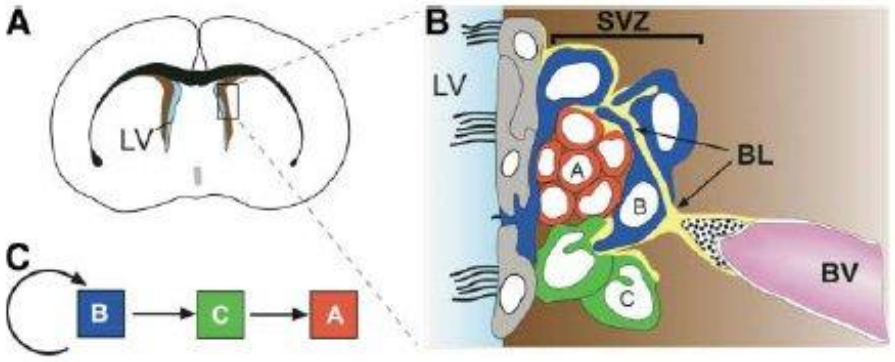

Fig. 1.6 Architecture of the subventricular zone

(A) shows a coronal section through a mouse brain. The subventricular zone is magnified in a schematic drawing in (B). The different cell types of the stem cell niche form a special architecture. The stem cells are in contact with ependymal cells (gray), blood vessels (BV) and the basal lamina (BL). (C) shows the hierarchy of the generated cells in the niche. From [Alvarez-Buylla and Lim, 2004].

1.3.2.2. The subgranular zone

The second stem cell niche is the subgranular zone of the dentate gyrus (SGZ) of the hippocampus. Previous studies have shown hippocampal neurogenesis in rodents [Altman and Das, 1965; Kaplan and Hinds, 1977; Kaplan and Bell, 1983, 1984; Cameron et al., 1993; Seki and Arai, 1993; Kuhn et al., 1996; Kempermann et al., 1997], non-human primates [Kornack and Rakic, 1999; Gould et al., 2001] and humans [Eriksson et al., 1998]. The SGZ is a narrow band of NPCs lining the inner part of the dentate gyrus. These NPCs are, similar to the structures in the SVZ, organized in a special way. The

stem cells of the niche are type 1 cells, which give rise to type 2a cells which then differentiate further into type 2b cells. These cells mature into neurons and glia and integrate into the granular layer of the dentate gyrus [Cameron et al., 1993] (Fig. 1.7). To confirm that these newly generated neurons are functional cells, receiving synaptic input [Kaplan and Bell, 1983; Markakis and Gage, 1999] and projecting connections *in vitro* [Song et al., 2002] and *in vivo* to the CA3 region [Stanfield and Trice, 1988; Markakis and Gage, 1999; van Praag et al., 2002], retrograde tracing studies were done. Like in the SVZ, the microenvironment of the SGZ is regulated by several factors e.g. Shh and VEGF [Alvarez-Buylla and Lim, 2004].

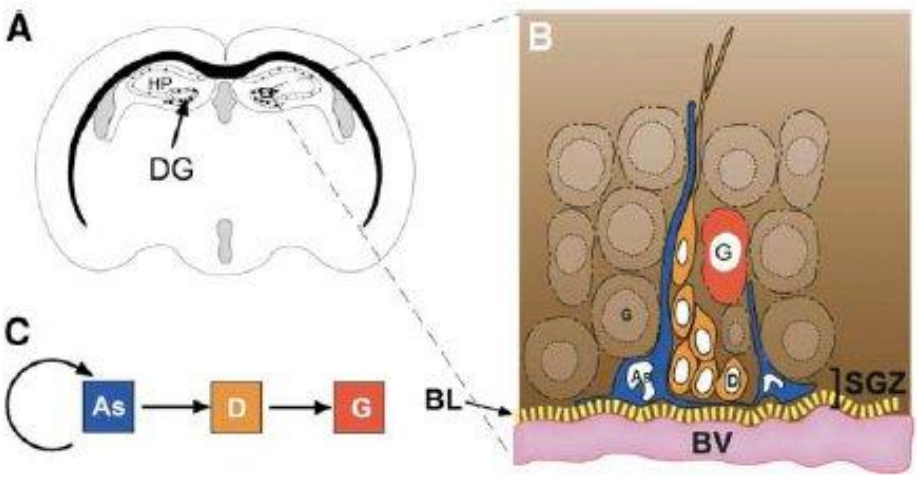

Fig. 1.7 Architecture of the subgranular zone

(A) shows a coronal section through a mouse brain. The subgranular zone of the dentate gyrus is magnified in a schematic drawing in (B). Similar to the SVZ, the different cell types of the stem cell niche form a special architecture as well. (C) shows the hierarchy of the generated cells in the niche. As – type 1 cells; D – type 2a/b cells; G – granule cells; BV - blood vessels. From [Alvarez-Buylla and Lim, 2004].

1.3.3. Neurogenesis

Neurogenesis is the generation of new neurons from neural stem and precursor cells. This process was first described in 1965 [Altman and Das, 1965], where tritiated thymidine

labeling studies were conducted to prove that cells are proliferating in the CNS [Altman and Das, 1967; Kaplan and Hinds, 1977]. Later, investigations using bromodeoxyuridine (BrdU) incorporation into the DNA of cells during the S-phase of the cell cycle confirmed the existence of adult neurogenesis in the brain [Corotto et al., 1993; Luskin, 1993; Seki and Arai, 1993].

Adult neurogenesis is important under physiological conditions e.g. for maintenance of cognitive functions [Gould and Gross, 2002; Song et al., 2002]. Neurogenesis has been linked to hippocampus-dependent functions [Bruel-Jungerman et al., 2007; Deng et al., 2010]. However, it remains unclear whether neurogenesis is a prerequisite for proper pattern separation in the dentate gyrus of the hippocampus and / or for memory resolution [Jessberger et al., 2008; Aimone et al., 2011; Sahay et al., 2011]. But also in pathological situations neurogenesis is of significance to limit the damage for instance in epilepsy [Parent, 2002], stroke [Darsalia et al., 2005] or brain tumors like high-grade astrocytomas [Glass et al., 2005].

1.3.3.1. Regulation of neurogenesis

Postnatal neurogenesis occurs in the first three weeks after birth, but both neural stem cell niches maintain neurogenesis into adulthood. Although, the activity of these neurogenic environments declines with increasing age in rodents [Corotto et al., 1993; Seki and Arai, 1995; Kuhn et al., 1996; Tropepe et al., 1997]. Nevertheless, NPCs can be isolated from SVZ and SGZ and cultured as neurospheres from older animals as well [Goldman et al., 1997; Tropepe et al., 1997].

Neurogenesis can be modulated by physiological and pathological stimuli in the brain (reviewed in [Abrous et al., 2005]). Physiologically, spatial learning and memory tasks, e.g. Morris water maze [Morris et al., 1982], can activate adult hippocampal neurogenesis

and lead to improved memory and increased synaptic plasticity [Kempermann, 2002; Garthe et al., 2009; Wolf et al., 2009]. But also physical exercising and enriched environment leads to an increase in neurogenesis [Kempermann et al., 1997; van Praag et al., 1999; Bick-Sander et al., 2006; Fabel et al., 2009; Wolf et al., 2011] and prevents age-related decline in precursor cell activity [Kronenberg et al., 2006]. Neurogenesis can be regulated by neurotransmitters. For instance, glutamate can increase neurogenesis through activation of AMPA receptors [Bai et al., 2003], but also decreases neurogenesis via NMDA receptors [Cameron et al., 1995]. Serotonin and nitric oxide exert positive modulations of neurogenesis [Brezun and Daszuta, 2000; Zhang et al., 2001]. Decreases in neurogenesis can be induced by environmental factors e.g. lack of maternal care [Mirescu et al., 2004] or social isolation [Lu et al., 2003b]. It has been also shown that chronic stress [Pham et al., 2003] and alcohol [Nixon and Crews, 2002] have a negative impact on hippocampal neurogenesis.

Pathological events can modulate neurogenesis as well. Neurological disorders e.g. traumatic brain injury [Dash et al., 2001; Lu et al., 2003a; Rice et al., 2003] or experimentally induced stroke by middle cerebral artery occlusion (MCAO) increase neurogenesis in SVZ and SGZ [Arvidsson et al., 2001; Arvidsson et al., 2002; Parent et al., 2002; Jin et al., 2003]. It is also shown that epilepsy [Parent et al., 1997] as well as antidepressants induce neurogenesis [Malberg et al., 2000; Sahay et al., 2011].

1.3.3.2. The influence of the endocannabinoid system on neurogenesis

Since the discovery of neurogenesis in the brain in 1965 by Altman and Das [Altman and Das, 1965], many endogenous and environmental influencing factors have been identified. In the recent years, the endovanilloid system came into focus as a novel intrinsic modulator system of neurogenesis.

There is a close interplay between the endovanilloid and the endocannabinoid system in the brain, since endocannabinoids like anandamide can also act on TRPV1 channels. The endocannabinoid system consists of the receptors CB1, CB2 and TRPV1, their ligands anandamide and 2-AG as well as the synthesizing and degrading enzymes of the ligands. The endogenous ligands are called endocannabinoids in contrast to the plant-derived or synthetic ones (see 1.1.). Endocannabinoids increase hippocampal NPC proliferation via CB1 receptors [Jin et al., 2004; Aguado et al., 2005]. They inhibit neuronal differentiation [Rueda et al., 2002] and favor gliogenesis instead [Aguado et al., 2006]. Nevertheless, cell viability is not affected [Rueda et al., 2002]. Neurosphere generation and self-renewal is modulated by CB1 receptors [Aguado et al., 2005]. CB1 also mediates baseline and activity-induced survival of new neurons in adult hippocampal neurogenesis [Wolf et al., 2010]. Furthermore, endocannabinoids inhibit neuritogenesis [Zhou and Song, 2001; Ishii and Chun, 2002] and lead to a decrease in synapse formation via CB1 *in vitro* [Kim and Thayer, 2001]. It is shown that the lack of CB1 results in the development of cognitive impairments in CB1 knockout mice [Bilkei-Gorzo et al., 2005]. CB1 expression is also found in human neural stem cells in the hNSC1 line *in vitro* [Rueda et al., 2002; Palazuelos et al., 2006] and in the subependymal layer in the adult human brain *in vivo* [Curtis et al., 2006].

Thus, the endocannabinoid system is a multimodal modulator of neurogenesis. However, so far only CB1 but not TRPV1 contribution to proliferation, neurosphere generation and differentiation is investigated in great detail, while TRPV1 contribution to the process is largely unknown.

1.4. Gliomas

Gliomas are the largest group of brain tumors (about 40%; [Kleihues et al., 1993]). They have an incidence of 5 in 100 000 annually [Friese et al., 2004].

1.4.1. Classification of gliomas

Gliomas can be classified according to different criteria. The first one is the anatomical location of the brain tumor, either in the cerebrum (supratentorial), in the cerebellum (infratentorial) or in the pons of the brainstem (pontine). The second classification is based on the cell type they histologically resemble (Tab. 1.1). Though, this does not specify the origin of the tumor.

Tab. 1.1 Classification of gliomas by cell type

Glioma	Share histological features with
Astrocytomas	Astrocytes
Ependymomas	Ependymal cells
Oligodendrogliomas	Oligodendrocytes
Mixed gliomas	Different types of glia

However, the most common system is the classification via World Health Organization (WHO) grades, which uses the cell type criteria as well [Louis et al., 2007]. The lower the grade, the less aggressive are the tumors and the better is the prognosis for the patient. WHO grades range from grade I tumors, which are non-invasive, benign tumors up to aggressive, highly proliferative and undifferentiated grade IV tumors (Tab. 1.2).

Tab. 1.2 Astrocytomas graded according to the World Health Organization (WHO)
(from [Louis et al., 2007])

Astrocytoma	I	II	III	IV
Subependymal giant cell astrocytoma	•			
Pilocytic astrocytoma	•			
Pilomyxoid astrocytoma		•		
Diffuse astrocytoma		•		
Pleomorphic xanthoastrocytoma		•		

Astrocytoma	I	II	III	IV
Anaplastic astrocytoma			•	
Glioblastoma multiforme				•
Giant cell glioblastoma				•
Gliosarcoma				•

1.4.2. Glioblastoma multiforme

Glioblastoma multiforme (GBM) is by far the most common (about 50 % of all gliomas) and most malignant primary brain tumor (for an example see Fig. 1.8). The occurrence of GBMs is age-related peaking between 50 and 55 years [Ohgaki and Kleihues, 2005, 2007; Ohgaki, 2009]. The prognosis is very poor, with a median survival of 14.6 months [Stupp et al., 2005], due to its high proliferation and invasiveness. Most GBMs emerge *de novo* as primary brain tumor and show a fast progression. Secondary GBMs, which arise from lower grade gliomas, are rare (~ 5 %) [Ohgaki and Kleihues,

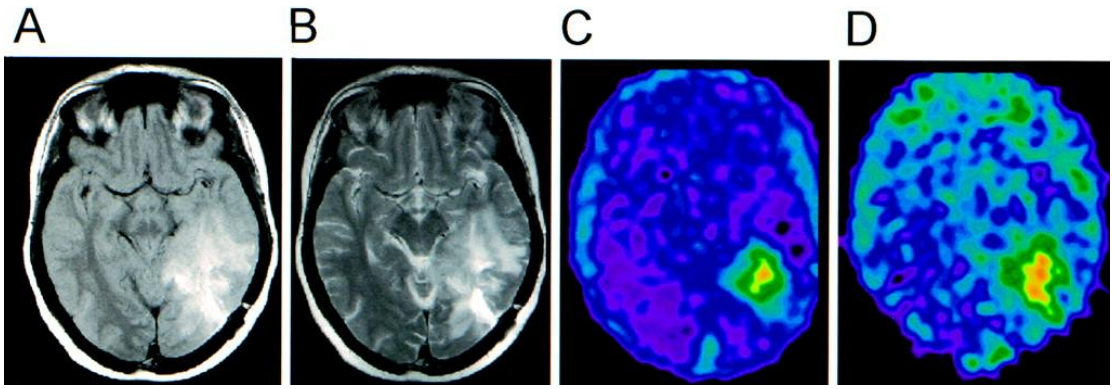

Fig. 1.8 Nuclear medicine diagnostics of glioblastoma multiforme in the left temporal lobe using magnetic resonance imaging and positron emission tomography

(A, B) Magnetic resonance imaging (MRI) is the most important diagnostic tool for assessing brain neoplasms. Two different types of MRI are shown (A: spin density MRI; B: T2-weighted MRI). (C, D) Positron emission tomography (PET), using radiolabeled amino acids, yields significant additional information that allows for a more accurate diagnostics of cerebral gliomas. A time series of PET scans after the injection of the tracer (radioactive ^{76}Br-bromide) is shown in (C: 60 to 90 min; D; 24 to 24.5 h). From [Bruehlmeier et al., 2003].

2007]. Due to the diversity of molecular mechanisms leading to GBMs and the tumor's high resistance to current therapies, up to now there is no cure. The treatments are mostly targeted at reducing the symptoms using resection, chemotherapy (e.g. using the alkylating cytostatic drug temozolomide) and radiation [DeAngelis, 2001; Stupp et al., 2005; Stupp et al., 2009; Strik et al., 2012].

Novel approaches lead to individualized therapies for patients depending on the molecular mechanism underlying their GBM formation. There is intense research going on to find predictive factors and biomarkers to better understand GBMs multiplicity and increase the patients' therapeutic options (for review see [Bleeker et al., 2012]).

1.4.3. Neurogenesis-glioma-relationship

As mentioned above, neurogenesis is the process by which neurons are generated from neural stem and precursor cells via certain maturation steps. Neural precursor cells (NPCs) with somatic mutations are likely the source for primary brain tumors such as high-grade gliomas (glioblastomas) [Sanai et al., 2005]. In extension to this concept, physiological NPCs also mediate paracrine tumor suppressive effects against glioblastomas [Aboody et al., 2000; Staflin et al., 2004; Glass et al., 2005; Suzuki et al., 2005; Walzlein et al., 2008; Staflin et al., 2009]. In 2010, it is shown that BMP7, which is released from NPCs, targets tumor stem cells and leads to cell death [Chirasani et al., 2010]. However, factors which act against the bulk tumor are not known yet. Interestingly, neurogenesis declines with age (see 1.3.3.) and is inversely correlated with the epidemiology of glioblastomas.

1.4.4. Cannabinoids and glioma

Cannabinoids, the active components of marijuana and their derivatives (plant-derived or synthetic), are already in clinical use as palliatives to alleviate tumor cachexy and side

effects of chemotherapy as for example nausea [Sallan et al., 1975; Tramer et al., 2001]. Direct effects on tumor cells are shown *in vitro* for a variety of cancers e.g. glioma [Sanchez et al., 1998], lung cancer [Munson et al., 1975] or skin cancer [Casanova et al., 2003]. Experiments in cultured glioma cells revealed that cannabinoid treatment leads to cell death via apoptosis [Sanchez et al., 1998]. *In vivo*, the application of cannabinoid receptor agonists lead to an increased survival of glioma bearing rats [Galve-Roperh et al., 2000; Piomelli, 2000; Sanchez et al., 2001a].

The mechanisms of anti-tumorigenic effects of cannabinoids are diverse. It is shown that they induce cell death via apoptosis [Guzman, 2003] or autophagy [Salazar et al., 2009], that they inhibit the migration of glioma cells [Vaccani et al., 2005] and they inhibit tumor angiogenesis and metastasis [Blazquez et al., 2003]. However, the cannabinoid-mediated effects seem to be restricted to transformed tumor cells since the endocannabinoid system also exerts a neuroprotective function in different neural cell types [Torres et al., 2011]. Nevertheless, resistance of glioma cells to cannabinoid-induced apoptosis is also reported, most probably due to the heterogeneity of expression profiles of cannabinoid receptors [Galve-Roperh et al., 2000; De Jesus et al., 2010]. Cannabinoids are tested in preclinical studies as possible combination therapy in addition to conventional glioma treatment [Radin, 2003; Torres et al., 2011]. They are also tested in clinical trials in patients with recurrent glioblastoma multiforme [Guzman et al., 2006] and might open a new therapeutic avenue towards a cure of gliomas.

However, cannabinoids for example anandamide can also act via TRPV1 channels. There are few reports showing that anandamide can induce glioma cell death via TRPV1-dependent apoptosis [Biro et al., 1998; Contassot et al., 2004; Amantini et al., 2007].

The term ‘glioma’ in the following refers to high-grade astrocytomas.

1.5. Aim of the thesis

The endocannabinoid system was shown to play an important role in regulating adult neurogenesis and glioma growth [Sanchez et al., 1998; Aguado et al., 2005]. In addition to cannabinoid receptors, soluble factors of the cannabinoid system can also stimulate vanilloid receptors. The contribution of vanilloid-dependent signaling pathways in adult neurogenesis and glioma pathology are so far largely unexplored.

The aim of this study is to investigate properties of TRPV1 channels under physiological conditions and in the glioma context in two independent projects.

Specific questions are:

Neurogenesis / Neural precursor cell physiology

1. Do NPCs express TRPV1 channels *in vitro* and *in vivo*?
2. Are TRPV1 channels on NPCs functional?
3. Which role do TRPV1 channels play in NPC homeostasis?
4. Does TRPV1 have an impact on learning-associated neurogenesis?

Neural precursor cells and glioma pathology

5. Which anti-tumorigenic factors are released from NPCs?
6. Which receptor is responsible for the anti-tumorigenic action of NPCs on glioma cells?
7. Which NPC-dependent signaling pathway leads to the anti-tumorigenic action in glioma cells?
8. Do synthetic vanilloids offer therapeutic potential for the treatment of gliomas?

2. Materials

Materials were purchased from the German branches of the given companies unless stated otherwise.

2.1. Technical equipment

Tab. 2.1 Technical products

Appliance	Product	Supplier
Balances	BL610	Sartorius (Göttingen)
	LA310S	Sartorius (Göttingen)
Block heater	Thermomixer compact	Eppendorf (Hamburg)
Centrifuges	Centrifuge 5403	Eppendorf (Hamburg)
	Centrifuge 5417R	Eppendorf (Hamburg)
	Centrifuge 5810R	Eppendorf (Hamburg)
Counting chamber	Neubauer	LaborOptik (Bad Homburg)
Cryostat	HM 560	Microm Laborgeräte GmbH (Walldorf)
Flow cytometry	FACSCalibur	BD Biosciences (Heidelberg)
Fluorescence lamp	HAL100	Carl Zeiss (Jena)
Gel documentation	G-Box	Syngene (Cambridge, United Kingdom)
Gel electrophoresis chamber	Agagel	Biometra (Göttingen)
Gel electrophoresis device	Standard power pack P25	Biometra (Göttingen)
Incubator	Heracell	Heraeus Instruments (Hanau)
Microliter syringe	7001N (blunt tip)	Hamilton (Bonaduz, Switzerland)
Microplate reader	Infinite M200	Tecan (Männedorf, Switzerland)
Microscopes	Axiovert 25 (fluorescence, inverse)	Carl Zeiss (Jena)
	Axiovert 40 CFL (fluorescence)	Carl Zeiss (Jena)
	Axiovert 200 (fluorescence, inverse)	Carl Zeiss (Jena)
	TCS SPE (confocal)	Leica microsystems (Wetzlar)
Microscope camera	Axiocam MRM	Carl Zeiss (Jena)
	SPOT-RT-SE18 CCD	Visitron Systems (Puchheim)
Microtome	AM2000R	Leica microsystems (Wetzlar)
Perfusion system (gravity-driven multi barrel)	WAS02	DITEL (Prague, Czech Republic)
pH meter	CG840	Schott (Mainz)
Photometer	SmartSpecTM3000	Bio-Rad (München)

Appliance	Product	Supplier
Pipette boy	Accu-Jet	Brand (Wertheim)
Pipettes	Research	Eppendorf (Hamburg)
Rota-Rod	47600 (mouse)	Ugo Basile (Comerio, Italy)
Shaker	Bühler Schüttler	Johanna Otto GmbH (Hechingen)
Spectrophotometer	Nanodrop ND-1000	Thermo Scientific (Schwerte)
Stereotactic head holder	Model 900	David Kopf Instruments, (Tajunga, USA)
Sterile hood	Herasafe (vertical)	Heraeus Instruments (Hanau)
Thermocycler (qPCR, SYBR green system)	Mastercycler ep realplex	Eppendorf (Hamburg)
Thermocycler (qPCR, Taqman system)	7700 Real-Time PCR System	Applied Biosystems (Foster City, USA)
Thermocycler (semi-quantitative PCR)	T3000	Biometra (Göttingen)
Vibratome	VT1000S	Leica microsystems (Wetzlar)
Vortex	Genie 2 vortexer	VWR (Darmstadt)
Water bath	1008	GFL (Burgwedel)

2.2. Chemicals and reagents

Tab. 2.2 Chemical products and reagents

Product	Supplier
Accutase	Life Technologies (Darmstadt)
Agar	Sigma-Aldrich (Taufkirchen)
Agarose	Peqlab (Erlangen)
Aqua-Poly/Mount	Polysciences Europe (Eppelheim)
ATP (Adenosine-5'-triphosphate)	Sigma-Aldrich (Taufkirchen)
B-27 supplement	Life Technologies (Darmstadt)
Beta-Mercaptoethanol	Life Technologies (Darmstadt)
BrdU (5-bromo-2-deoxyuridine)	Sigma-Aldrich (Taufkirchen)
Bromphenol blue	Sigma-Aldrich (Taufkirchen)
BSA (Bovine serum albumin)	Roth (Karlsruhe)
$CaCl_2$ (Calcium chloride)	Roth (Karlsruhe)
Capsaicin	Tocris Bioscience (Bristol, United Kingdom)
Cyanoacrylate glue	UHU (Bühl)
D(+)-Glucose	Roth (Karlsruhe)
DAPI (4',6-Diamidino-2-Phenylindol-2HCl)	Sigma-Aldrich (Taufkirchen)
Dispase II	Roche (Mannheim)
DMEM (Dulbecco's Modified Eagle Medium)	Life Technologies (Darmstadt)
DMEM medium, high glucose	Life Technologies (Darmstadt)

Product	Supplier
DMSO (Dimethyl sulfoxide)	Sigma-Aldrich (Taufkirchen)
DNA ladder 100 bp	Fermentas (St. Leon-Rot)
DNAse (desoxyribonuclease)	Worthington Biochemical (Lakewood, USA)
dNTPs (desoxyribonucleosidtriphosphates)	Takara Bio Europe S.A.S. (St Germain en Laye, France)
Donkey serum	Sigma-Aldrich (Taufkirchen)
EDTA (Ethylenediaminetetraacetic acid)	Sigma-Aldrich (Taufkirchen)
EGF (endothelial growth factor)	Cell systems (Troisdorf)
Endoplasmic reticulum tracker	Life Technologies (Darmstadt)
Ethanol	Merck (Darmstadt)
Ethidium bromide	Roth (Karlsruhe)
FCS (Fetal calf serum)	Life Technologies (Darmstadt)
FGF-2 (fibroblast growth factor-2)	Cell systems (Troisdorf)
FuGene transfection reagent	Roche (Mannheim)
Fura-2 acetoxymethyl ester	Life Technologies (Darmstadt)
Glycerol	Sigma-Aldrich (Taufkirchen)
HBSS (Hanks' Balanced Salt Solution)	Life Technologies (Darmstadt)
HEPES (4-(2-hydroxyethyl)-1-piperazine-ethanesulfonic acid)	Roth (Karlsruhe)
Horse serum	Biochrom (Berlin)
Insulin	Sigma-Aldrich (Taufkirchen)
Isopropanol	Sigma-Aldrich (Taufkirchen)
KCl (potassium chloride)	Roth (Karlsruhe)
Ketanest S	Bela-Pharm (Vechta)
Laminin	Life Technologies (Darmstadt)
L-Glutamine	Life Technologies (Darmstadt)
Liposomes (Clodronate- or PBS-filled)	Department of Molecular Cell Biology, Free University of Amsterdam (Netherlands)
$MgCl_2$ (Magnesium chloride)	Life Technologies (Darmstadt)
NaCl (Sodium chloride)	Roth (Karlsruhe)
Narcoren (Pentobarbital)	Merial (Hallbergmoos)
Neurobasal-A medium	Life Technologies (Darmstadt)
Oligo (dT)-Primer	Roche (Mannheim)
Papain	Cell systems (Troisdorf)
PBS (phosphate buffered saline)	Life Technologies (Darmstadt)
PCR Buffer (10x, Mg^{2+} plus)	Takara Bio Europe S.A.S. (St Germain en Laye, France)
Penicillin/streptomycin	Biochrom (Berlin)
PFA (paraformaldehyde)	Sigma-Aldrich (Taufkirchen)
Pluronic acid	Sigma-Aldrich (Taufkirchen)

Product	Supplier
Poly-L-ornithine	Sigma-Aldrich (Taufkirchen)
Potassium iodide	Sigma-Aldrich (Taufkirchen)
Puromycin	Sigma-Aldrich (Taufkirchen)
Reverse transcriptase	Roche (Mannheim)
RNAse inhibitor	Roche (Mannheim)
Rompun	Bayer Health Care (Leverkusen)
RPMI medium	Life Technologies (Darmstadt)
Sodium pyruvate	Life Technologies (Darmstadt)
Sucrose	Merck (Darmstadt)
Sutures	Johnson & Johnson (Langhorne, USA)
Thapsigargin	Tocris Bioscience (Bristol, United Kingdom)
Tris	Sigma-Aldrich (Taufkirchen)
TritonX-100	Sigma-Aldrich (Taufkirchen)
Trypan blue	Life Technologies (Darmstadt)
Trypsin-EDTA (10x)	Life Technologies (Darmstadt)

Tab. 2.3 Enzymes

Product	Supplier
GoTaq Polymerase (for quantitative PCR)	Life Technologies (Darmstadt)
Taq Polymerase (for semi-quantitative PCR)	Takara Bio Europe S.A.S. (St Germain en Laye, France)

Tab. 2.4 Kits used for molecular biology, cell culture and protein biochemistry

Product	Supplier
Amaxa Cell Line Nucleofector Kit V	Lonza (Basel, Switzerland)
BCA Protein Assay	Thermo Fisher Scientific (Rockford, USA)
CytoTox-Fluor Cytotoxicity Assay	Promega (Mannheim)
iScript cDNA Synthesis Kit	Bio-Rad (München)
RNeasy Mini RNA Isolation Kit	Qiagen (Hilden)
Taqman gene expression assay TRPV1 (Mm01246301_m1)	Applied Biosystems (Foster City, USA)
Tyramide signal amplification (TSA Biotin System)	PerkinElmer (Waltham, USA)

2.3. Cell culture

2.3.1. Primary cells and cell lines

Tab. 2.5 Primary cells and cell lines

Category	Origin	Cells	Label
Primary	mouse	neural precursor cells	mNPC
	human	neural precursor cells	NPC-A (BLV1)
		neural precursor cells	NPC-B (BLV4)
		neural precursor cells	NPC-C (NPC5)
		glioblastoma cells	GBM1 (TU7/2000)
		glioblastoma cells	GBM2 (B4)
		glioblastoma cells	GBM3 (TU3/2006)
Cell lines	mouse	high-grade astrocytoma cells	GL261
	mouse	high-grade astrocytoma cells	GL261-GFP
	human	virus producing cells	HEK 293T

2.3.2. Cell culture equipment

Glass materials were obtained from Schott (Mainz).

Tab. 2.6 Cell culture plastic ware

Consumables	Manufacturer
µ-slide 8 wells	ibidi GmbH (Martinsried)
Cell culture inserts (for 6-well plate)	Becton Dickinson (Heidelberg)
Cell Strainer 40 µm Nylon	BD Falcon (Bedford, USA)
Cryovials (1, 1.8 ml)	Nunc (Wiesbaden)
Multiwell culture dishes (4-, 6,- 12-, 24- or 96-well)	Nunc (Wiesbaden)
Parafilm M	Pechiney Plastic Packaging (Chicago, USA)
PCR strip tubes 0.2 ml	Peqlab (Erlangen)
Petri dishes (3.5, 6, 10 cm)	BD Biosciences (Heidelberg)
Round bottom tubes - 12x75 mm	BD Biosciences (Heidelberg)
Serological pipettes (1, 2, 5, 10, 25 ml)	BD Biosciences (Heidelberg)
Syringe filter (0.2, 0.45 µm)	Sarstedt (Nuembrecht)
Syringes (1, 10, 20 ml)	BD Biosciences (Heidelberg)
Tissue culture dishes (3.5, 6, 10 cm)	BD Biosciences (Heidelberg)
Tissue culture flasks (25 cm^2, 75 cm^2)	TPP (Switzerland)
Tubes (0.5, 1.5, 2 ml)	Greiner Bio-One (Solingen)
Tubes (15, 50 ml)	Greiner Bio-One (Solingen)

2.3.3. Cell culture media

Before use, all cell culture reagents were sterile filtered through a Millipore filtration unit (Millipore, Billerica, USA) except for growth factors.

All basal media were obtained from Life Technologies (Darmstadt).

2.3.3.1. Cultivation of mouse cells

Tab. 2.7 Media for cultivation of mouse cells

Medium	Composition
Cultivation medium for mouse NPCs (proliferation medium)	2 % B-27 100 U/ml penicillin 100 µg/ml streptomycin 2 mM L-glutamine 3 mg/ml D(+)-glucose 20 ng/ml FGF-2 20 ng/ml EGF in Neurobasal-A
Differentiation medium for mouse NPCs	2 % B-27 100 U/ml penicillin 100 µg/ml streptomycin 2 mM L-glutamine 3 mg/ml D(+)-glucose 0.1 % FCS in Neurobasal-A
Freezing medium for mNPCs	5 % DMSO in NPC cultivation medium
Cultivation medium for mouse high-grade glioma cells (GL261)	10 % FCS 100 U/ml penicillin 100 µg/ml streptomycin 2 mM L-glutamine in DMEM-high glucose
Freezing medium for mouse high-grade glioma cells (GL261)	10 % DMSO 15 % FCS in DMEM-high glucose
Cultivation medium for mouse dorsal root ganglia neurons (DRGs)	10 % horse serum 100 U/ml penicillin 100 µg/ml streptomycin 2 mM L-glutamine 0.8 % D(+)-glucose in DMEM
Preparation medium for organotypic brain slices	10 % FCS 100 U/ml penicillin 100 µg/ml streptomycin 2 mM L-glutamine in DMEM-high glucose

Medium	Composition
Cultivation medium for organotypic brain slices	25 % FCS 50 mM sodium bicarbonate 2 % L-glutamine 25 % HBSS 1 µg/ml insulin 2.46 mg/ml D(+)-glucose 0.8 µg/ml ascorbic acid 100 U/ml penicillin, 100 µg/ml streptomycin 5 mM Tris in DMEM

2.3.3.2. Cultivation of human cells

Tab. 2.8 Media for cultivation of human cells

Medium	Composition
Cultivation medium for human NPCs	2 % B-27 100 U/ml penicillin 100 µg/ml streptomycin 2 mM L-glutamine 3 mg/ml D(+)-glucose 20 ng/ml FGF-2 20 ng/ml EGF in Neurobasal-A
Freezing medium for human NPCs	5 % DMSO in NPC cultivation medium
Cultivation medium for human high-grade glioma cells (GBM1 and 3)	10 % FCS 100 U/ml penicillin 100 µg/ml streptomycin 2 mM L-glutamine 20 ng/ml FGF-2 20 ng/ml EGF in RPMI
Cultivation medium for human high-grade glioma cells (GBM2)	2 % B-27 100 U/ml penicillin 100 µg/ml streptomycin 2 mM L-glutamine 3 mg/ml D(+)-glucose 20 ng/ml FGF-2 20 ng/ml EGF in Neurobasal-A
Freezing medium for human high-grade glioma cells (GBM1 and 3)	5 % DMSO in GBM1/3 cultivation medium
Freezing medium for human high-grade glioma cells (GBM2)	5 % DMSO in GBM2 cultivation medium
Cultivation medium HEK-293T cells	10 % FCS 100 U/ml penicillin 100 µg/ml streptomycin 2 mM L-glutamine in DMEM-high glucose
Freezing medium for HEK-293T cells	5 % DMSO in HEK-293T cultivation medium

2.3.4. Coatings

Laminin

Laminin 1 µg/ml
in PBS

Poly-L-lysine (PLL)

Poly-L-lysin 1 µg/ml
in ddH_2O
Incubation: 1 h, room temperature

For PLL/laminin-coating:
incubation with PLL 1 h room temperature,
wash 3x with PBS,
incubation with laminin for 2 h (37°C)

Poly-L-ornithine (PO)

Poly-L-ornithine 1.5 µg/ml
in ddH_2O
Incubation: o/n, 37°C

For PO/laminin-coating:
incubation with PO o/n 37°C,
wash 3x with PBS,
incubation with laminin for 2 h (37°C)

2.3.5. Cell dissociation reagents

Accutase

ready to use solution

PPD solution

2.5 U/ml papain
1 U/ml dispase II (neutral protease)
250 U/ml DNAse
in DMEM-high glucose

Trypsin/DNAse

10 g/l Trypsin
500 mg/l DNAse
in HBSS

Trypsin/EDTA

10x Trypsin-EDTA 1:10
in PBS

2.3.6. Cell culture stock solutions

Tab. 2.9 Cell culture stocks

Reagent	Concentration	Solvent
3,3,5-Triiodothyronone (T3)	30 µg/ml	H_2O
Ascorbic acid	100 mg/ml	H_2O
B-27	50x, used directly from Life Technologies	
D(+)-glucose	300 mg/ml	H_2O

Reagent	Concentration	Solvent
EGF	20 µg/ml	Diluted acetic acid + 0.1% BSA
FGF-2	20 µg/ml	PBS + 0.1% BSA
Insulin	5 mg/ml	10 mM NaOH
Laminin	1 µg/ml, used directly from Sigma	
L-Glutamine	200 mM, used directly from Sigma	
Penicillin/Streptomycin	Used directly from Biochrom	
Puromycin	0.875 µg/ml	DMEM
Putrescine	0.1 M	H_2O
Sodium selenite	500 µM	H_2O
Transferrin	10 mg/ml	H_2O

2.4. Buffers and solutions

2.4.1. Buffers for molecular biology

Gel loading buffer

50 % H_2O
49 % Glycerol
0.5 % Bromphenol blue
0.5 % Xylene cyanol

50x Tris-actetate-EDTA buffer (TAE)

242 g Tris
100 ml 0.5 M EDTA (pH 8)
57.1 ml Water-free acetic acid
add dd$H_2$0 to 1 l

For use 50x TAE was diluted in H_2O 1:50

2.4.2. Solutions for immunolabeling

Blocking buffer (TBS+)

0.1 % Triton X-100
5 % donkey serum
in TBS

Cryoprotection buffer (CPS)

25 % glycerol
25 % ethylenglycol
in 0.05 M phosphate buffer

Fixation reagent

4 % Paraformaldehyde
in 0.1M PB

0.9 % Saline solution

0.9 % NaCl
in ddH_2O

30 % Sucrose
Sucrose (300 g/l)
in 0.05 M phosphate buffer

TritonX-100 (10 % stock solution)

100 mg/ml Triton-X-100
in PBS

Washing buffer (TBS)

100 mM Tris
150 mM NaCl, pH 7.4
in ddH_2O

2.4.3. Solutions for live-cell endoplasmic reticulum labeling

ER tracker (1 mM)

For use 1 mM ER tracker was diluted 1:2000 in
HBSS containing calcium and magnesium

2.4.4. Solutions for calcium imaging

FURA-2 AM (5 mM)

5 µg/µl in DMSO with pluronic acid

For use 5 mM FURA-2 AM was diluted in
HEPES buffer 1:1000

HEPES buffer

150 mM NaCl
5.4 mM KCl
1 mM $CaCl_2$
2 mM $MgCl_2$
5 mM HEPES
10 mM D(+)-Glucose
in ddH_20
adjust pH to 7.4

2.4.5. Solutions for mass spectrometry

Denaturizing buffer

6 M Urea
2 M Thiourea
20 mM HEPES
in ddH20
adjust pH to 8.0

Elution buffer

chloroform/methanol/Tris HCl 50 mM
2:1:1, v/v
adjust pH to 7.4

Homogenization buffer

chloroform/methanol
9:1 v/v

2.5. Immunolabeling

2.5.1. Primary antibodies

Tab. 2.10 Primary antibodies

Gp = guinea pig, Gt = goat, Ms = mouse, Rb = rabbit, Rt = rat

Epitope	Origin and Isotype	Dilution	Provider
5-Bromodeoxy-uridine (BrdU)	rt IgG	1:500	Biozol (Eching)
Doublecortin (Dcx)	gt IgG	1:200	Santa Cruz Biotechnology (Santa Cruz, USA)
Doublecortin (Dcx)	rb IgG	1:200	Abcam (Cambridge, United Kingdom)
Glial fibrillary acidic protein (GFAP)	gp IgG	1:500	Synaptic Systems (Goettingen)
Glial fibrillary acidic protein (GFAP)	rb IgG	1:1000	DAKO (Glostrup, Denmark)
Green fluorescent protein (GFP)	gt IgG	1:500	Acris Antibodies (Herford)
Ki67	rb IgG	1:400	Novocastra (Newcastle upon Tyne, United Kingdom)
Nestin	ms IgG	1:80	Millipore (Schwalbach)
Neuronal Nuclei (NeuN)	ms IgG	1:100	Millipore (Schwalbach)
Parvalbumin	rb IgG	1:1000	Millipore (Schwalbach)
Sex determining region Y-box 2 (Sox2)	gt IgG	1:200	Acris Antibodies (Herford)
Transient receptor potential vanilloid 1 (TRPV1)	rb IgG	1:10000	Neuromics (Edina, USA)

2.5.2. Secondary antibodies

All secondary antibodies were obtained from Dianova (Hamburg).

Tab. 2.11 Secondary antibodies

Antigen	Conjugation	Origin	Dilution
goat IgG	DyLight 488	donkey	1:200
goat IgG	Cy5	donkey	1:200

guinea pig IgG	DyLight 649	donkey	1:200
mouse IgG	Cy3	donkey	1:200
mouse IgG	DyLight 488	donkey	1:200
mouse IgG	Cy5	donkey	1:200
rabbit IgG	Cy3	donkey	1:200
rabbit IgG	DyLight 488	donkey	1:200
rabbit IgG	Cy5	donkey	1:200
rabbit IgG	Biotin-SP	donkey	1:125
rat IgG	Rhodamine Red-X	donkey	1:125
rat IgG	Biotin-SP	donkey	1:125
Biotin-SP	Streptavidin-Horseradish Peroxidase		1:200

2.6. PCR primers

Tab. 2.12 Primers for qRT-PCR

Gene product	Product length	Primer sequence	Annealing temperature	Cycles
beta-3-Tubulin	100 bp	fw: 5'-gatgatgacgaggaatcggaa-3' rev: 5'-cagatgctgcttgtcttggc-3'	59°C	35
beta-Actin	238 bp	fw: 5'-cgtgggccgccctaggcacca-3' rev: 5'-cttagggttcaggggggc-3'	56-62°C	25
CB1^{+}	255 bp	fw: 5'-ccaagaaaagatgacggcag -3' rev: 5'-aggatgacacatagcaccag -3'	58°C	35
CB2	200 bp	fw: 5'-tccaacgctatcttcctgct-3' rev: 5'-ggactagggcaacaagtcca-3'	60°C	35
CNP$^{\#}$	136 bp	fw: 5'-gagctggtcagctactttgga-3' rev: 5'-ggccttgccatacgatctct-3'	56°C	35
DAGL^{+}	194 bp	fw: 5'-ttccgagggtgacattcttagc-3' rev: 5'-aatggctatcatctggctgagc-3'	60°C	35
FAAH^{+}	343 bp	fw: 5'-aaggcctgggaagtgaacaaagg-3' rev: 5'-aacctcctggactcttggagg-3'	62°C	35
GAPDH	203 bp	fw: 5'-acgacccctcattgacctcaact-3' rev: 5'-atatttctcgtggttcacacccat-3'	60°C	25
GFAP$^{\#}$	198 bp	fw: 5'-gagtaccacgatctactcaac-3' rev: 5'-ccacagtctttaccacgatgt-3'	62°C	35
MAGL^{+}	288 bp	fw: 5'-atggtgtccacgtgttgcagc-3' rev: 5'-ttgtagatactggaagccc-3'	62°C	35

Gene product	Product length	Primer sequence	Annealing temperature	Cycles
NAPE-PLD[+]	207 bp	fw: 5'-aagtgtgtcttctaggttctcc-3' rev: 5'-ttgtcaagttcctctttggaacc-3'	62°C	35
Nestin*	107 bp	fw: 5'-ggacaggaccaagaggaaca-3' rev: 5'-tctggatccacctttctgg-3'	56°C	35
PLP[#]	70 bp	fw: 5'-cacttacaacttcgccgtcct-3' rev: 5'-gggagtttctatgggagctcaga-3'	56°C	35
S100beta[#]	311 bp	fw: 5'-gagcccatgagcctttgctgtg-3' rev: 5'-gggtgacaagcacaagctgaagaa-3'	62°C	35
Sox2*	204 bp	fw: 5'-agaaccccaagatgcacaac-3' rev: 5'-ctccgggaagcgtgtactta-3'	56°C	35
TRPV1	132 bp	fw: 5'-catgctcattgctctcatgg-3' rev: 5'-aggccttcctcatgcacttc-3'	57°C	35

* from [Liu et al., 2009] [#] from [Stock et al., 2010] [+] from [Bari et al., 2011]

2.7. Plasmids for TRPV1 knockdown and rescue

pLKO.1 or pLKO.1-TRPV1-shRNA or pLKO.1-scrambled-shRNA (Biocat, Heidelberg) and packaging plasmids (pMD2.g for VSV-G, PAX2 for gag/pol; Addgene, Cambridge, USA) were used for TRPV1 knockdown.

The TRPV1 rescue construct contained a full-length open reading frame of mouse TRPV1 (NM_001001445, expressed in pIRES2-EGFP), which was mutated in the seed-region of the shRNA knockdown construct [Cullen, 2006] and coded for a wildtype TRPV1 protein (by alternative codon-usage): 5´- TATCTTGTATTTTTATTCGGT TTC-3´ (the seed region is underlined; the first mutant basepair is at position 1753 of the open reading frame of mouse TRPV1).

2.8. Software

Tab. 2.13 Software products

Product	Supplier
Adobe Illustrator CS	Adobe Systems (München)
Adobe Photoshop CS	Adobe Systems (München)
ANY-maze	Stoelting Co. (Wood Dale, USA)
CELLQuest (for FACS)	BD Biosciences (Heidelberg)
Fiji - Image J	http://fiji.sc/wiki/index.php/Downloads
Leica LAS AF	Leica (Wetzlar)
MetaFluor Fluorescence Ratio Imaging Software 7.01	Molecular Devices (Sunnyvale, USA)
Microsoft Office 2007	Microsoft (Mountain View, USA)
Microsoft Windows XP	Microsoft (Mountain View, USA)
MultiQuant (for Mass spectromoetry)	AB SCIEX (Darmstadt)
SPSS 11.5	SPSS Inc., IBM (Chicago, USA)
StereoInvestigator	MBF Bioscience (Williston, USA)
Thomson Reuters EndNote X1	Thomson Reuters (Carlsbad, USA)
Volocity LE	PerkinElmer (Waltham, USA)

3. Methods

3.1. Cell culture

Generally, all cell culture techniques were performed under sterile conditions in a hood with sterile media, glass and plastics.

3.1.1. Cell culture of mouse cells

3.1.1.1. Cell culture of mouse neural precursor cells

C57BL/6 mice (p14) were decapitated and skin and skull were removed. The brain was dissected and transferred into cold PBS/D(+)-Glucose (4.5 g/l). The cerebellum and olfactory bulb were taken off and cross sections of the brain containing the SVZ or hippocampus were made. The lateral ventricles of the SVZ or the hippocampus were microdissected, collected in a 15 ml tube and centrifuged (500 g, 5 min, 4°C). The collected tissue was incubated with occasional mixing in PPD solution (2.5 U/ml papain, 1 U/ml dispase II (neutral protease) and 250 U/ml DNAse in DMEM 4.5 g/l D(+)-glucose) (5 ml / animal) for 40 min at 37°C. The tissue was washed three times with PBS to remove the PPD solution. Cells were plated in 10 cm-dishes in cultivation medium for mouse NPCs. Cultures were incubated at 37°C / 5 % CO_2 and the medium was changed on the next day. The cells were cultured until they formed neurospheres. For splitting, NPCs were collected by centrifugation (500 g, 5 min, 4°C) and dissociated enzymatically by Accutase according to the manufacturer's instructions. The cells were counted and seeded in a clonal density of 0.5 x 10^6 per 10 cm-dish in cultivation medium.

To investigate NPC proliferation, 0.5 x 10^6 cells were replated in a 10 cm-dish in cultivation medium after each subculturing passage and the average growth factor per passage was calculated.

3.1.1.2. Limiting dilution assay

Clonal efficiency was assessed using a limiting dilution assay. Briefly, 10 to 500 cells per well (96-well plate) were incubated in 200 µl medium. Per cell concentration twelve wells were seeded. After different time points, wells containing at least one neurosphere were counted using an inverted microscope. Clonal efficiency was quantified as the cell concentration needed to obtain at least one clone per well.

3.1.1.3. Differentiation

For differentiation experiments, NPCs were cultured for two weeks adherently on poly-L-ornithine/laminin coated T75 flasks, growth factors were withdrawn and 0.1 % FCS was added to the cultivation medium.

3.1.1.4. Cell culture of mouse high-grade astrocytoma cells (GL261)

The high-grade astrocytoma cell line GL261 (C57BL/6 background) was obtained from the National Cancer Institute (Frederick, USA). The cells were cultured in cultivation medium for mouse high-grade glioma cells (GL261). Cultures were incubated at 37°C / 5 % CO_2 and the medium was changed every other day. The cells were cultured until confluency. For splitting, GL261 cells were dissociated enzymatically by Trypsin/EDTA according to the manufacturer's instructions.

3.1.1.5. Cell culture of dorsal root ganglia neurons

Dorsal root ganglia (DRG) neurons were prepared from both wildtype and TRPV1 knockout adult mice (4-10 weeks old) as described previously [Sturzebecher et al., 2010]. Neurons were plated on poly-L-lysine (1 µg/ml) and laminin (1 µg/ml) coated glass coverslips and maintained in DRG cultivation medium at 37°C and 5 % CO_2.

3.1.2. Cell culture of human cells

3.1.2.1. Cell culture of human neural precursor cells

Human neural precursor cells (NPC-A, NPC-B, NPC-C) were isolated from access tissue of planned resections from patients with the required neuroendoscopy and ethical approval. The normal SVZ specimens were obtained during anterior temporal lobectomy for the treatment of intractable epilepsy from mesial temporal sclerosis at the Charité university clinic Berlin (Department of Neurosurgery). The cells were isolated from the tissue using the same protocol as for mouse NPCs (see 3.1.1.1.). Cells were plated in T75 flasks in human NPC cultivation medium. Cultures were incubated at 37°C / 5 % CO_2 and the medium was changed on the next day. The cells were cultured until they formed neurospheres. For splitting, human NPCs were collected by centrifugation (500 g, 5 min, 4°C) and dissociated enzymatically by Accutase according to the manufacturer's instructions. The cells were counted and seeded in a clonal density of 0.5 x 10^6 per T75 flask in cultivation medium.

3.1.2.2. Cell culture of human glioblastoma cells

Tumor samples were obtained from glioblastoma multiforme (GBM) patients according to governmental and internal (Charité university clinic, Berlin) rules and regulations: all patients were diagnosed with primary GBMs, without any prior clinical history; all samples were obtained from initial surgical treatment and none of the patients had yet received chemo- or radiation-therapy.

The human glioblastoma cells GBM1, GBM2 and GBM3 were derived from tumor resections. The material was washed 3 times in HBSS and cut into small pieces using a scalpel in a sterile petridish. The tissue was digested in a 15 ml falcon tube for 4 min at room temperature using 1 ml Trypsin/DNAse and titruated first using a plastic and then a glass Pasteur pipette. The reaction was stopped with cultivation medium and the

dissociated cell suspension was centrifuged for 10 min (800 rpm, 4°C). The cell pellet was resuspended in cultivation medium and transferred to a T25 flask. After 2 days the cells were washed with PBS and the medium was changed. Cultures were incubated at 37°C and 5 % CO_2.

GBM1 and 3 cells were cultured adherently until confluency and were dissociated enzymatically by Trypsin/EDTA according to the manufacturer's instructions. GBM2 cells were grown as tumorspheres and splitted as described for neurospheres. The cells were counted and seeded in a clonal density of 0.5 x 10^6 per T75 flask in cultivation medium.

3.1.2.3. Cell culture of human HEK-293T cells

HEK-293T cells were obtained ATCC (Manassas, USA) and cultured in cultivation medium for HEK-293T cells. Cultures were incubated at 37°C and 5 % CO_2 and medium was changed every other day. The cells were cultured until confluency. For splitting, HEK-293T cells were dissociated enzymatically by Trypsin/EDTA according to the manufacturer's instructions.

3.1.2.4. Cytotoxicity assay

Human GBM cells (0.3 x 10^4/well) were seeded in PLL-coated 96-well plates. The next day the medium was removed and replaced by agonist/antagonist containing medium (normal NB/B-27 and 1 µM digitonin served as negative and positive controls respectively). After 24, 48 and 72 h of incubation, 100 µl of CytoTox-Fluor Cytotoxicity reagent was added to the wells and incubated at 37°C for 1 h. The CytoTox-Fluor Assay measures a distinct protease activity associated with cytotoxicity. The assay uses a fluorogenic peptide substrate (bis-alanyl-alanyl-phenylalanyl-rhodamine 110; bis-AAF-R110) to measure dead-cell protease activity, which has been released from cells that have lost membrane integrity. The bis-AAF-R110 Substrate cannot cross the intact

membrane of living cells and therefore gives no signal from living cells. After 1 h of incubation the resulting fluorescence was measured (485/520 nm) with the fluorometer. For antagonist treatment, the cells were preincubated with antagonists for 3 h in control medium. Afterwards, the medium was exchanged with treatment medium (containing agonist and antagonist).

3.1.2.5. Measurement of endoplasmic reticulum (ER) size

Human GBM cells (1 x 10^4/well) were seeded in PLL-coated µ-slide 8 well-plates. The next day the medium was removed and replaced by agonist/antagonist containing medium (normal NB/B-27 served as negative control). After 72 h of incubation, the ER stress inducer thapsigargin (30 ng/ml) was added to the positive control wells for 6 h. For live-cell ER labeling, the cells were washed with HBSS (containing calcium and magnesium) and the prewarmed ER tracker solution (500 nM) was added to the cells for an incubation time of 30 min at 37°C. Afterwards, the stained cells were fixed with 4 % PFA for 15 min at room temperature. The staining was evaluated using a DAPI longpass filter. The relative increase in ER-size after incubation with human NPC-conditioned medium was quantified by confocal microscopy z-stacks (non-conditioned medium is used as control; incubation with thapsigargin is set as 100%). For antagonist treatment, the cells were preincubated with antagonist for 3 h in control medium. Afterwards, the medium was exchanged with treatment medium (containing agonist and antagonist).

3.1.3. Organotypic brain slice cultures

3.1.3.1. Preparation of organotypic brain slices

Organotypic brain slices were prepared from 16 day-old C57BL/6 mice as described previously [Markovic et al., 2005]. The mice were decapitated and the brain was placed in ice-cold PBS solution. After removing the cerebellum, the brain was mounted on a cutting block with cyanoacrylate glue. An agar block (2 %) stabilized the brain. Coronal 250 µm sections were cut using a vibratome. The brain slices were collected with a glass pipette (7 mm diameter) and transferred onto cell culture inserts in 6-well plates. Excess PBS was removed in a sterile cell culture hood. The brain slices were cultivated at the air-liquid interface in 1 ml of preparation medium for organotypic brain slices per well. The next day, the medium was changed to cultivation medium.

3.1.3.2. Depletion of microglia in organotypic brain slices

Organotypic brain slices were prepared as described in 3.1.3.1. Two hours after preparation, the medium was exchanged for preparation medium supplemented with clodronate-filled liposomes (1:10) or PBS-filled liposomes (1:10) as control. The slices were incubated with the liposomes for 24-28 h. Afterwards, the cell culture inserts containing the organotypic brain slices were transferred into a new 6-well plate with cultivation medium (1 ml per well) and the slices were resting for 72 h.

3.1.3.3. Glioma cell injection into organotypic brain slices

Organotypic brain slices were injected with 5000 GFP-expressing GL261 high-grade astrocytoma cells per hemisphere. Therefore, the glioma cells were diluted to 25 000 cells/µl and a total volume of 0.2 µl was injected using a 1 µl blunt tipped microsyringe mounted to a self-constructed micromanipulator. An injection cavity was

formed and the cells were slowly injected into the caudate putamen region in 100-150 µm depth of the slice. Careful control of the injection procedure ensured that no cells spilled onto the surface of the slices, which could then migrate over this surface rather than invade through the tissue.

The fluorescent glioma area was quantified using the ImageJ software. The scale of the images was calibrated. The area was measured as fluorescent pixels above threshold and is given as mm^2.

3.1.4. TRPV1 knockdown and FACS analysis

293T cells were cotransfected with pLKO.1, pLKO.1-TRPV1-shRNA or pLKO.1-scrambled-shRNA and packaging plasmids (pMD2.g for VSV-G, PAX2 for gag/pol) using FuGene transfection reagent according to the manufacturer's instructions. The virus-containing supernatant was collected for infection of GL261 mouse high-grade glioma cells. Stable cell lines were selected in growth medium containing 1 µg/ml puromycin.

The ready-made shRNAs (set of five: RMM3981-97057125, RMM3981-97057126, RMM3981-97057127, RMM3981-97057128, RMM3981-985011490) contained sequences complementary to TRPV1 (NM_001001445). The shRNA from clone RMM3981-97057126 (source-ID: TRCN0000068739), with the sequence: 5´-CCTCGTGTTCTTGTTTGGATT-3´ produced the most efficient TRPV1 knockdown. The validity of the shRNA mediated knockdown (compared to empty-vector and scrambled shRNA controls) was affirmed on protein level, by Western blot and FACS analysis against a TRPV1-GFP fusion protein, as described [Grunweller et al., 2003] and also on the functional level, by Ca^{2+} imaging and cell-death induction.

For TRPV1 rescue, a TRPV1 wildtype sequence was used which was protected from shRNA degradation by alternative codon-usage. The rescue construct was transfected (by Amaxa electroporation according to the manufacturer's instructions) into GL261 cells

stably expressing TRPV1-KD. GFP-expressing cells were purified by fluorescence activated cell sorting (FACS). Therefore cells were collected and centrifuged at 1000 g for 2 min. The cell pellet was washed and suspended in PBS. Cells expressing GFP (TRPV1 shRNA, empty vector and scrambled shRNA) were analyzed using a FACS Calibur (BD Biosciences). CELLQuest (BD Biosciences) software was used for data analysis and quantifications.

3.2. Molecular biology

3.2.1. mRNA isolation and cDNA synthesis

The total RNA of the cells was extracted using the RNeasy Mini Kit according to the manufacturer's instructions (spinning protocol) including the optional DNAse digest. The isolated RNA was quantified photometrically and 1 µg was used for the synthesis of cDNA using the iScript cDNA synthesis kit according to the manufacturer's instructions.

3.2.2. Semiquantitative PCR

Semiquantitative PCR for the endocannabinoid / -vanilloid system and human TRPV1 detection was done using the TaKaRa Taq system (Tab. 3.1) in a Biometra T3000 thermocycler. Negative controls (H_2O) were always included. Beta-actin or GAPDH housekeeping genes were used as positive controls and reference genes.

Tab. 3.1 Semiquantitative PCR mix per reaction

Component	Volume (µl)
TaKaRa Taq™ (5 units/µl)	0.2
10× PCR Buffer (Mg^{2+} plus)	2.5
dNTP Mixture (2.5 mM each)	2.0
Primer fw (10 µM)	0.5
Primer rv (10 µM)	0.5
Sterilized distilled water	17.3
TOTAL	**23**

70 ng of cDNA (2 µl) was added to the master mix and pipetted into the PCR stripes.

The individual steps were performed as follows (the lid was kept at 95°C):

Initial Denaturation	94°C	3 min	
Denaturation	94°C	30 s	x cycles
Annealing	x°C	1 min	
Extension	72°C	60 s	
Final Extension	72°C	5 min	
Pause	4°C	∞	

The annealing temperature was adapted to the primer set used. For most genes 35 cycles were used, the PCRs for the house keeping genes were performed using 25 cycles.

After the PCR reaction, the samples were electrophoretically separated on an agarose gel (2 % agarose in TAE-buffer, 1 µl ethidiumbromide / 10 ml buffer) at 80 V for approximately 30 min. The agarose gels were exposed to UV light (254 nm) in a gel documentation system to visualize DNA bands.

3.2.3. Quantitative PCR

Real-time quantitative PCR for TRPV1 was performed with TaqMan probes (Mm01246301_m1) obtained from Applied Biosystems (Tab. 3.2). Amplifications were run as triplicates in a 7700 Real-time PCR system and values were adjusted using beta-actin in-well-controls as reference.

Tab. 3.2 Quantitative TaqMan PCR mix per reaction

Component	Volume (µl)
2x TaqMan Gene Expression Master Mix	10
20x TaqMan Gene Expression Assay	1
20x Mouse beta-actin Endogenous Control (VIC/MGB Probe, Primer Limited)	1
Sterilized distilled water	5
TOTAL	**17**

50 ng of cDNA (3 µl) was added to the master mix and pipetted into the PCR plates.

The PCR protocol was run according to the manufacturer's instructions as follows (the lid was kept at 95°C):

Initial Denaturation	95°C	10 min	
Denaturation	95°C	15 s	40 cycles
Annealing	60°C	60 s	
Extension	72°C	45 s	
Final Extension	72°C	10 min	
Pause	4°C	∞	

Real-time quantitative PCR for differentiation markers was done in triplicates using the SYBR Green fluorescence method (Tab. 3.3) in an Eppendorf realplex mastercycler.

Tab. 3.3 Quantitative SYBR Green PCR mix per reaction

Component	Volume (µl)
Promega goTaq PCR mix (2x)	10
Primer fw (10 µM)	0.5
Primer rv (10 µM)	0.5
Sterilized distilled water	8
TOTAL	19

The cDNA (10 ng, 1µl) was added to the master mix and pipetted into the PCR stripes.

The individual steps were performed as follows (the lid was kept at 95°C):

Initial Denaturation	94°C	3 min	
Denaturation	94°C	30 s	35 cycles
Annealing	x°C	30 s	
Extension	72°C	60 s	
Final Extension	72°C	3 min	
Pause	4°C	∞	

The annealing temperature was adapted to the primer set used. After completing the run, melting curves of the amplified PCR products were obtained to control for specificity.

After the PCR reaction, the samples were electrophoretically separated on an agarose gel (2 % agarose in TAE-buffer, 1 µl ethidiumbromide / 10 ml buffer) at 80 V for approximately 30 min. The agarose gels were exposed to UV light (254 nm) in a gel documentation system to visualize DNA bands.

3.3. HPLC and mass spectrometry for lipids

The HPLC and mass spectrometry for lipids were conducted at the Institute of Biomolecular Chemistry of the National Research Council (ICB-CNR) in Pozzuoli, Naples, Italy. Cells were homogenized in homogenization buffer containing internal standards (10 pmol of d8-AEA and 50 pmol of d5-2-AG, d4-PEA and d2-OEA) [Devane et al., 1992; Bisogno et al., 1997]. The lipid-containing organic phase was purified by open-bed chromatography on silica gel and fractions eluted with elution buffer (containing AEA, 2-AG, PEA, OEA) were analyzed by isotope dilution-liquid chromatography/atmospheric pressure chemical ionization/mass spectrometry (LC APCI-MS) carried out under conditions described previously [Marsicano et al., 2002]. MS detection was carried out in the selected ion monitoring (SIM) mode using mass-to-charge ratio values of 356 and 348 (molecular ions +1 for deuterated and undeuterated AEA), 384.35 and 379.35 (molecular ions +1 for deuterated and undeuterated 2-AG), 304 and 300 (molecular ions +1 for deuterated and undeuterated PEA), 328 and 326 (molecular ions +1 for deuterated and undeuterated OEA). The amounts of endocannabinoids, PEA and OEA were calculated on the basis of their area ratio with the internal deuterated standard signal area, and were expressed as pmol/mg of lipid extract compared by ANOVA followed by the Bonferroni's *post-hoc* test.

3.4. Detection of TRPV1 by mass spectrometry in total cell lysates

The mass spectrometry analysis was conducted at the mass spectrometry technology platform at the MDC Berlin. Peptides for the development of a SRM method (selected reaction monitoring) were selected based on the peptide sieve prediction method (www.peptideatlas.org). Based on the prediction several peptides were synthesized (in house peptide synthesis, Intavis ResPep SL). The SRM method was set up based on the fragmentation and retention time information generated with these model peptides. Cells were grown as described above. Cells were resuspended in denaturizing buffer and lysed by sonication. After centrifugation the soluble fraction was subjected to a two-step protease digest as described [de Godoy et al., 2008]. Peptides were captured on a stage-tip micro column and desalted. The purified peptides were separated on a 15 cm reverse phase column (75 µm inner diameter, 3 µm C18-reverse phase beads, Dr. Maisch, Reprosil-AQ Pur), with 155 min gradient from 5 % to 40 % acetonitrile in 0.5 % acetic acid using an Proxeon EASY-nLC nanoLC HPLC system. The effluent was directly electrosprayed into the mass spectrometer [Rappsilber et al., 2007]. Data was recorded on an ABSciex Q-TRAP 4000 in SRM mode. Several transitions of the QFVNASYTDSYYK peptide were followed and normalized to the SYELPDGQVITIGNER peptide of actin. MultiQuant software (ABSciex) was used for data analysis.

3.5. Calcium imaging

Cultured cells were loaded for 30 min with 5 µM of the membrane permeable fluorescent dye Fura-2 acetoxymethyl ester. Inside the cells, the acetoxymethyl groups are removed by cellular esterases generating the calcium indicator. The loaded cells were transferred to the PBS containing recording chamber of a fluorescence microscope (Zeiss Axiovert 200). Applications of stimuli were done using a gravity-driven multi barrel perfusion system (WAS02). Cells were illuminated alternately at 340 and 380 nm for 500 ms and

ratio images were collected every 1.6 s using MetaFluor software and a SPOT-SE18 CCD camera. All ratios were normalized to the mean of the first 10 ratio images (R_0) and plotted as R/R_0. At the end of each individual experiment cells were perfused with 40 mM KCl for DRGs or 500 µM ATP for NPCs. All cells that did not respond to the control stimulation were excluded from analysis. The acquired data were analyzed using MetaFluor software and Microsoft Excel. Signals were considered, if they lay outside the confidence interval of the R/R_0 values using the statistical level of alpha = 0.05.

3.6. Animals

All animals were handled according to governmental and internal (MDC) rules and regulations. Wildtype C57BL/6 mice, TRPV1 knockout mice [Caterina et al., 2000], Nestin-GFP mice [Yamaguchi et al., 2000], cdk2 knockout mice [Sicinski et al., 1996] (from in-house breeding) and NOD/SCID mice (from Charles River Breeding Laboratories; Schöneiche, Germany) were housed with a 12 h light / dark cycle and received food *ad libitum*. In TRPV1 knockout mice, a targeting vector was used to disrupt an exon encoding part of the fifth and all of the sixth putative transmembrane domains together with the pore-loop region of TRPV1 [Caterina et al., 2000].

All experiments involving animals were conducted under the following licenses and approved by Landesamt für Gesundheit und Soziales Berlin (LAGeSo):

TVV: T 0014_08 (for primary cell culture or slice culture)

TVV: O 0360 (for perfusion and analysis of organs)

TVV: O 0416-9 (for tail cuts for genotyping)

TVV: G 0343/10 (for tumor inoculation and Nestin-GFP animals)

TVV: G 0268/10 (for tumor inoculation, TRPV1 knockout animals, BrdU injections, behavioral analysis).

3.6.1. BrdU injections

For the analysis of cell survival, the mice received an injection of 50 µg BrdU / g body weight at a concentration of 10 mg/ml BrdU in sterile 0.9 % NaCl solution for three days.

3.6.2. *In vivo* inoculation of glioma cells into the mouse brain

3.6.2.1. Anesthesia

Mice were anesthetized by intraperitoneal injections of a 0.1 % xylazyne (Rompun) and 1.5 % ketamine hydrochloride (Ketanest) mixture in 0.9 % NaCl. 10 µl of the anesthetic mixture was injected per gram of mouse body weight. The eyes of the mice were carefully covered with glycerin fat to avoid cornea drying.

3.6.2.2. Tumor implantation

Surgical procedures were performed as described previously [Glass et al., 2005; Walzlein et al., 2008]. Anaesthetized wildtype, Nestin-GFP or NOD/SCID mice were immobilized and mounted into a stereotactic head holder in the flat-skull position. The skin of the skull was dissected with a scalpel blade and the skull surface was disinfected with 10 % potassium iodide solution. Approximately 1 mm anterior and 1.5 mm lateral to the bregma (for p30 animals) or 1.5 mm posterior and 1.5 mm lateral to the bregma (for p90 animals) the skull was carefully drilled with a 20-gauge needle tip. Then, a 1 µl microsyringe was inserted to a depth of 4 mm, retracted to a depth of 3 mm from the dural surface and cell suspensions were injected. The needle was slowly taken out from the injection canal and the skin was sutured. Wildtype C57BL/6 or Nestin-GFP mice (at p30 or p90) received murine glioma cells that are syngeneic with the genetic background of these mouse strains (GL261 wildtype, TRPV1 knockdown, or scrambled controls) alone (2×10^4 GL261 cells / 1 µl) or in combination with exogenously cultivated C57BL/6-derived

NPCs (6 x 10^4 precursor cells / 4 µl plus 2 x 10^4 GL261 cells / 1 µl - total volume of 5 µl). Immune deficient mice (NOD/SCID) were implanted with primary human GBM1, 2 or 3 cells (1 µl containing 20 000 cells).

3.6.2.3. Tumor size quantification by unbiased stereology

Tumor size determination was performed in at least 6 animals per group. Two weeks after orthotopic implantation of GFP expressing tumor cells, brains were sectioned and every 12^{th} axial section 1.8 to 4.2 mm from dural surface was sampled (representing the area that was infiltrated by the tumor). Quantification of tumor area was determined in an unbiased approach using the optical fractionator procedure of the StereoInvestigator software. The coefficient of error (CE) of the probe was consistently ≤ 0.08. Tumor volume was quantified according to the Cavalieri principle by determining tumor area in every 6^{th} 40 µm brain slice and then multiplying by 6 x 40 µm (to obtain a tumor volume).

3.6.3. Survival studies

All mice that were used for glioma survival studies have been obtained from commercial providers in the same delivery and were then randomly distributed to the respective experimental groups. All survival studies were performed in parallel. In all experiments using immune-deficient mice and arvanil (alone, together with temozolomide or vehicle as a control), the experiments of the control or treated groups (for each single experiment) were performed in parallel.

3.6.4. Paraformaldehyde fixation

The mice were anesthetized with pentobarbital (Narcoren) at a dose of 500 µg / g body weight intraperitoneally and perfused with an intracardiac injection of a 0.9 % NaCl solution, followed by freshly prepared 4 % paraformaldehyde (PFA) solution (30 ml per animal). The PFA perfusate was replaced by a 0.9 % NaCl solution. Afterwards, the skull was opened and the brain was carefully removed and postfixed for 2 h or o/n in 4 % PFA. Then, the brains were cryopreserved in 30 % sucrose.

3.7. Immunolabeling

3.7.1. Immunocytochemistry

Immunocytochemical analysis of the cells was performed using primary antibodies and appropriate fluorophore-labeled secondary antibodies. Nuclei were visualized by DAPI (4',6-diamidino-2-phenylindole dihydrochloride) counterstaining (1:200 in TBS, 10 min). Cells were fixed in 4 % PFA for 10 min at room temperature and washed with TBS. Cells were then blocked in blocking buffer for 30 min and incubated with primary antibodies diluted in blocking buffer overnight at 4°C. After washing, the secondary antibodies were diluted in blocking buffer (TBS+), applied to the cells and incubated for 2 h at room temperature in darkness. The cells were washed three times with TBS, subsequently counterstained with DAPI, washed again with TBS and mounted in Aqua-Poly/Mount mounting medium. The coverslips were stored at 4°C until used for microscopical analysis.

3.7.2. Immunohistochemistry of brain sections (floating sections)

The PFA perfused and cryoprotected brains were rapidly frozen in dry ice and mounted onto a sliding microtome. 40 µm thick sections were collected into a CPS-cryoprotecting

solution. Before immunolabeling, the sections were washed with TBS and for 3,3'-Diaminobenzidine (DAB) reaction blocked in 0.6 % H_2O_2 (in PBS) for 30 min at room temperature on a shaker. The sections were washed again with TBS and incubated in blocking buffer (TBS+) for 1 h for permeabilization. Then, the sections were incubated o/n at 4°C with the primary antibody. Sections were washed with TBS and blocked again for 30 min. For DAB-staining, the slices were incubated for 2 h in the secondary antibody solution (Biotin-SP-conjugated, at room temperature). After washes with TBS the third antibody was incubated for 1 h (HRP-conjugated streptavidin), following detection via DAB. The reaction was stopped with water. For immunofluorescence labeling, the slices were labeled directly by incubation with a fluorophore-labeled antibody or a Biotin-SP-conjugated secondary and a fluorophore-streptavidin labeled tertiary antibody. For TRPV1 immunolabeling, the primary antibody was incubated for 48 h and the reaction was enhanced using tyramide signal amplification for 8 min (TSA kit). After a final wash they were mounted in Aqua-Poly/Mount mounting medium onto microscope glass slides and stored at 4°C until used for microscopical analysis.

3.8. Behavioral testing of animals

3.8.1. Morris water maze spatial learning task

Female C57BL/6 and TRPV1 knockout mice were trained in the reference memory version of the Morris water maze task to locate a hidden escape platform in a circular pool (1.89 m diameter) [Morris et al., 1982; Wolfer et al., 1997]. The water was made opaque with non-toxic white paint and kept at room temperature. Ten mice were tested per group and each mouse was given six trials a day for five consecutive days. The experiment was subdivided into acquisition (day 1-3), probe trial (without platform, day 4), reversal (day 4-5). Platform position was changed on day four. Mice were released from one of six fixed possible starting points and allowed to search up to 100 s for the platform. Irrespective of

trial performance, mice were guided to the platform and allowed to remain there for at least 15 s. Performance during acquisition phase, probe trial and reversal phase was recorded and analyzed using Any-MAZE software.

3.8.2. Rota-Rod performance test

Female C57BL/6 and TRPV1 knockout mice were set on the Rota-Rod device at a starting speed of 4 rpm. Up to 4 mice were tested in parallel. The speed was accelerating from 4 to 40 rpm and the latency to fall was monitored automatically. Eight mice were tested per group and each mouse was tested five times.

3.9. Microscopy

3.9.1. Fluorescence microscopy

Fluorescent gliomas in organotypic brain slices were visualized with a fluorescence microscope (Zeiss Axiovert).

3.9.2. Confocal microscopy

For confocal microscopy, I used a Leica SPE microscope with appropriate gain and black level settings (determined on negative controls, where the primary antibodies were omitted). Images were recorded as z-stacks and analyzed using Photoshop and Volocity software.

3.9.3. Cell counting and unbiased stereology

Cell counts were determined in an unbiased approach using the optical fractionator procedure of the StereoInvestigator software. For further phenotypic analysis of $BrdU^+$ cells, 50 cells in the dentate gyrus were counted on a confocal microscope for

colocalization with Dcx or NeuN. Six different tissue sections were analyzed and tissue from at least three different mice was used.

3.10. Statistical analysis

Data sets were analyzed statistically using SPSS 11.5 software and tested for normality by Shapiro-Wilks test. Two-sided levels of significance were determined at the $p < 0.05$ level. For non-parametric analysis, the Mann-Whitney-U test was used. Parametric testing was done with the t-test. The water maze data were tested with repeated measures ANOVAs. Comparisons between multiple groups were done using a one-way ANOVA with Scheffé *post-hoc* test. Significances are depicted as *: $p < 0.05$, **: $p < 0.01$, ***: $p < 0.001$. Data are presented as mean ± SEM.

4. Results

4.1. The vanilloid receptor TRPV1 modulates neural precursor cell functions

4.1.1. Neural precursor cells continuously release anandamide

Neural precursor cells (NPCs) were cultured as neurospheres in suspension. This so-called conditioned medium (NPC-CM) was collected after three days of culture and was screened for soluble factors (n = 3). The analysis revealed a high release of anandamide (N-arachidonoyl-ethanolamide, AEA) from undifferentiated NPCs (Fig. 4.1 A), which is an agonist on TRPV1 and CB1 receptors. Furthermore, two other endovanilloids were found in the medium of NPCs, N-palmitoyl-ethanolamide (PEA) and N-oleoyl-ethanolamide (OEA). They are known to exert anandamide function through TRPV1 channels [Ho and Gardiner, 2009] (Fig. 4.1 B). In addition, 2-Arachidonoylglycerol (2-AG), which is a ligands on CB1 receptors only, was found in higher amounts in differentiating NPCs than in undifferentiated ones (not shown).

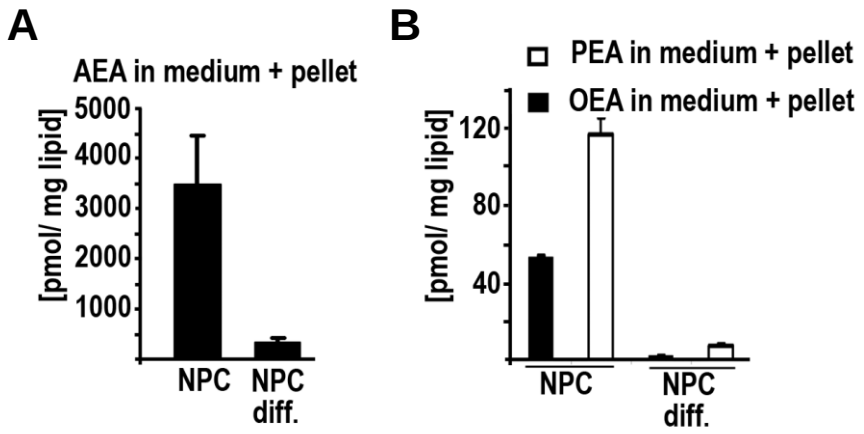

Fig. 4.1 NPCs release endovanilloids

The medium and pellet of undifferentiated and differentiated NPC cultures have been analyzed for N-arachidonoylethanolamide (AEA) (A), N-palmitoylethanolamide (PEA) and N-oleoyl-ethanolamide (OEA) (B) concentrations. All lipids are found predominantly in undifferentiated NPC cultures.

NPC-CM of proliferating NPCs was applied to wildtype dorsal root ganglia (DRG) neurons to show by calcium imaging that substances released by NPCs can act on TRPV1 channels (Fig. 4.2). About 30 % of DRG neurons express high levels of TRPV1 [Caterina et al., 2000]. TRPV1 channel activation results in an increase in intracellular calcium in DRGs. To exclude an effect via CB1 receptors, the cells were pre-incubated for 5 min with the CB1 antagonist AM251 (3 µM) [Fischbach et al., 2007] before starting calcium imaging.

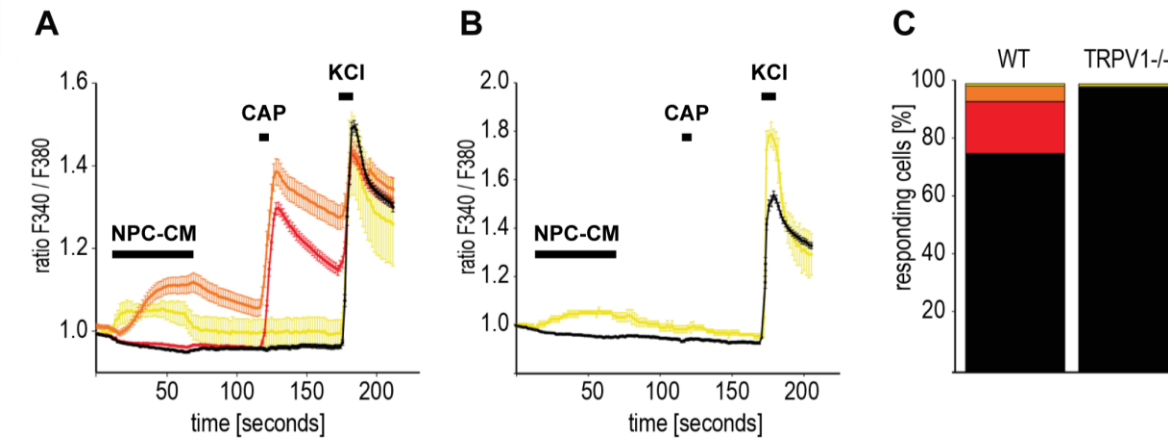

Fig. 4.2 Conditioned medium excites a subpopulation of capsaicin-sensitive DRG neurons

(A) Averaged example traces show that a population of wildtype DRG neurons is activated by 1 µM capsaicin (CAP, red) and that a second population is activated by both capsaicin and NPC-CM (orange). NPC-CM alone (yellow) also activates some DRG neurons. (B) Averaged example traces from TRPV1 knockout mice show that there are no DRG neurons responding to capsaicin, but that some respond to NPC-CM alone. Quantification of (A) and (B) is shown in (C). The black bar shows non-responsive DRGs, the red one DRGs reacting to capsaicin and the orange bar represents the fraction of cells reacting to NPC-CM and capsaicin. Courtesy of Dr. Ewan St. John Smith.

DRG neurons could be activated by NPC-CM as well as by capsaicin, the specific agonist for TRPV1 (Fig. 4.2 A). The same experiment was performed using TRPV1 knockout mice (Fig. 4.2 B). DRG neurons from TRPV1 knockout mice did not respond to capsaicin and the percentage of responders to NPC-CM was ~ 1 %. The co-activation of many DRG

neurons in wildtype mice by both capsaicin and NPC-CM, in combination with the lower percentage of NPC-CM responders in TRPV1 knockout mice suggests that a substance is present in NPC-CM that activates TRPV1. In total 1171 DRG neurons were analyzed from three different wildtype mice, 211 responded to capsaicin only, 63 to capsaicin and NPC-CM and ten responded to NPC-CM only. 544 DRG neurons were analyzed from three different TRPV1 knockout mice, five responded to NPC-CM (Fig. 4.2 C).

4.1.2. Postnatal NPCs express functional TRPV1 channels *in vitro*

To investigate the expression of TRPV1 in cultured NPCs, I isolated cells from the subventricular zone (SVZ) und hippocampal subgranular zone (SGZ) of p14 C57BL/6 wildtype mice and cultured them as described above. The expression of endogenous TRPV1 was analyzed on mRNA level using qRT-PCR (Fig. 4.3 A) and on protein level by mass spectrometry (Fig. 4.3 B). To verify that the cultured NPCs are undifferentiated, the culture was stained for the stem / precursor cell markers Sox2 (sex determining region Y-box 2), Nestin and GFAP (Glial fibrillary acidic protein, here used for detection of GFAP-expressing neural stem cells; n = 3) (Fig. 4.3 C-E).

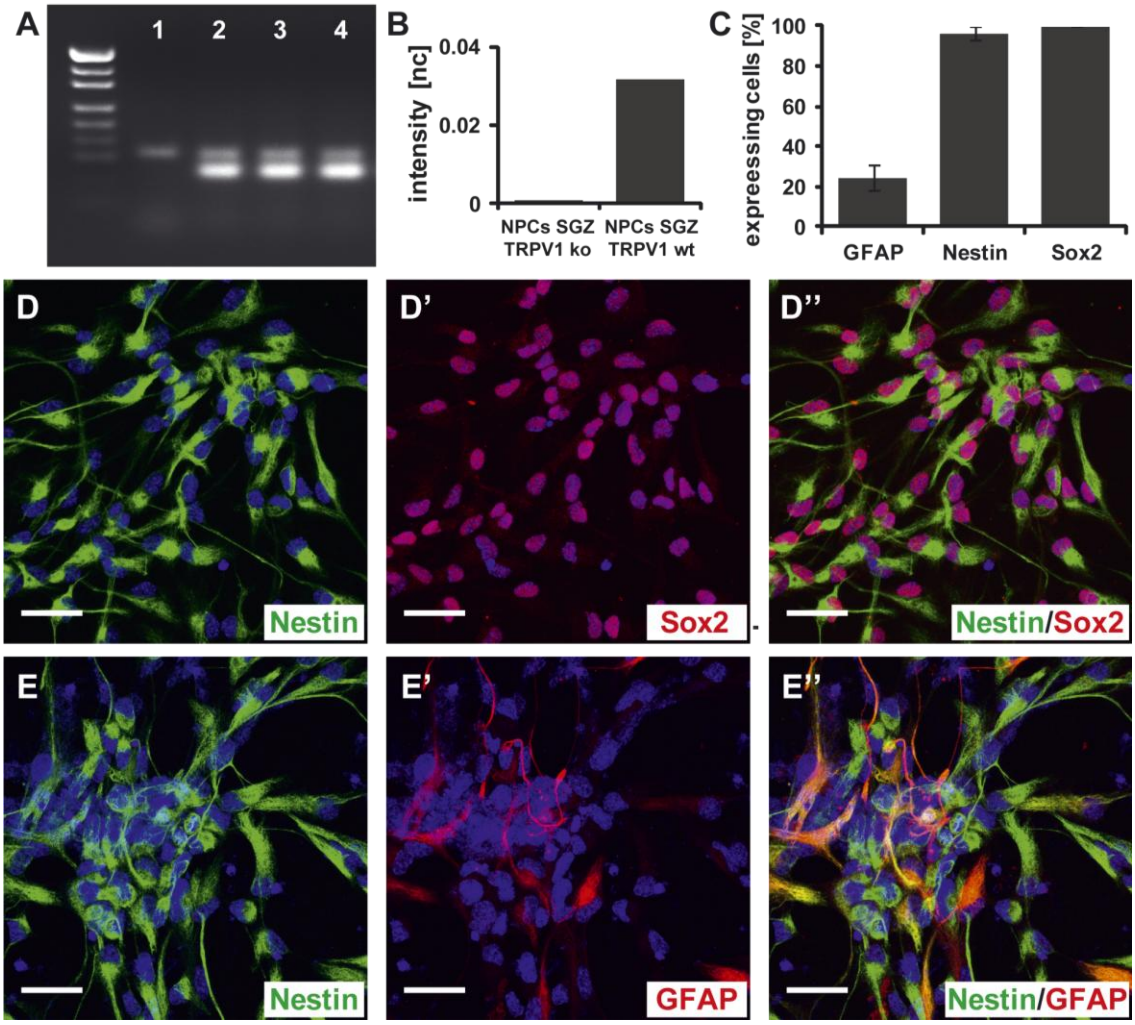

Fig. 4.3 TRPV1 is expressed in undifferentiated NPCs

Expression of TRPV1 is shown on mRNA level (A). RT-PCR products for TRPV1 (lower band) can be found in wildtype NPCs from both stem cell niches, but not in NPCs isolated from TRPV1 knockout animals (1: NPC TRPV1 ko SGZ; 2: NPC TRPV1 wt SGZ; 3: NPC TRPV1 wt SVZ; 4: GL261 astrocytoma cells). The upper band represents the beta-actin loading control. TRPV1 protein expression is confirmed by mass spectrometry (B). Values are given as normalized counts (nc). (C-E) NPCs are cultured adherently on poly-L-ornithine/laminin coated coverslips under proliferating conditions. NPC cultures express markers for undifferentiated neural precursor cells: Sox2 (100 %), Nestin (98 ± 2 %) and GFAP (25 ± 6 %). The cell nuclei are counterstained with DAPI (blue). Scale bars: 20 µm (D, E).

The analysis revealed that undifferentiated NPCs express the TRPV1 channel on mRNA and protein level (Fig. 4.3).

Furthermore, NPCs have the potential to differentiate into the neurogenic and gliogenic lineage. That is why I wanted to prove the differentiation potential of the isolated NPCs as well. Therefore, NPCs were cultured adherently in differentiation medium without growth factors but including 0.1 % FCS (differentiating conditions) for one week (Fig. 4.4).

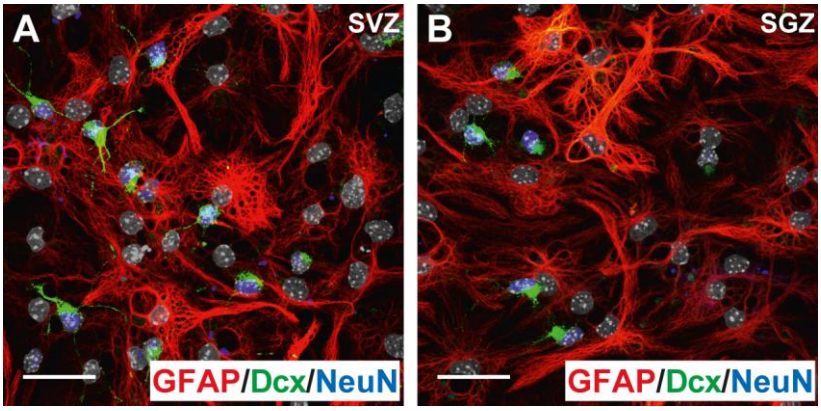

Fig. 4.4 Isolated NPCs can differentiate into neurons and astrocytes

Isolated NPCs from both stem cell niches are plated on poly-L-ornithine/laminin coated coverslips. They are cultured under mild differentiating conditions for one week and stained for astrocytic (GFAP) and neuronal (Dcx; NeuN) differentiation markers. The cell nuclei are counterstained with DAPI (gray). Scale bars: 20 µm.

Adherently cultured NPCs differentiated into astrocytes as shown by glial fibrillary acidic protein (GFAP) staining as well as into neurons maturing from a Doublecortin$^+$ (Dcx) immature neuronal stage to a mature NeuN$^+$ (neuronal nuclei) one, which proves their differentiation potential. However, for the following experiments undifferentiated NPCs are used unless indicated otherwise.

After the finding that TRPV1 is expressed in undifferentiated NPCs under proliferating conditions, I investigated whether they express also other components of the endovanilloid / -cannabinoid system.

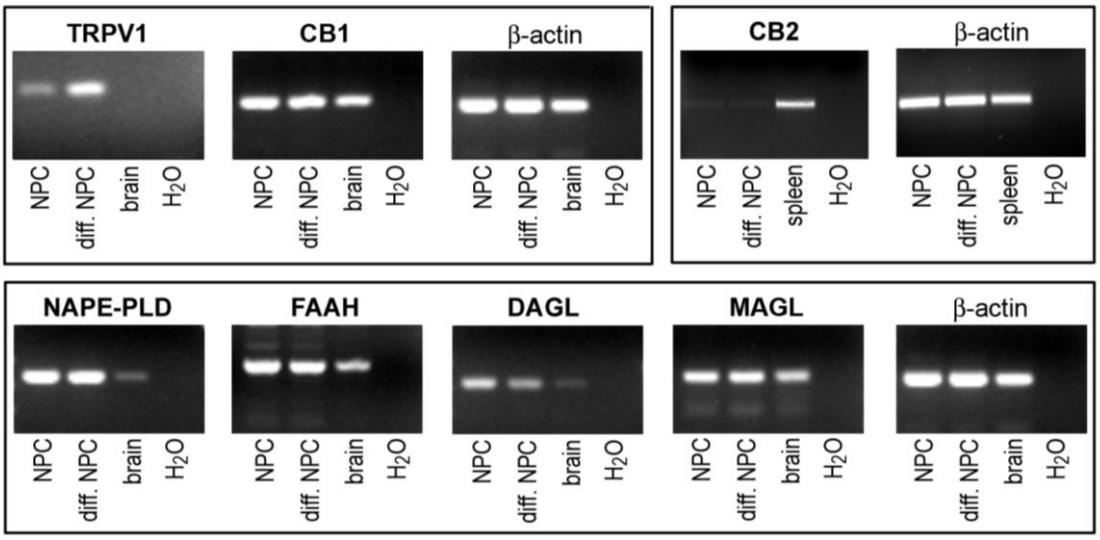

Fig. 4.5 NPCs express the complete endovanilloid / -cannabinoid system

The endoendovanilloid / -cannabinoid system is composed of the three receptors CB1, CB2 and TRPV1, the ligands anandamide (N-arachidonoylethanolamine, AEA) and 2-AG (2-Arachidonoyl-glycerol) and the production and hydrolysis machinery. AEA is produced by the activity of a NAPE-specific phospholipase D (NAPE-PLD) and binds to all receptors. It is degraded by fatty acid amide hydrolase (FAAH). 2-AG is released from membrane lipids through the activity of diacylglycerol lipase (DAGL). It binds only to CB receptors and can be hydrolyzed by FAAH or monoacylglycerol lipase (MAGL). All components can be detected in undifferentiated NPCs using RT-PCR, although CB2 expression is very low.

I found the complete endovanilloid / -cannabinoid system for the production and degradation of the two major compounds anandamide and 2-AG to be expressed in NPCs. Furthermore, findings from previous studies were confirmed, that they express CB1 and CB2 receptors [Aguado et al., 2005; Arevalo-Martin et al., 2007], although the latter one at very low levels (Fig. 4.5).

To test for functionality of the expressed receptor, I used calcium imaging to detect an increase in the intracellular calcium concentration upon TRPV1 activation. Therefore, NPCs from TRPV1 wildtype and knockout mice were exposed to capsaicin, the specific agonist on TRPV1 channels. The number of responding cells was analyzed and referred to cells responding to ATP (Adenosine-5'-triphosphate). The application times for 1 µM capsaicin and 500 µM ATP are marked in the figures (Fig. 4.6 A, C, E).

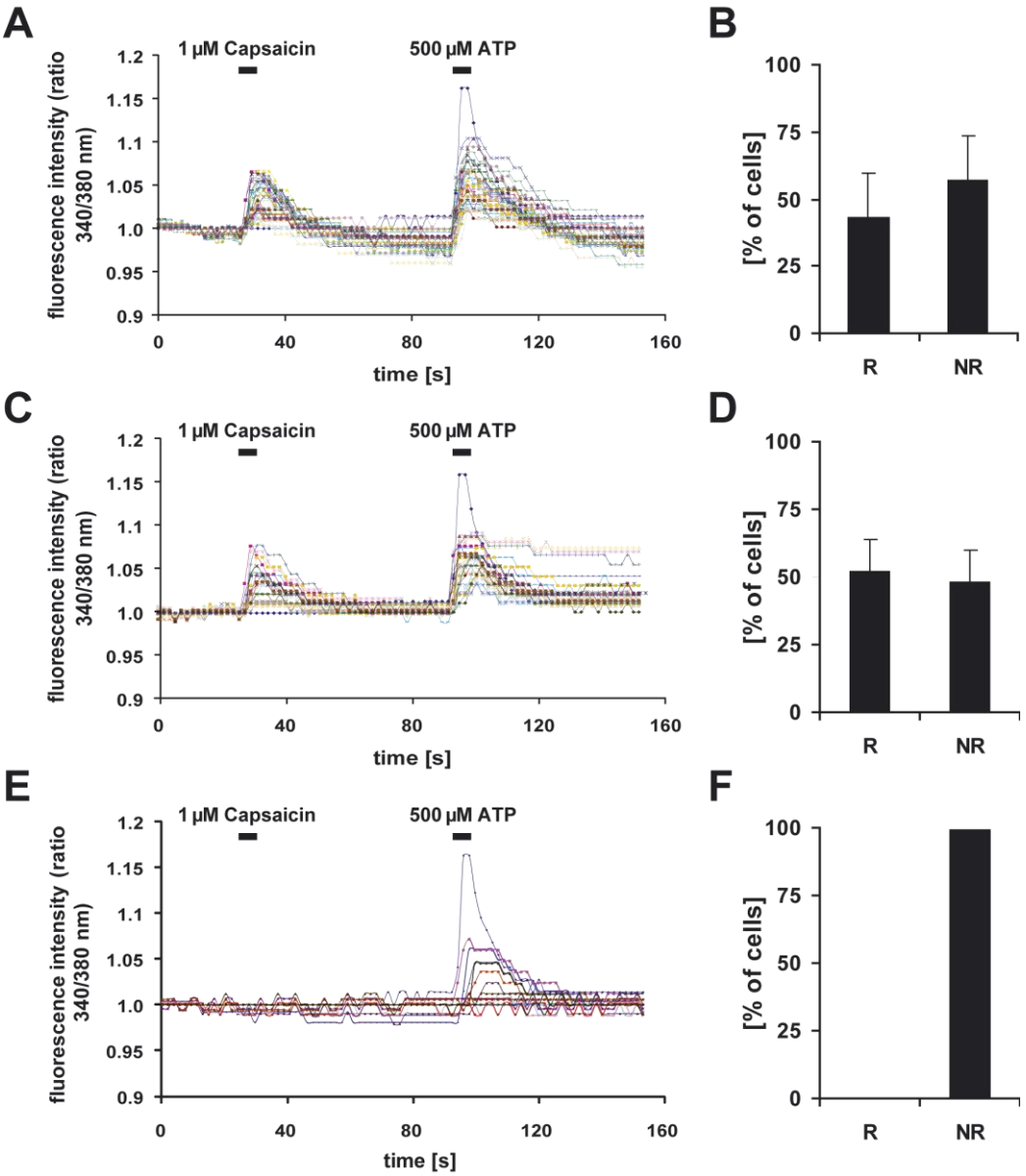

Fig. 4.6 TRPV1 on NPCs from SVZ and SGZ is functional

Functionality of TRPV1 is tested by calcium imaging to detect an increase of the intracellular calcium concentration upon TRPV1 activation. Therefore, NPCs from TRPV1 wildtype and from TRPV1 knockout animals are exposed to capsaicin, the specific agonist on TRPV1 channels, and the fluorescence intensity ratio 340/380 nm is measured. The following protocol is applied: 25 s buffer - 5 s 1 µM capsaicin – 60 s buffer - 5 s 500 µM ATP - 60 s buffer. The calcium signal is exclusively detected in TRPV1 wildtype NPCs from SVZ (A, B) and SGZ (C, D) and absent in TRPV1 knockout cultures (E, F). Calcium imaging was performed on NPCs SVZ (n = 528 cells / 12 coverslips), NPCs SGZ (n = 668 cells / 16 coverslips) and NPC TRPV1 knockout SGZ (n= 101 cells / 6 coverslips). The fraction of responding cells was analyzed and referred to cells responding to ATP. About half of both cell populations respond to 1 µM capsaicin. R: responders, NR non-responders.

For SVZ NPCs 43.2 ± 16.5 % responded to 1 µM capsaicin (Fig. 4.6 A, B) and for SGZ NPCs 51.8 ± 11.7 % showed an increase in the intracellular calcium concentration (Fig. 4.6 C, D). TRPV1 knockout NPCs did not respond to capsaicin application (Fig. 4.6 E, F).

4.1.3. Loss of TRPV1 in postnatal NPCs changes their properties

In order to assess the effect of TRPV1 expression in cultured NPCs, I studied the growth features of TRPV1 wildtype and knockout cultures. For that reason, freshly isolated NPCs were cultured in cultivation medium including growth factors (20 ng/µl EGF and 20 ng/µl FGF-2, proliferating conditions). TRPV1 knockout NPCs formed a remarkably higher number of spheres which were bigger than wildtype ones (Fig. 4.7 A-D). Interestingly, clonal efficiency analysis showed, that the sphere formation capacity (Fig. 4.7 E, F), i.e. the cell density needed to form secondary spheres, was not affected by TRPV1 knockout (n = 3). To investigate the growth curve, 500 000 cells were replated in a 10 cm-dish after each subculturing passage in cultivation medium and the proliferation rate was plotted (Fig. 4.7 G-H). The average growth factor per passage is increased in both TRPV1 knockout cell populations (n = 3): SVZ (TRPV1 ko: 8.35 ± 6.19; TRPV1 wt: 4.98 ± 2.88; ** for $p < 0.01$), SGZ (TRPV1 ko: 9.94 ± 6.90; TRPV1 wt: 5.32 ± 3.04; * for $p < 0.05$ Mann-Whitney-U test).

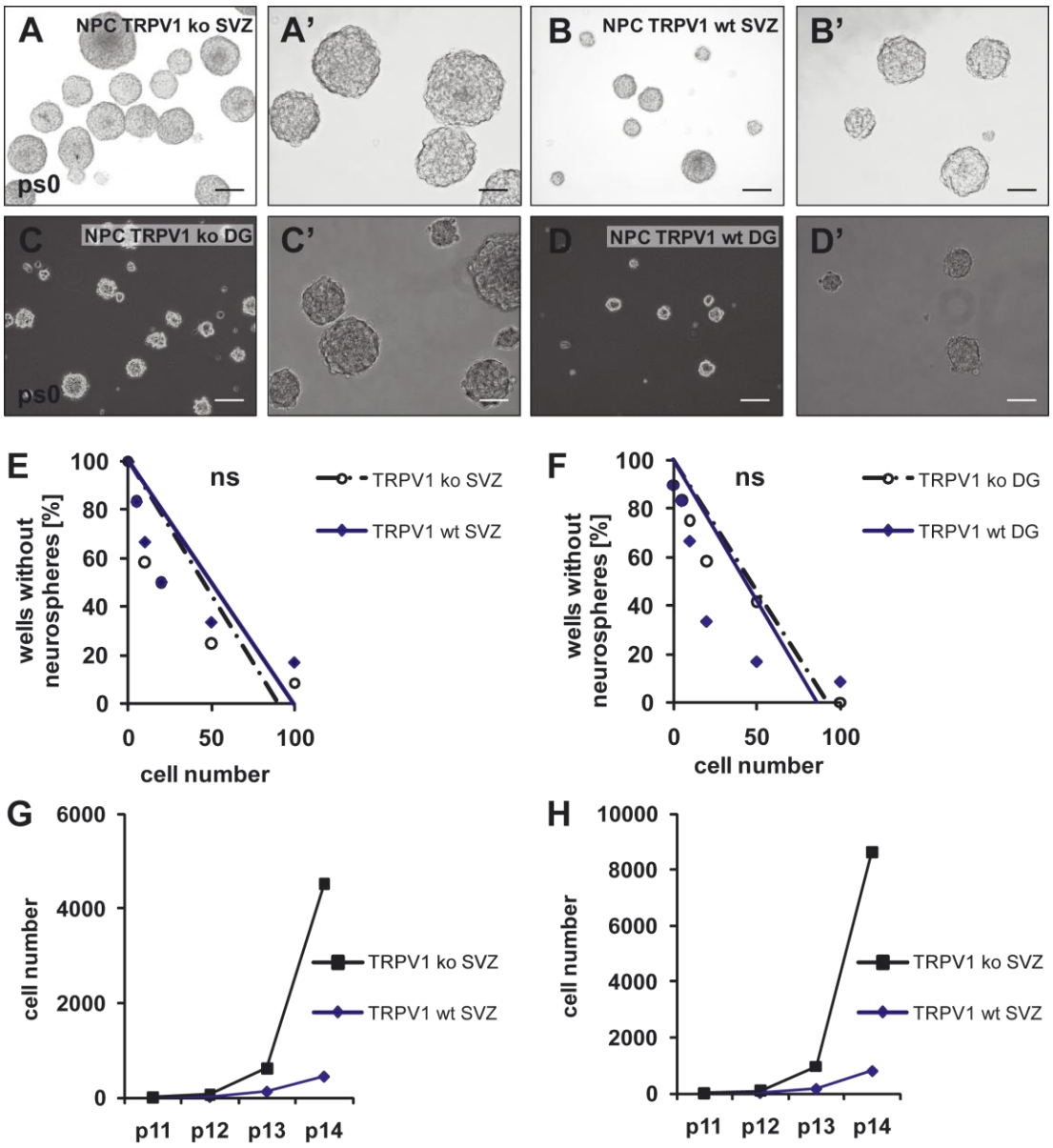

Fig. 4.7 TRPV1 knockout NPCs show a higher proliferation rate than wildtype cells

TRPV1 wildtype and knockout NPCs from SVZ (A, B) and SGZ (C, D) are cultured under proliferating condions for one week. TRPV1 knockout cells show an increased sphere size compared to wildtype cells. Cells are plated at limiting dilution in 200 µl volume of medium to investigate the sphere forming capacity of wildtype and knockout cells from SVZ (E) and SGZ (F). The mean x-intercept values calculated from limiting dilution analysis reveal that the number of cells required to form at least one neurosphere/well is not changed in TRPV1 knockout NPCs. TRPV1 wildtype and knockout NPCs from SVZ (G) and SGZ (H) are cultured under proliferating condions. Four passages exemplify the effect of the TRPV1 knockout on the proliferation of NPCs. TRPV1 knockout NPCs show a significantly increased proliferation (NPC SVZ: * for $p < 0.05$; NPC SGZ ** for $p < 0.01$, Mann-Whitney-U test). Scale bars: 100 µm (A-D), 50 µm (A'-D').

After investigating the proliferating properties of TRPV1 knockout NPCs, I studied the differentiating capacities. Therefore, NPCs were cultured adherently in cultivation medium without growth factors including 0.1 % FCS (differentiating conditions) for two weeks and gene expression was analyzed in qRT-PCR (n = 3). TRPV1 knockout NPCs showed a significantly reduced expression of the astrocytic markers glial fibrillary acidic protein (GFAP, 0.30 ± 0.04 fold expression, relative to wildtype) and S100 calcium binding protein B (S100b, 0.29 ± 0.11) as well as the neuronal marker beta-3-tubulin (b3Tub, 0.30 ± 0.13). Additionally, the stem cell markers Nestin (1.68 ± 0.10) and sex determining region Y-box 2 (Sox2, 1.71 ± 0.07) were increased (Fig. 4.8).

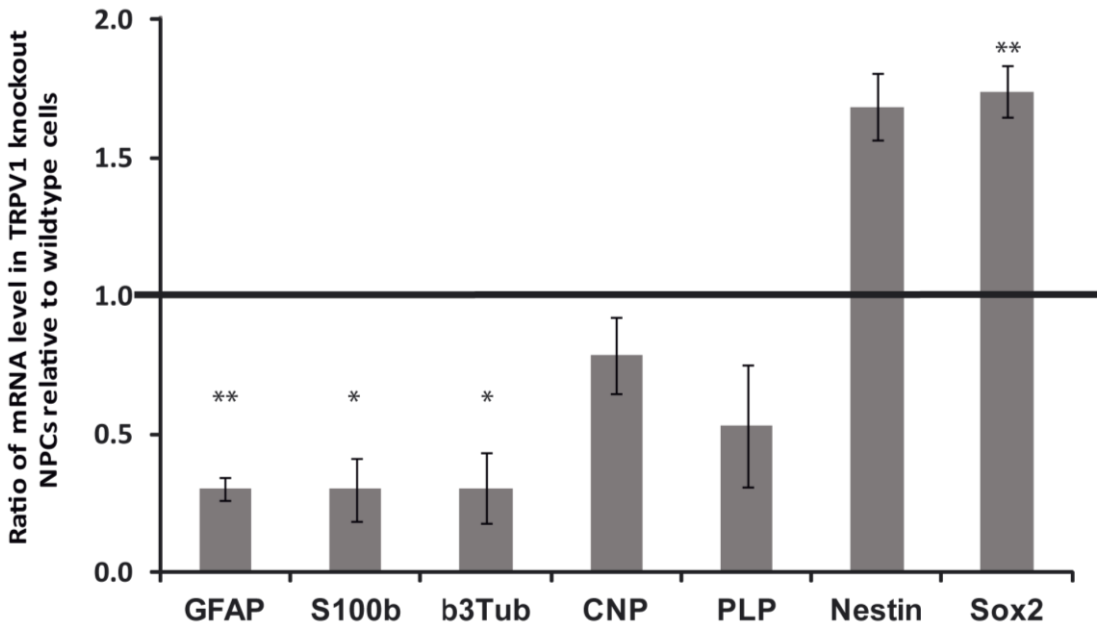

Fig. 4.8 TRPV1 modulates differentiation

TRPV1 wildtype and knockout NPCs are differentiated for two weeks and expression levels of differentiation markers are analyzed by qRT-PCR. Values are normalized to beta-actin controls. The graph shows the TRPV1 knockout expression pattern relative to wildtype NPCs. Significances: * for $p < 0.05$, ** for $p < 0.01$, t-test.

4.1.4. NPCs express TRPV1 channels *in vivo* during postnatal neurogenesis

After the finding that NPCs which are lacking the TRPV1 channel show an increased proliferation and sphere size, I investigated the TRPV1 knockout *in vivo*.

Due to an increased stem cell activity during postnatal neurogenesis, brain slices from p21 Nestin-GFP mice were prepared. The tissue containing SVZ was stained for TRPV1 expression along the lateral ventricle (n = 6).

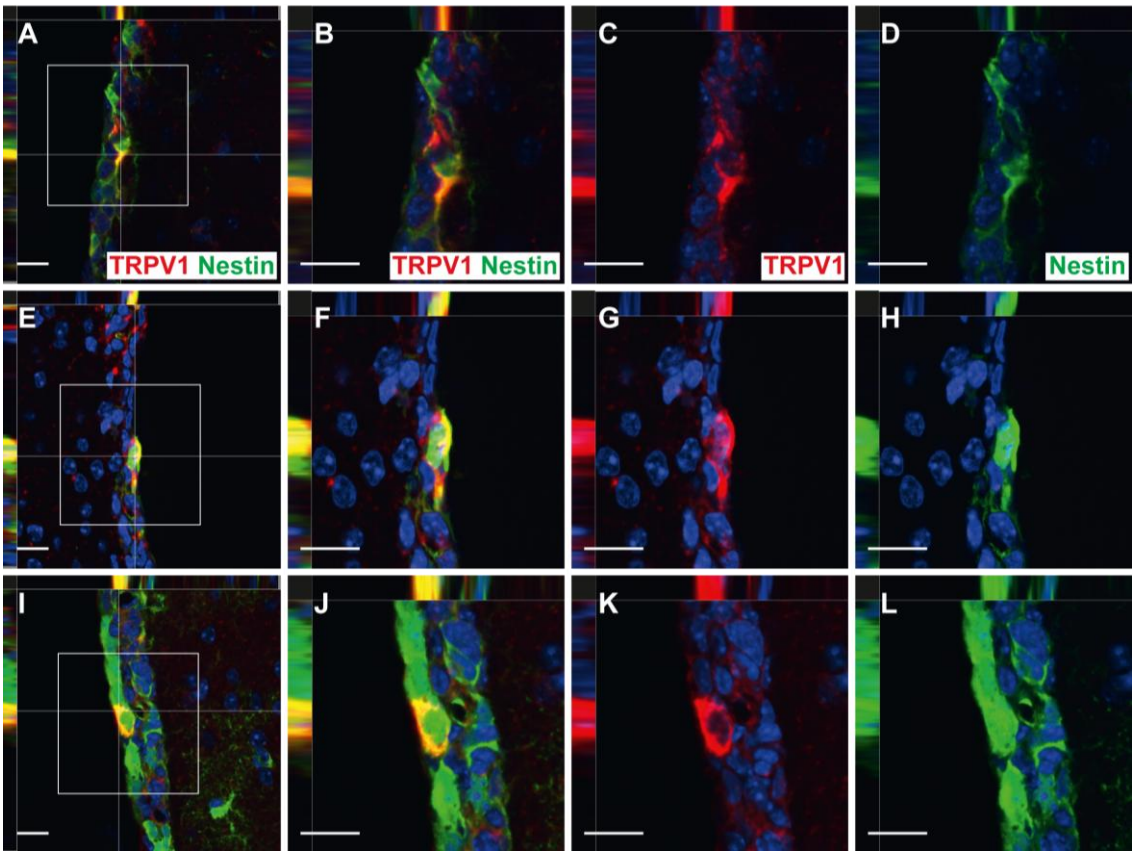

Fig. 4.9 TRPV1 is expressed in the SVZ during postnatal neurogenesis

Brain sections from p21 Nestin-GFP mice are stained for TRPV1 (red) and Nestin-GFP (green) (A, E, I). Nestin^{+} neural precursors in the SVZ are partially stained for TRPV1. Double-positive cells are magnified in (B-D), (F-H) and (J-L). Nuclei are counterstained with DAPI (blue). Scale bars: 50 µm (A, E, I), 20 µm (B-D, F-H, J-L). Colocalization is confirmed by confocal microscopy orthogonal view.

Representative example pictures from p21 Nestin-GFP mice show that a subpopulation of Nestin$^+$ NPCs expressed TRPV1 in the SVZ during postnatal neurogenesis *in vivo* (Fig. 4.9).

Since both stem cell niches are active postnatally, I also investigated the dentate gyrus of the hippocampus for TRPV1 expression in NPCs (n = 6).

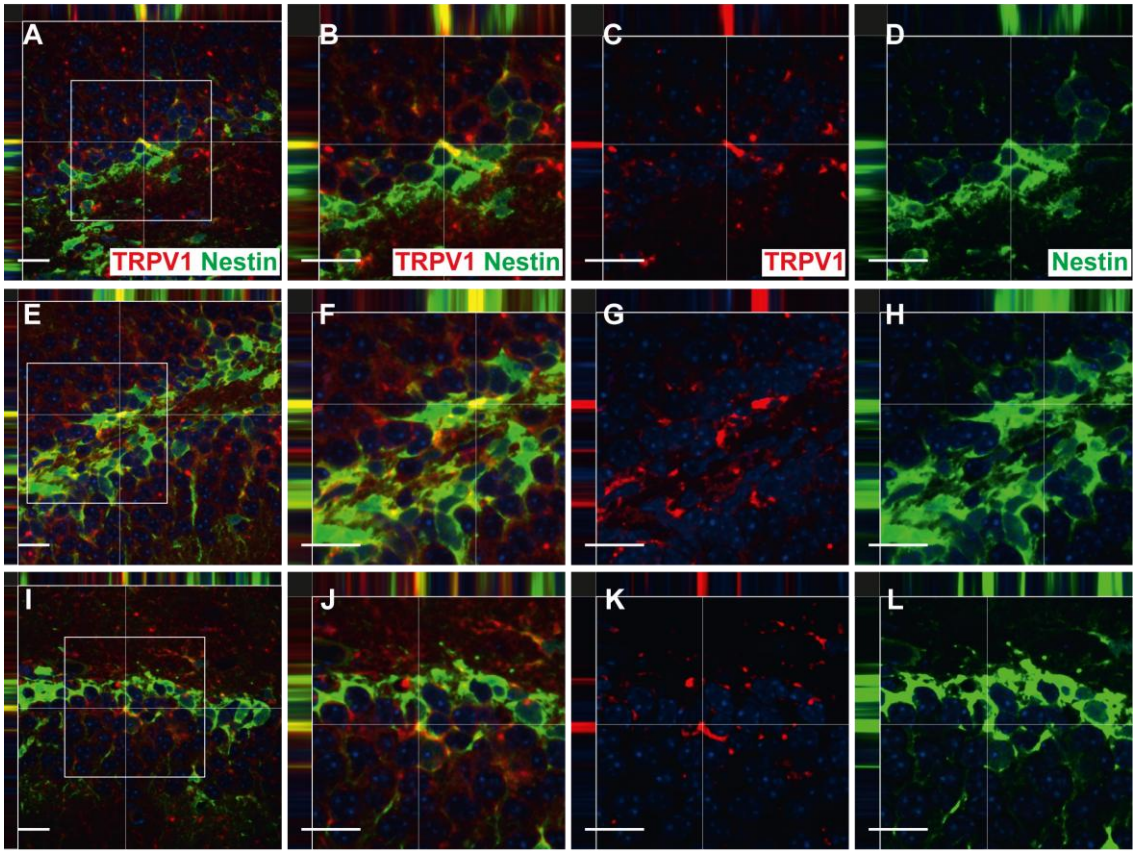

Fig. 4.10 TRPV1 is expressed in the dentate gyrus during postnatal neurogenesis

Hippocampal brain sections from postnatal Nestin-GFP animals (p21) are stained for TRPV1 (red) and Nestin-GFP (green) (A, E, I). Nestin$^+$ neural precursors are partially stained for TRPV1 in the dentate gyrus. Double-positive cells are magnified in (B-D), (F-H) and (J-L). Nuclei are counterstained with DAPI (blue). Scale bars: 50 µm (A, E, I), 20 µm (B-D, F-H, J-L). Colocalization is confirmed by confocal microscopy orthogonal view.

TRPV1 expression *in vivo* in the postnatal dentate gyrus is shown by immunostainings in coronal brain sections. There was a low expression of TRPV1 in the stem cell niche,

which colocalizes either with Nestin$^+$ NPCs (Fig. 4.10) or Parvalbumin$^+$ interneurons (Fig. 4.11).

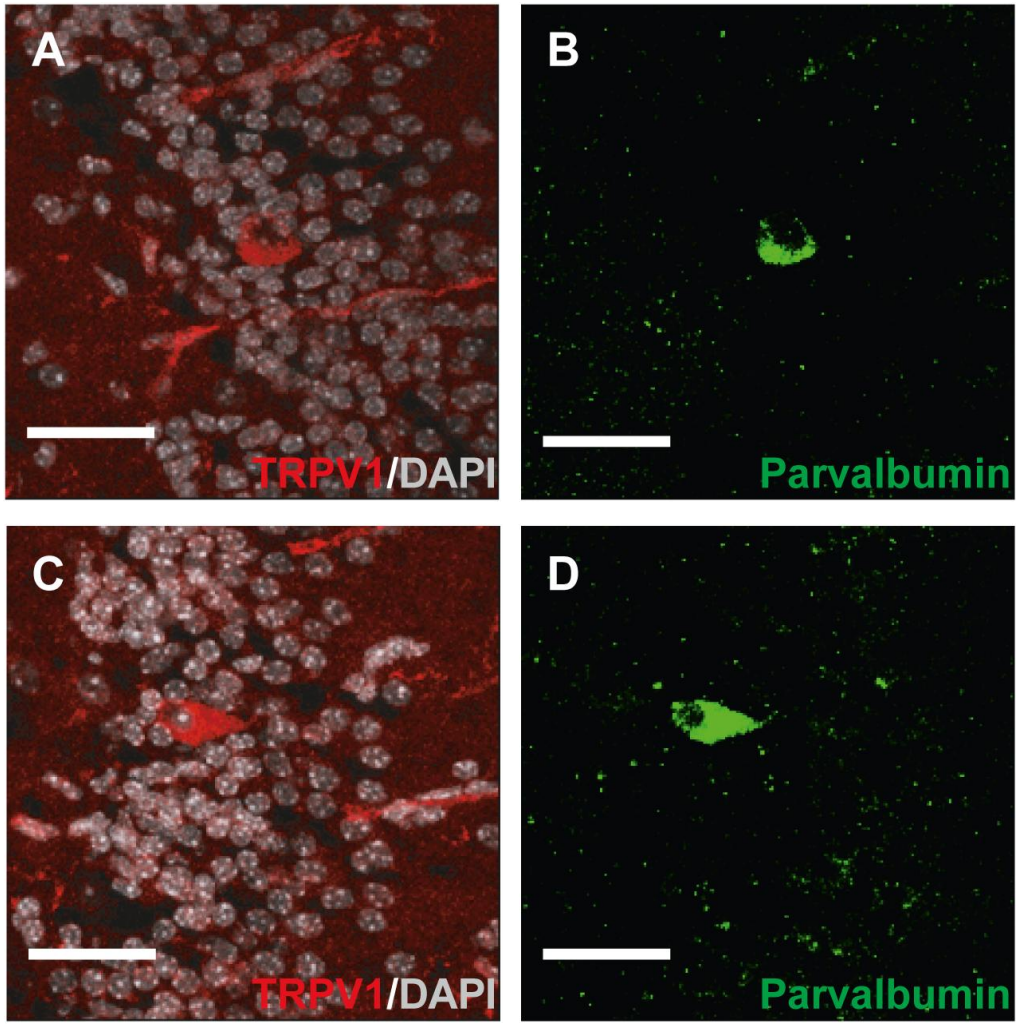

Fig. 4.11 TRPV1 is expressed in interneurons in the dentate gyrus *in vivo*

Brain sections from hippocampus are stained for TRPV1 (red), Parvalbumin (blue) and DAPI (gray). TRPV1 is expressed by Parvalbumin$^+$ interneurons in the dentate gyrus. Two examples are shown in (A, B) and (C, D). Scale bars: 20 µm.

Furthermore, TRPV1 was detected for example in the cortex and striatum (not shown). This is in agreement with previous studies [Mezey et al., 2000; Liapi and Wood, 2005; Toth et al., 2005; Cristino et al., 2006].

4.1.5. Loss of TRPV1 *in vivo* affects the neurogenic niches in postnatal neurogenesis

To test the proliferation of NPCs *in vivo*, TRPV1 wildtype and knockout mice were perfused at different time points (p7, p14, p21 and p39) and the brains were removed and cut into horizontal slices. The brain slices were stained for the proliferation marker Ki67 ($n \geq 3$). Proliferation could be observed in the neurogenic regions of the adult brain, the SVZ and the SGZ of the dentate gyrus of the hippocampus (Fig. 4.12).

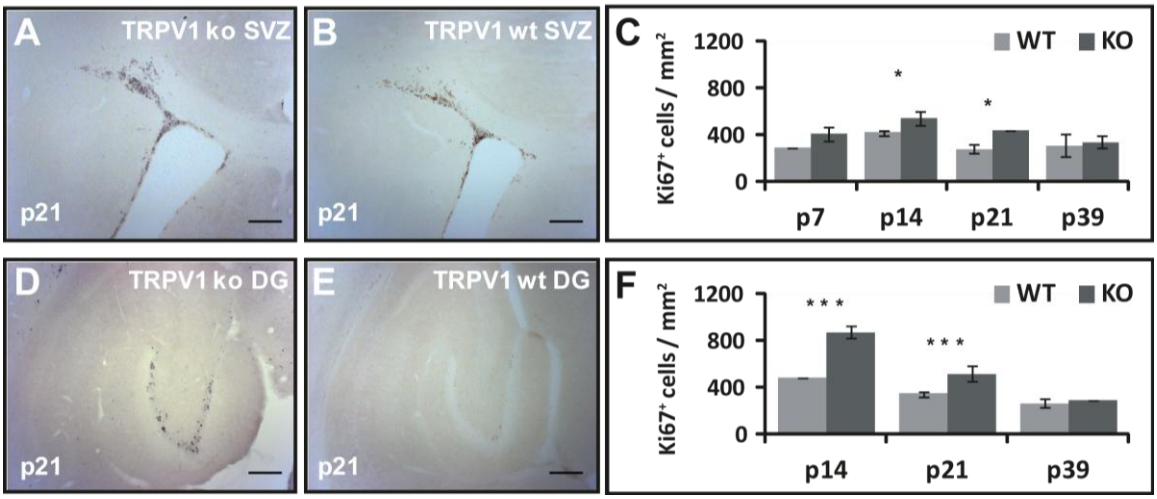

Fig. 4.12 TRPV1 knockout mice show an increased proliferation in the SVZ and dentate gyrus

(A, B, D, E) Brain slices from TRPV1 wildtype and knockout animals are stained for the proliferation marker Ki67 and the proliferation in SVZ and dentate gyrus (DG) is analyzed. TRPV1 knockout mice show an increased proliferation in both neurogenic areas. Quantification of proliferation in SVZ and DG is shown in (C) and (F). Light gray bars show TRPV1 wildtype, dark gray bars TRPV1 knockout mice. The increased proliferation in TRPV1 knockout mice is age-dependant. Scale bars: 200 µm (A, B, D, E). Significances shown: * for $p < 0.05$, *** for $p < 0.001$, t-test.

TRPV1 knockout mice showed also an increased proliferation *in vivo*. Interestingly, this effect was only observed up to postnatal day 21 and correlates with the proliferation processes occurring during neurogenesis in the postnatal brain.

4.1.6. Physiological stimulation of adult neurogenesis is modulated by TRPV1 channels

Since TRPV1 presence or absence had an effect on postnatal neurogenesis, I wanted to investigate whether TRPV1 knockout has an impact on spatial memory, which is closely associated with hippocampal neurogenesis [Kempermann, 2002]. Therefore, adult TRPV1 wildtype and knockout mice were tested in Morris water maze (MWM; n = 10) [Morris et al., 1982; Wolfer et al., 1997]. For this experiment, the animals were set into a pool filled with water and needed to find a hidden platform (P1) by orienting themselves in space using cues in the room. The experiment is subdivided into three phases: 1. acquisition (day 1-3), 2. probe trial (day 4), 3. reversal (day 4-5). The experimental setup is schematically shown in Fig. 4.13 F.

TRPV1 knockout mice showed significantly higher learning slopes during the acquisition from day one to two ($p = 0.004$) and from day one to three ($p = 0.037$) as well as the reversal phase ($p = 0.014$, Fig. 4.13 A). The statistical analysis revealed a trend for the overall performance especially during hippocampus associated reversal as well (latency: training phase $p = 0.996$, reversal $p = 0.181$ (Fig. 4.13 A); distance: training phase $p = 0.395$, reversal 0.366 (Fig. 4.13 B)). There was no significant difference for the swimming distance to reach the platform (Fig. 4.13 B). TRPV1 knockout mice show a significantly reduced swim speed as compared to wildtypes (training $p < 0.001$; reversal $p < 0.001$; Fig. 4.13 C). Furthermore, the time the animals spent immobile during the task was significantly higher in the knockout group (training $p < 0.001$; reversal $p < 0.001$; Fig. 4.13 D). Next, the path efficiency of the animals was investigated, which is how efficient an animal is at getting to the platform zone. Ideal path efficiency would have a value of one. TRPV1 knockout mice performed better in the training phase ($p = 0.011$) but not in the reversal ($p = 0.425$; Fig. 4.13 E).

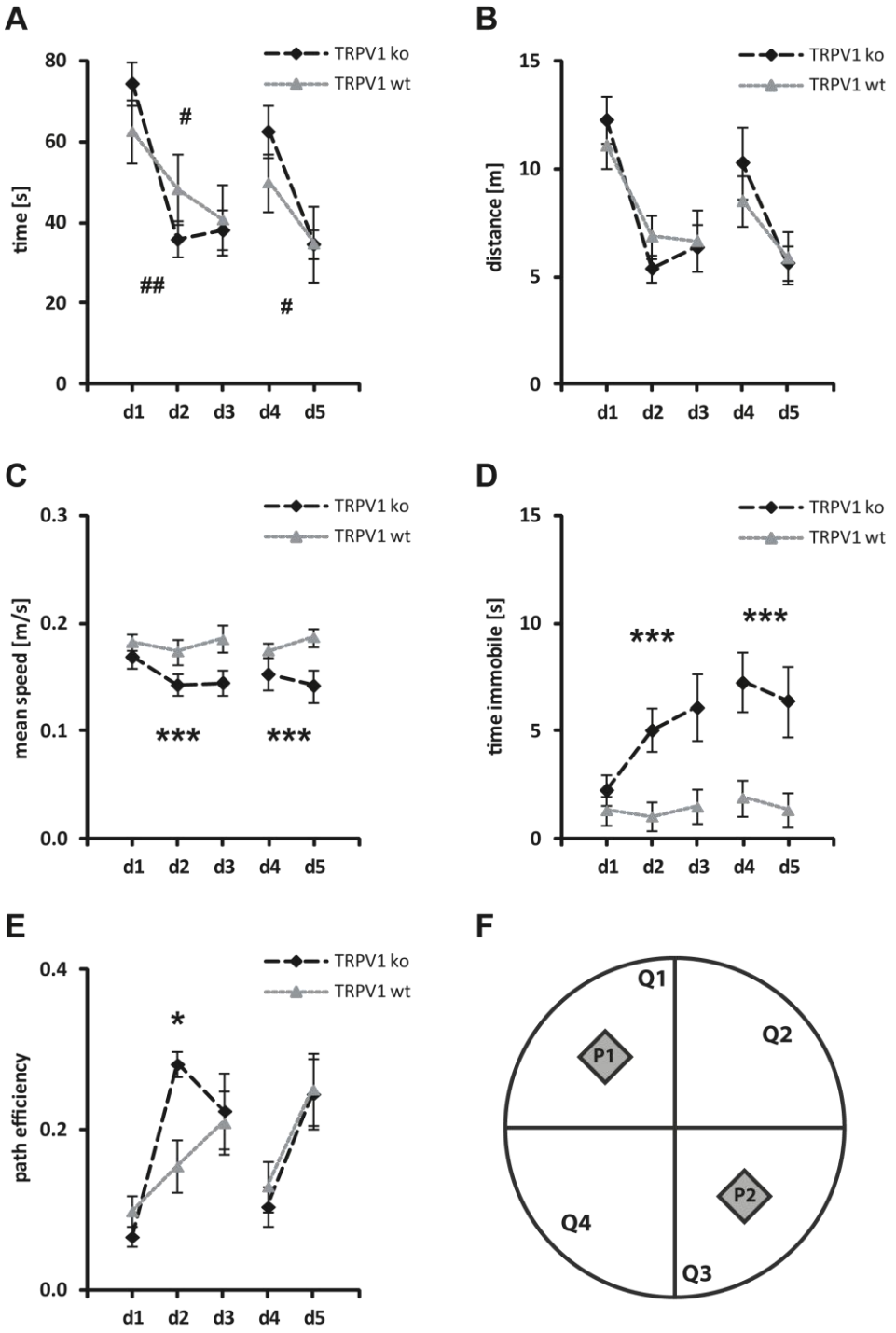

Fig. 4.13 TRPV1 knockout mice show differences in spatial learning

TRPV1 wildtype and knockout animals are tested for spatial memory in the Morris water maze task. TRPV1 knockout mice show steeper learning slopes in time (A) and distance to reach the platform (B). They apply a different search strategy compared to wildtype mice as seen in mean speed (C), immobility time (D) and path efficiency of the animals (E). The setup of the water maze tank is shown schematically in (F). Significances shown: * for $p < 0.05$, *** for $p < 0.001$, Repeated Measures ANOVA; $^{\#}$ for $p < 0.05$, $^{\#\#}$ for $p < 0.01$ for slopes, t-test.

In the second phase, a probe trial without a platform was done at day 4. Here, the entries into the platform zone during the trial were investigated (Fig. 4.14 A). TRPV1 knockout mice entered this area significantly more often compared to wildtype animals ($p < 0.05$).
In the third part of the MWM, the hidden platform was put into another position (reversal learning, P2). Here, the knockout mice spent significantly less time in the new quadrant (Q3) compared to the former platform quadrant (Q1) during the first day of reversal learning ($p < 0.01$; Fig. 4.14 B).

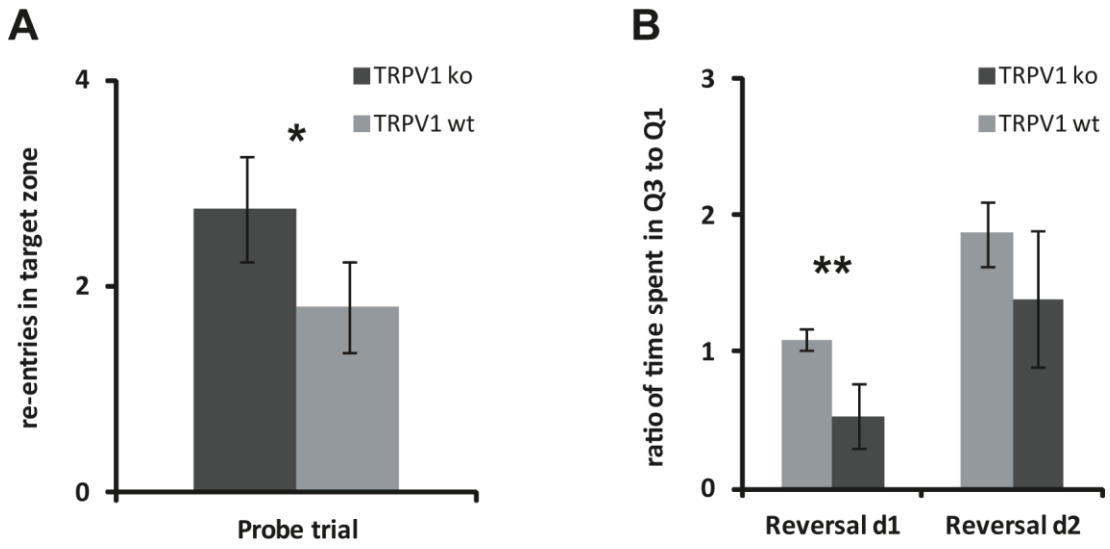

Fig. 4.14 Morris water maze performance

Spatial memory of TRPV1 wildtype and knockout animals is tested in the Morris water maze task. TRPV1 knockout mice are more effective in discriminating the previously trained zone as they re-enter the former platform zone significantly more often than wildtype mice (A). In the reversal, knockout mice persist longer in searching in the previous platform quadrant at day 1, but aquire the task at day two to the same level than wildtype mice (B). Significances shown: * for $p < 0.05$, ** for $p < 0.01$, Mann-Whitney-U test.

To exclude an impact of different motor coordination abilities of the mice, I tested TRPV1 wildtype and knockout animals on the Rota-Rod [Jones and Roberts, 1968]. During this task the mice need to walk continuously on an accelerating rotating wheel and need to

show motor coordination and balance to prevent falling from the rod. They are placed on the slowly turning rod, which is high enough that the animals try to avoid falling down. The rod is accelerating and the latency to fall is a measure of their balance, physical condition and motor function (Fig. 4.15).

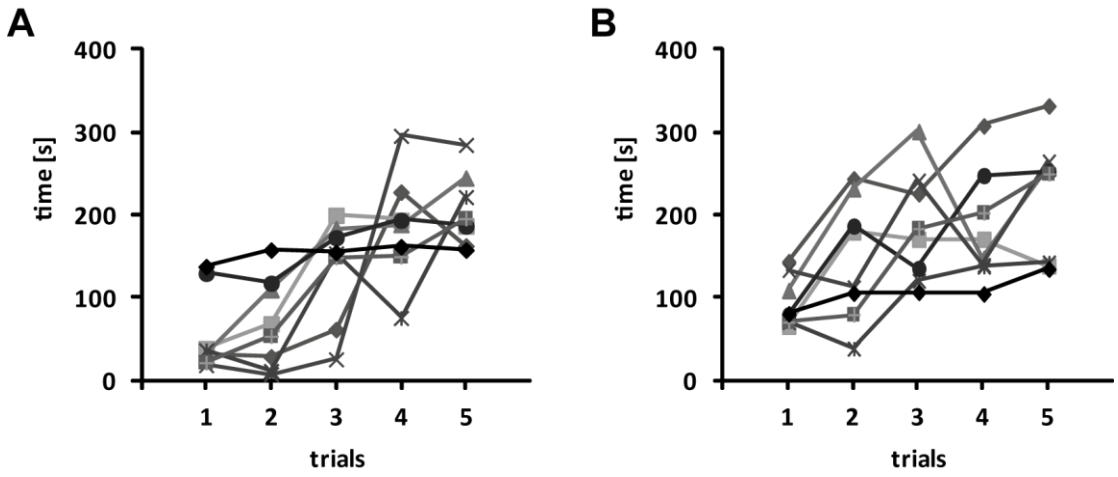

Fig. 4.15 The motor coordination and balance abilities are not affected by TRPV1 knockout

The Rota-Rod test is a behavioral task assessing motor coordination performance. The mice are set on an accelerating rod and the latency to fall is monitored. Both, TRPV1 wildtype (A, $p < 0.001$) and knockout animals (B, $p < 0.001$) learn to stay on the Rota-Rod over time. There is no significant difference in the performance between the groups ($p = 0,09$). Repeated Measures ANOVA.

TRPV1 knockout mice show no differences in motor coordination and balance in comparison to wildtypes in the Rota-Rod test ($n = 8$) (Fig. 4.15). So, the different performances in the water maze are not due to motor coordination problems of the animals.

Since hippocampal neurogenesis is associated with improved spatial learning and memory which can be tested in the MWM task [Kempermann, 2002], I studied the hippocampal neurogenesis in adult TRPV1 wildtype and knockout mice with spatial

learning task (MWM) and without stimulation. The animals received three i.p. BrdU injections during the last three days of the MWM and were analyzed four weeks later.

First of all, TRPV1 expression in the dentate gyrus was investigated. TRPV1 expression *in vivo* is shown by immunostainings in coronal brain sections (n = 3) (Fig. 4.16).

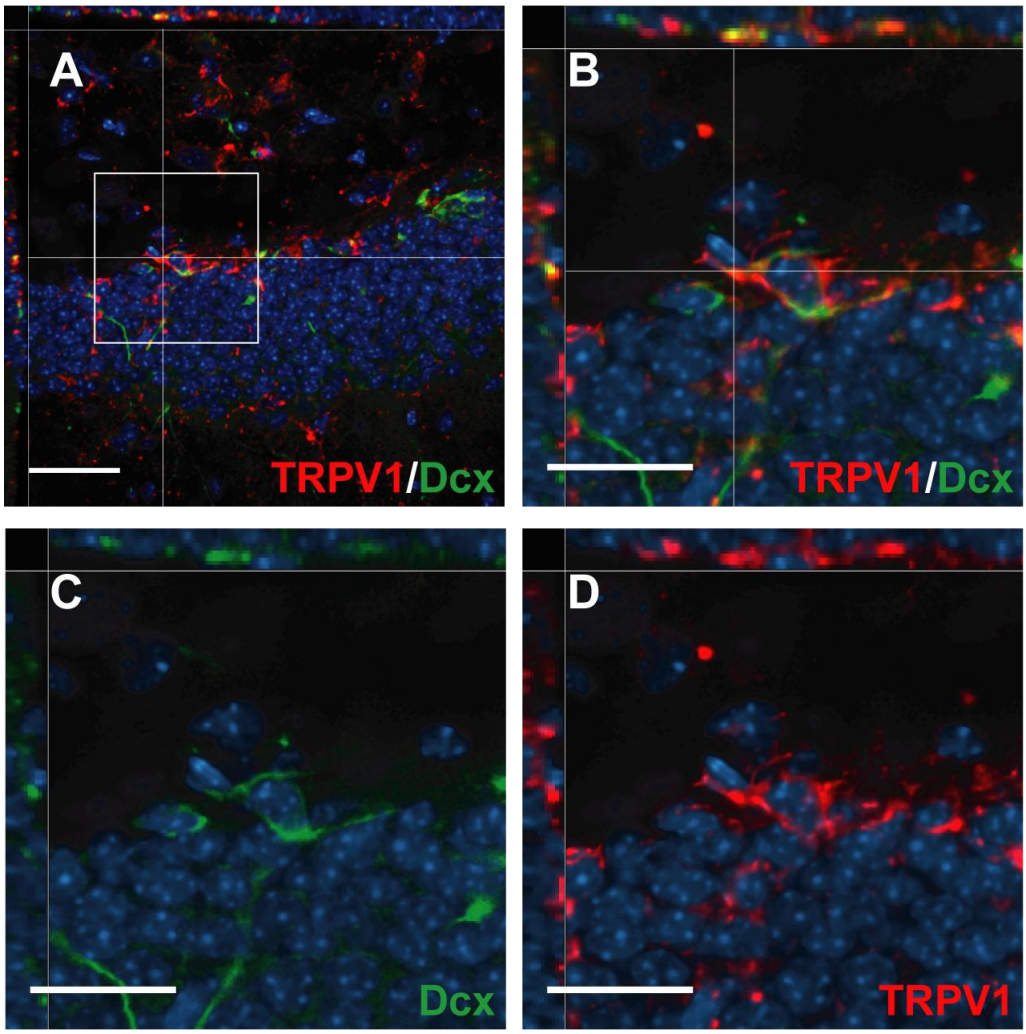

Fig. 4.16 TRPV1 is expressed after physiological stimulation of neurogenesis in NPCs *in vivo*

TRPV1 wildtype brain sections from hippocampus are stained for TRPV1 (red) and Dcx (green) (A). Dcx-positive neural precursors are partially stained for TRPV1. A double-positive cell is magnified in (B-D). Nuclei are counterstained with DAPI (blue). Scale bars: 50 µm (A), 20 µm (B-D). Colocalization is confirmed by confocal microscopy orthogonal view.

There was a low expression of TRPV1 in the dentate gyrus, which colocalizes with Doublecortin$^+$ (Dcx$^+$) NPCs.

After ensuring that TRPV1 is expressed in NPCs after MWM, the number of BrdU$^+$ cells four weeks after injection was examined.

Adult TRPV1 wildtype and knockout mice showed no difference in cell survival of BrdU$^+$ proliferating cells in the SVZ and dentate gyrus under baseline conditions without any stimulus (n = 4). Cell numbers were counted four weeks after BrdU injection in SVZ (BrdU$^+$: wildtype: 100 ± 5 %; knockout: 85 ± 67 %) and SGZ (BrdU$^+$: wildtype: 100 ± 67 %; knockout: 102 ± 69 %; normalized to wildtype) (Fig. 4.17 A). As well, the acquired phenotype of BrdU$^+$ cells did not change significantly between TRPV1 wildtype (BrdU$^+$: 13 ± 3 %; BrdU$^+$/Dcx$^+$: 20 ± 2 %; BrdU$^+$/NeuN$^+$: 67 ± 1 %) and knockout animals (BrdU$^+$: 13 ± 5 %; BrdU$^+$/Dcx$^+$: 24 ± 7 %; BrdU$^+$/NeuN$^+$: 63 ± 3 %) (Fig. 4.17 B).

However, after performing the learning task (MWM), TRPV1 knockout mice showed a significant increase in BrdU$^+$ cells in the SGZ of the dentate gyrus of the hippocampus (wildtype: 100 ± 27 %; knockout: 141 ± 22 %; normalized to wildtype; n = 5), which resembles the increased proliferation in postnatal neurogenesis shown in Fig. 4.12. As expected, there was no difference in BrdU$^+$ cells in the SVZ, because it is known that the MWM task affects only hippocampal neurogenesis [Kempermann, 2002] (wildtype: 100 ± 30 %; knockout: 102 ± 15 %; normalized to wildtype) (Fig. 4.17 C). Furthermore, there was no change in the phenotype of BrdU$^+$ cells between TRPV1 wildtype (BrdU$^+$: 14 ± 0 %; BrdU$^+$/Dcx$^+$: 8 ± 3 %; BrdU$^+$/Dcx$^+$/NeuN$^+$: 17 ± 7 %; BrdU$^+$/NeuN$^+$: 61 ± 4 %) and knockout animals (BrdU$^+$: 15 ± 1 %; BrdU$^+$/Dcx$^+$: 8 ± 3 %; BrdU$^+$/Dcx$^+$/NeuN$^+$: 17 ± 10 %; BrdU$^+$/NeuN$^+$: 60.0 ± 6 %) (Fig. 4.17 D). A representative series of stainings is shown in Fig. 4.17 E-H.

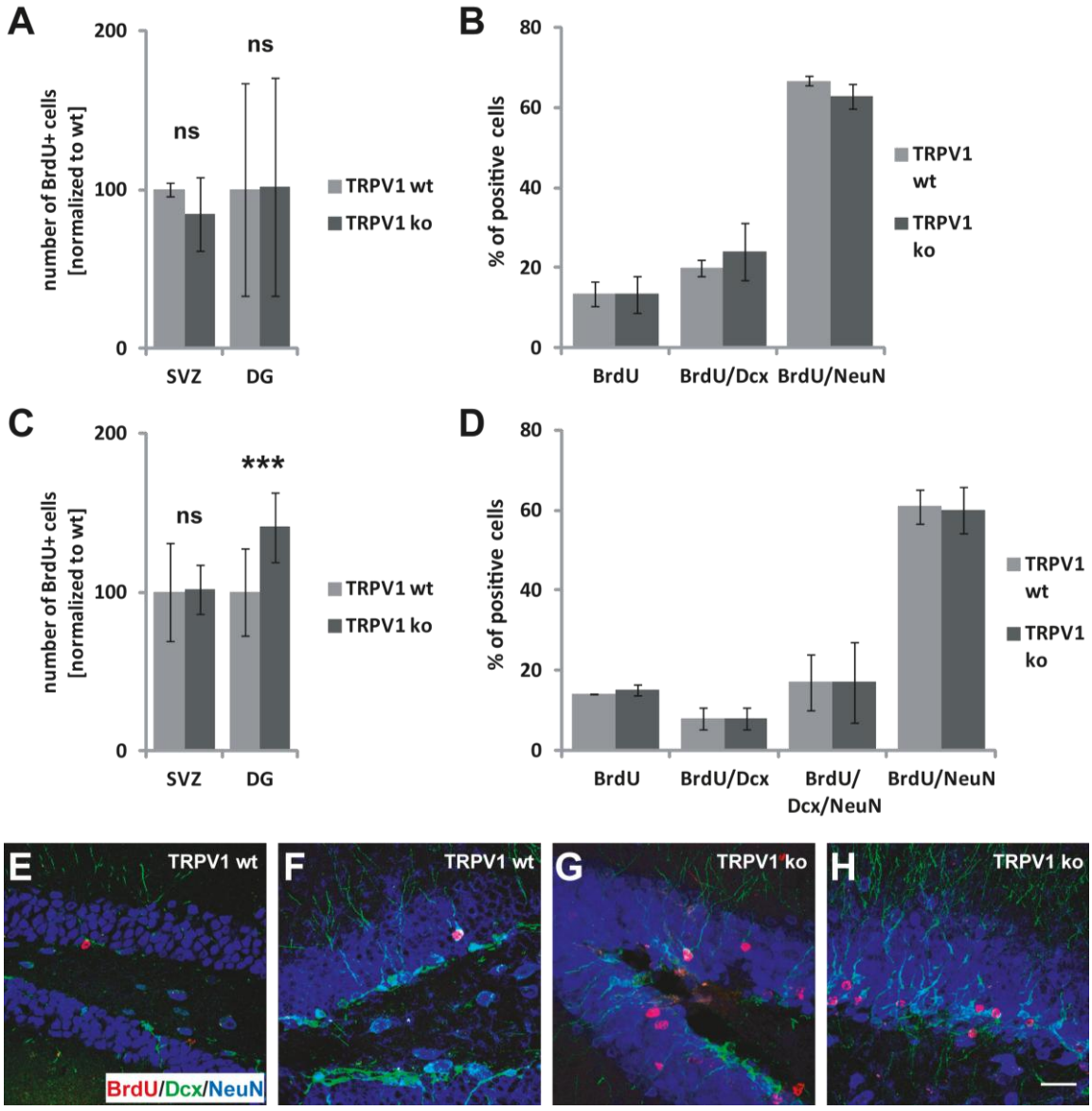

Fig. 4.17 TRPV1 knockout mice show an increased neurogenesis after spatial learning

Adult TRPV1 wildtype and knockout mice received three BrdU injections. After four weeks, the animals were perfused, stained for BrdU and survival of dividing cells in the SVZ and dentate gyrus was analyzed. There is no difference in the numbers of surviving $BrdU^+$ cells (A), as well as the phenotype (B). After performing the spatial learning task (MWM), TRPV1 knockout mice show significantly more surviving $BrdU^+$ cells as compared to wildtype (C). However, the phenotype of cells is not altered (D). Example pictures of BrdU double-positive cells from TRPV1 wildtype (E, F) and knockout (G, H) animals after performing MWM are shown. Scale bar: 100 µm (E-H). Significances shown: *** for $p < 0.001$, t-test.

To conclude, TRPV1 is expressed in NPCs *in vitro* and *in vivo*. Loss of TRPV1 expression resulted in an increase in proliferation and survival of NPCs, leading to a larger pool of stem cells. Mice lacking TRPV1 expression performed better in MWM, although they were less flexible after a paradigm shift of the task. Additionally, they pursued a different strategy in the water maze. Furthermore, TRPV1 knockout mice showed an increase in hippocampal neurogenesis after fulfilling the task. However, the increase in proliferation did not alter the differentiation paradigm of the cells.

4.2. Neural precursor cells induce cell-death of high-grade astrocytomas via stimulation of TRPV1

4.2.1. Human primary NPCs and human primary glioblastoma cells express TRPV1

As shown in the first part of the study, mouse NPCs express TRPV1 channels to modulate neurogenesis. Additionally, it was found by our group that mouse high-grade astrocytoma cells (GL261) express TRPV1. So, I wanted to investigate the expression of TRPV1 in both cell types in the human system.

Therefore, primary human NPCs (huNPCs) and human glioblastoma cells (huGBMs) from resections of three independent patients were analyzed for TRPV1 expression on mRNA level (Fig. 4.18).

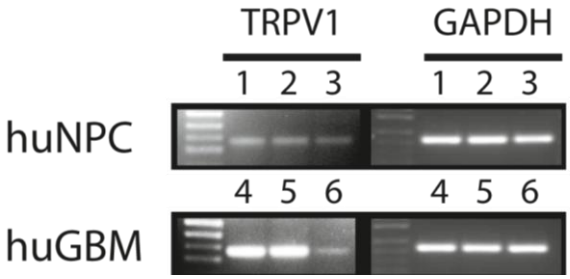

Fig. 4.18 TRPV1 is expressed in primary huNPCs and high-grade huGBMs
mRNA is isolated from huNPCs (upper pannel) and huGBMs (lower pannel) and transcribed into cDNA. Semiquantitative PCR shows TRPV1 expression in NPCs and glioma cells (left). GAPDH serves as loading control (right). huNPCs: 1-NPC-A, 2- NPC-B, 3- NPC-C. huGBMs: 4-GBM1, 5-GBM3, 6-GBM2.

All human NPCs and GBM cells expressed TRPV1 on mRNA level (n = 3). The housekeeping gene glyceraldehyde-3-phosphate dehydrogenase (GAPDH) served as loading control. There was a lower TRPV1 expression in NPCs, however also in GBMs, there are tumors with higher and lower expression of the receptor (Fig. 4.18).

4.2.2. NPC-released TRPV1-agonists induce glioma cell death

Neural precursor cells migrate to experimental gliomas *in vivo* and perform anti-tumorigenic actions [Glass et al., 2005; Walzlein et al., 2008; Chirasani et al., 2010]. Furthermore, NPCs secrete vanilloid factors like anandamide (see 4.1.1.). Therefore, I wanted to test whether soluble factors released by NPCs can act on glioma cells *in vitro*. HuGBM cells were plated, huNPC-conditioned medium (huNPC-CM) was added one day later and I studied the effect of this exposure.

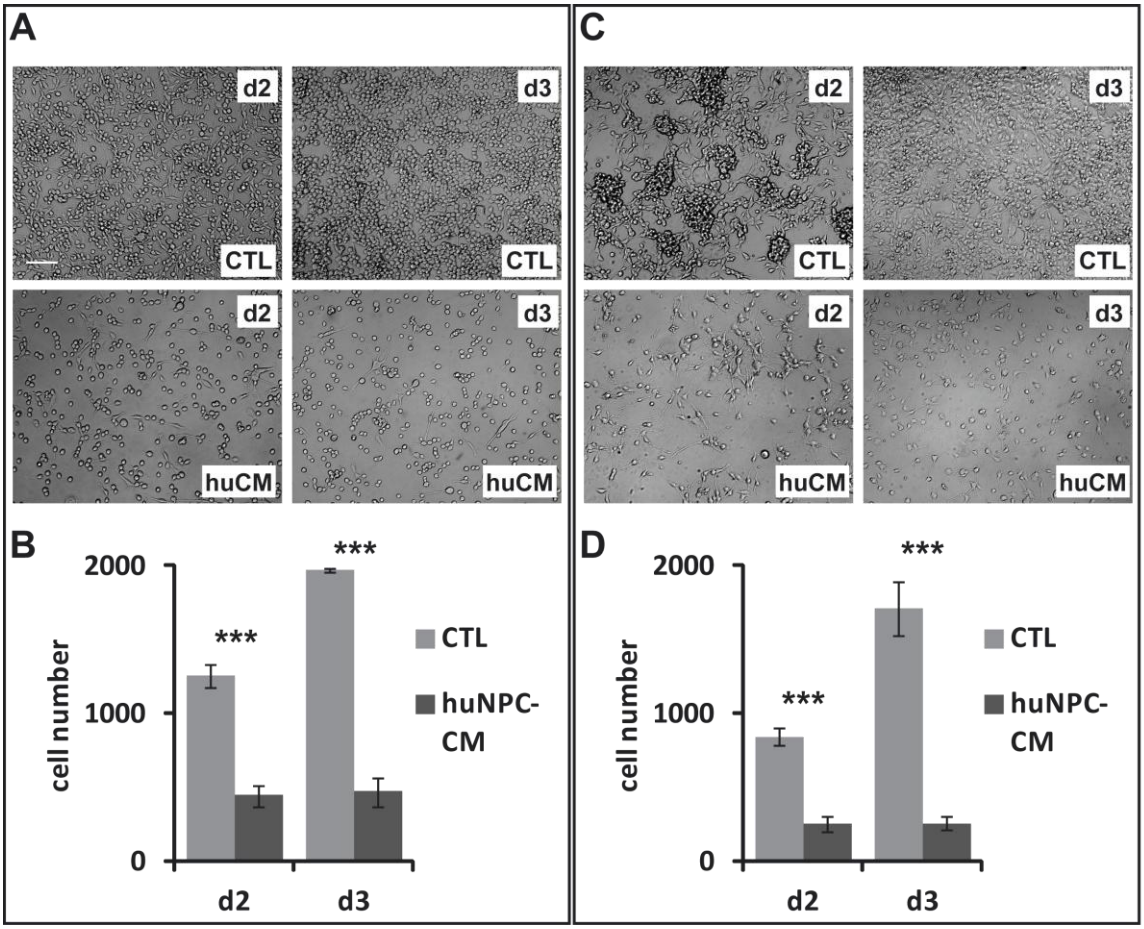

Fig. 4.19 HuNPC-CM causes decrease in number of huGBM cells

HuGBM cells are plated and one day later huNPC-CM is added. Exposure of GBM1 (A, B) and GBM2 cells (C, D) to CM leads to a significant decrease in cell numbers after two and three days of incubation as compared to control medium. Scale bar: 100 µm (A, C). Significances shown: *** for $p < 0.001$, t-test.

First of all, it was visible that the exposure to huNPC-CM led to a lower cell number after two and three days as compared to cells receiving control medium. GBM1-huGBM cells (Fig. 4.19 A, B) as well as GBM2-huGBM cells (Fig. 4.19 C, D) showed a significant reduction in counted cells for both time points (n = 3).

Furthermore, the signaling pathway that is activated by this exposure should be investigated. The cells were tested for the induction of cytotoxicity, i.e. a reduction in viability of the cells and an increase in cell death (n = 4) (Fig. 4.20). The assay was performed as a time course, investigating incubation with huNPC-CM for one day (d1), two days (d2) and three days (d3). After the exposure of huNPC-CM, cytotoxicity is strongly increased (dark gray bar), this effect could be blocked by capsazepine (CZP), a specific antagonist for TRPV1 channels (light gray bar). Capsazepine alone did not show cytotoxic effects (white bar). Cytotoxicity values are normalized to the negative control (NB medium) and shown as percentage of highest possible cytotoxicity of the cells (Digitonin-permeabilized, positive control).

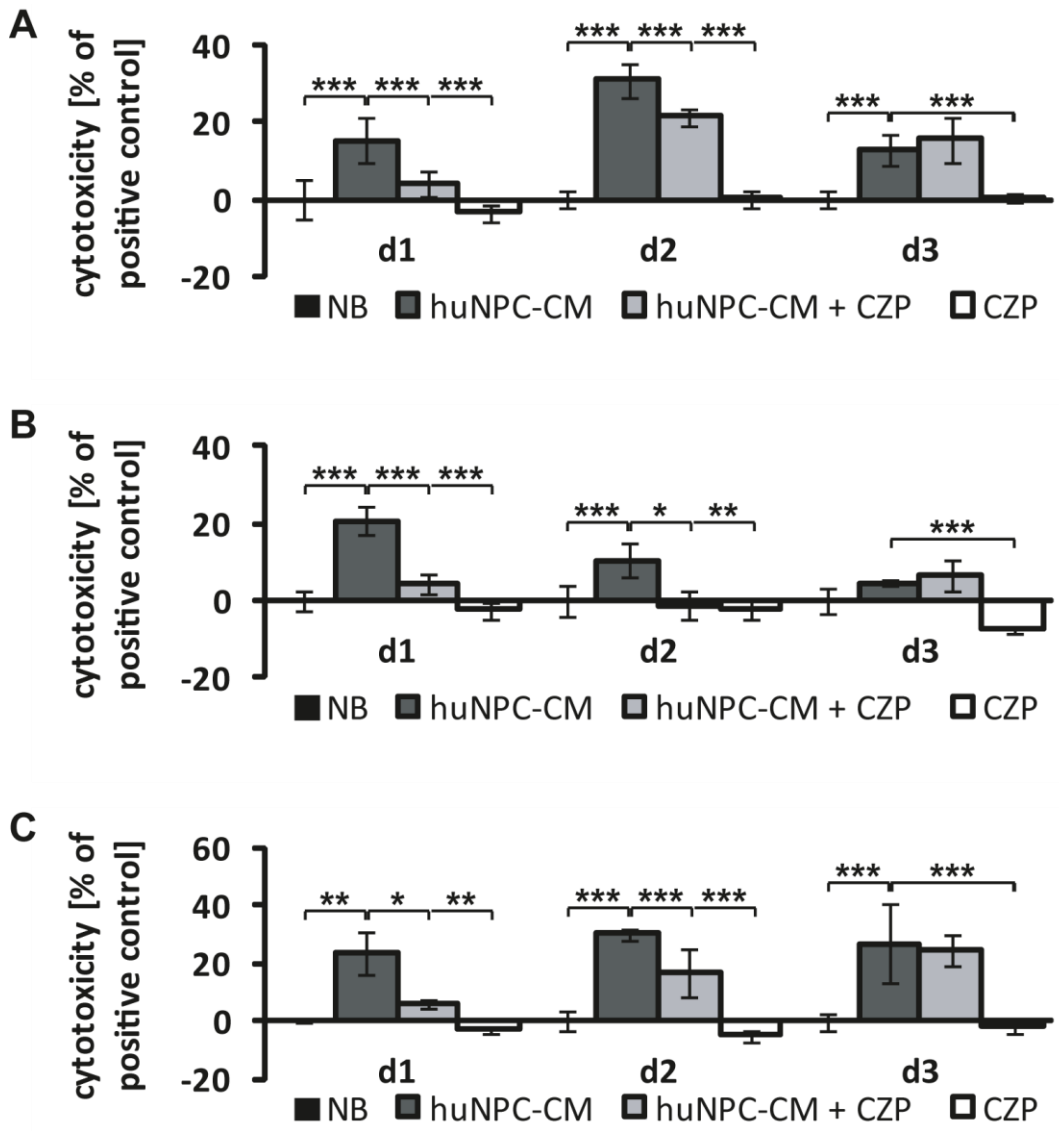

Fig. 4.20 HuNPC-released TRPV1 agonists induce huGBM cell death

HuGBMs are treated with huNPC-CM for one (d1), two (d2) or three (d3) days. Relative cytotoxicity induced by huNPC-CM is shown for three huGBM cells: GBM1 (A), GBM2 (B) and GBM3 (C). Cytotoxicity effects could be blocked by the TRPV1 antagonist capsazepine (CZP). Significances shown: * for $p < 0.05$, ** for $p < 0.01$, *** for $p < 0.001$, one-way ANOVA with Scheffé *post-hoc* test.

This huNPC-CM-induced cytotoxicity effect was observed in all three primary GBM cells, although all of them showed slightly different kinetics and time courses. This reflects the heterogeneity of GBMs which is a therapeutic challenge as well. All three GBM cells showed similar cytotoxicity values at day one, but differed at day two and three. GBM2

cells (Fig. 4.20 B; Tab. 4.1 B) exhibited the strongest increase in cytotoxicity upon stimulation at day one (20.8 ± 3.4 %), which was almost fully blocked by CZP (4.4 ± 2.7 %). At later time points cytotoxicity was decreasing. For GBM1 and GBM3 cells (Fig. 4.20 A, C; Tab. 4.1 A, C), the cytotoxicity peaked at day two (31.0 ± 4.5 % and 30.1 ± 2.3 %), but in contrast to day one the antagonist reduced the effect only to 21.6 ± 2.2 % and 16.7 ± 8.2 %, respectively (for complete values see Tab. 4.1).

Tab. 4.1 Human NPC-conditioned medium leads to cytotoxicity of human glioblastoma cells

A	NB		CM		CM + CZP		CZP	
	Mean [%]	SD [%]	Mean [%]	SD [%]	Mean [%]	SD [%]	Mean [%]	SD [%]
d1	0.0	4.9	15.3	5.8	3.8	3.3	-3.4	2.1
d2	0.0	2.2	31.0	4.5	21.6	2.2	0.1	2.0
d3	0.0	2.2	13.1	4.0	15.7	5.9	0.3	1.3

B	NB		CM		CM + CZP		CZP	
	Mean [%]	SD [%]	Mean [%]	SD [%]	Mean [%]	SD [%]	Mean [%]	SD [%]
d1	0.0	2.6	20.8	3.4	4.4	2.7	-2.5	2.1
d2	0.0	4.0	10.6	4.6	-1.2	3.8	-2.5	2.5
d3	0.0	3.4	4.5	0.8	6.6	3.7	-7.7	0.8

C	NB		CM		CM + CZP		CZP	
	Mean [%]	SD [%]	Mean [%]	SD [%]	Mean [%]	SD [%]	Mean [%]	SD [%]
d1	0.0	0.8	23.1	7.3	6.0	1.8	-2.9	1.0
d2	0.0	3.1	30.1	2.3	16.7	8.2	-5.1	1.7
d3	0.0	2.9	27.0	13.5	24.8	5.5	-2.1	2.6

4.2.3. NPC-released TRPV1-agonists induce endoplasmic reticulum-stress

Since it is known that TRPV1 activation can lead to endoplasmic reticulum (ER) stress [Thomas et al., 2007; Sanchez et al., 2008], I investigated this cell death pathway further. I used a fluorescent dye which specifically marks the ER of cells (ER tracker). HuGBM cells were plated and huNPC-CM was added after one day. The GBM cells were stained three days after exposure to CM using ER tracker and analyzed by confocal microscopy using z-stack recordings (n = 5). The ER size was calculated by the normalization of the area of ER tracker fluorescence to the cell size and is given as percentage of the total cell size. To compare multiple cells, these values were normalized to the positive control, an incubation with the potent ER stress-inducer Thapsigargin (30 ng/ml) for 6 h, which is set as 100 %.

All three GBM cells showed an increase in ER size upon huNPC-CM stimulation (Fig. 4.21), which was reduced by application of the specific TRPV1 antagonist CZP comparable to values of cells receiving normal NB/B-27 medium.

4.2.4. NPC-mediated tumor suppression is restricted to the young brain

After investigating the signaling pathway of endovanilloid factors in NPC-CM on glioma cells *in vitro*, an established animal model was used to study *in vivo* effects [Glass et al., 2005; Walzlein et al., 2008; Chirasani et al., 2010]. Mouse high-grade astrocytoma cells (GL261) were injected into syngeneic Nestin-GFP mice, where NPCs are labeled in green, and tumor size was measured 14 days after inoculation into young (p30) and old (p90) mice (n = 6). To test the specific effect of TRPV1, GL261 cells with a knockdown for TRPV1 were injected in a second set of animals (n = 6).

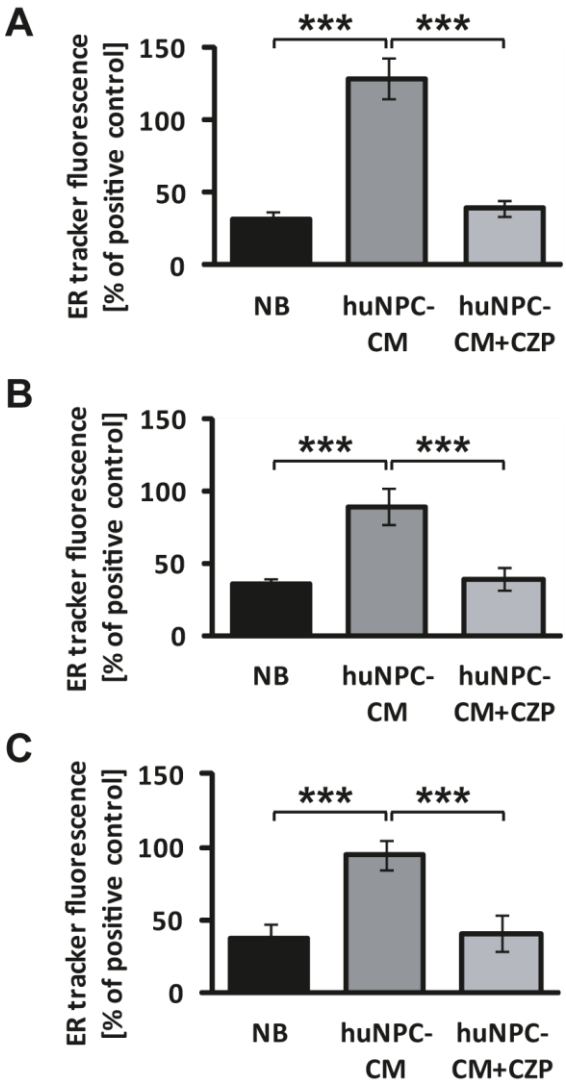

Fig. 4.21 HuNPC-CM results in cell death of huGBM cells via ER stress

HuGBMs are treated with huNPC-CM for three days and stained with an ER tracker dye. Relative ER tracker fluorescence is shown for three primary huGBM cells: GBM1 (A), GBM2 (B), GBM3 (C). HuNPC-CM exposure leads to a significant increase in ER size of huGBM cells. This could be blocked by capsazepine (CZP). Values are normalized to maximal possible increase in ER size via Thapsigargin treatment. Significances shown: *** for $p < 0.001$, one-way ANOVA with Scheffé *post-hoc* test.

In the group of young mice, the loss of TRPV1 on glioma cells resulted in a significantly increased tumor size (8.2 ± 0.9 mm^3) as compared to control glioma cells (4.8 ± 0.8 mm^3), carrying control shRNA (Fig. 4.22 A, B). Many Nestin-GFP$^+$ NPCs were found in the tumor vicinity, which has been shown previously [Glass et al., 2005; Walzlein et al., 2008;

Chirasani et al., 2010]. In contrast, there was no difference between knockdown or control cell injections in p90 mice (control: 9.6 ± 1.4 mm^3; TRPV1 knockdown: 11.1 ± 1.2 mm^3).

Since p90 mice have a reduced neurogenesis compared to their younger counterparts [Corotto et al., 1993], another established mouse model, namely cyclin D2 (cdk2) knockout mice, was used. These mice show a reduction in neurogenesis *per se* [Kowalczyk et al., 2004; Walzlein et al., 2008]. 14 days after injection of either GL261 control or TRPV1 knockdown cells into cdk2 knockout or wildtype mice, tumor sizes were compared (n = 4). In wildtype mice, the injection of TRPV1 knockdown cells led to an increase in tumor size as shown before (see Fig. 4.22 B). The tumor size after control glioma cell inoculation differed significantly between C57BL/6 wildtype (3.1 ± 0.4 mm^3) and cdk2 knockout mice (8.4 ± 2.0 mm^3) (Fig. 4.22 C). Mice with reduced neurogenesis showed larger tumors. The injection of TRPV1 knockdown tumor cells did not result in significant changes in tumor size in C57BL/6 wildtype (10.6 ± 1.0 mm^3) and cdk2 knockout mice (8.4 ± 2.6 mm^3). That indicates that both components, the neurogenesis, i.e. NPCs releasing a vanilloid factor, and the TRPV1 channel triggering cell death of the glioma cells must be present to reduce tumor size.

In a survival study, young (p30) and old (p90) C57BL/6 mice received GL261 control glioma cells or TRPV1 knockdown cells ($n \geq 10$) (Fig. 4.22 D). Young mice with TRPV1 knockdown cells injected (blue line) died earlier than young mice receiving GL261 control cells (green line; cumulative survival). This effect was recovered using GL261-TRPV1 knockdown cells which carry TRPV1 that has a mutation in the seeding region of the shRNA and thus can rescue the knockdown effect. Mice injected with GL261-TRPV1 rescue cells (gray line) showed the same survival time as mice injected with GL261 control cells. For older mice the survival time did not differ between the groups

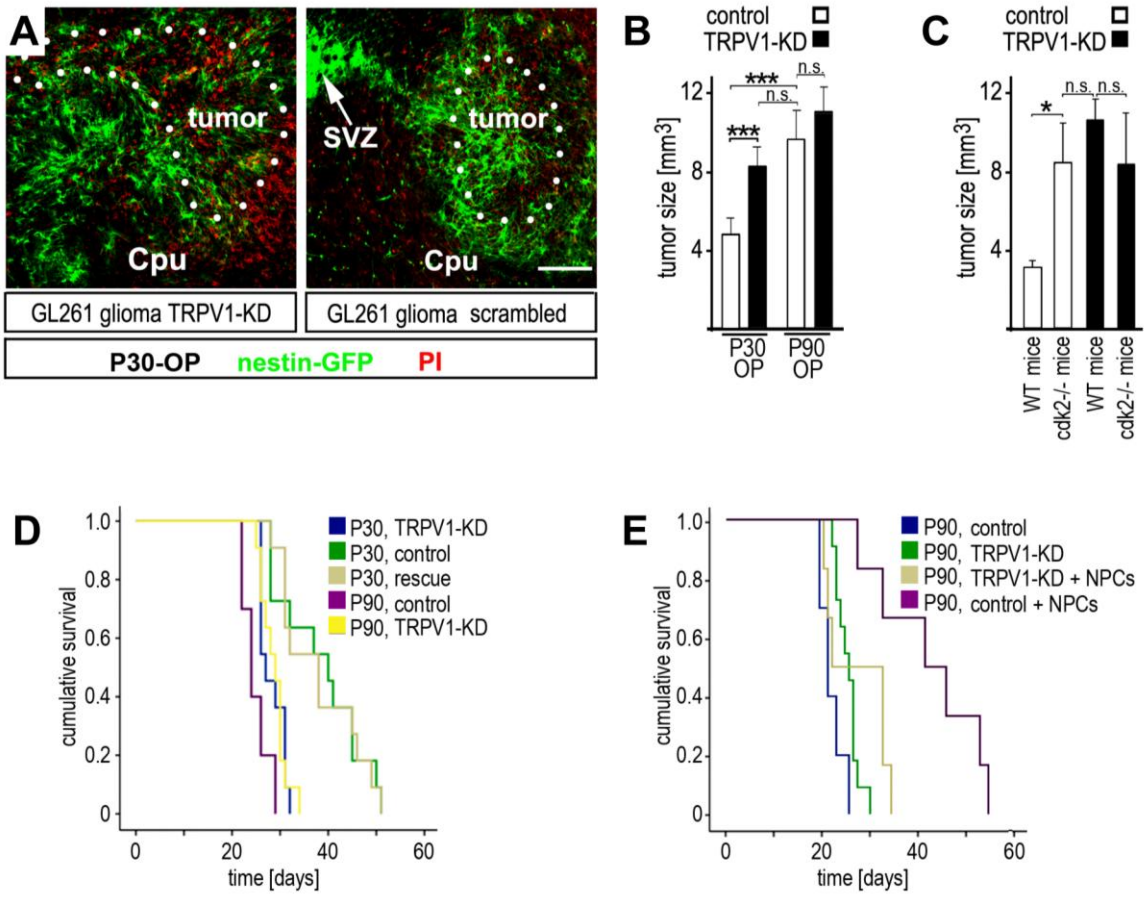

Fig. 4.22 NPC-mediated tumor suppression by endovanilloids is restricted to the young brain

GL261 high grade-astrocytoma cells with TRPV1 knockdown (TRPV1-KD) or controls (scrambled) were inoculated into the caudate putamen (CPu) of Nestin-GFP mice at P30 or P90 (P30-OP or P90-OP) (A). Tumors (indicated by a dotted line) developed for 14 days and dying cells were labeled with propidium iodide (PI), which also stains dying parenchymal cells (subventricular zone, SVZ). Quantification of tumor sizes in young (P30) and old (P90) mice are shown in (B). GL261 control cells or TRPV1-KD cells were inoculated in young (P30) wildtype (WT) or cyclin-D2 knockout mice (cdk2-/-, which have reduced neurogenesis) and tumor sizes are compared two weeks later (C). The survival of mice bearing gliomas is shown in (D). P30 or P90 mice received control (scrambled or rescue) or TRPV1-KD GL261 cells. P30-OP mice outlive P90-OP mice, unless given TRPV1-KD GL261 cells. P90-OP mice were co-implanted either with NPCs and control GL261 cells (scrambled) or with NPCs and TRPV1-KD cells (E). The co-implantation of NPCs improves the survival of adult mice with control astrocytomas, but not with TRPV1-KD tumors. Significances shown: *** for $p < 0.001$; * for $p < 0.05$, t-test. Survival is statistically different with: $p < 0.001$.

injected with GL261 wildtype (purple line) or TRPV1 knockdown cells (yellow line). Next, it was investigated whether the additional application of NPCs into older mice can increase survival times (Fig. 4.22 E). Older mice injected with GL261 wildtype (blue line) or TRPV1 knockdown cells (green line) did not show a difference in the survival as shown before. However, restoring NPCs by co-injection with GL261 control cells (purple line) led to a significantly increased survival in p90 mice, but not the combination of NPCs injected together with TRPV1 knockdown cells (gray line) ($n \geq 6$).

In summary, an active neurogenesis with NPCs releasing endovanilloids and TRPV1 channels on the glioma cells are needed to achieve anti-tumorigenic effects.

4.2.5. Synthetic vanilloids are promising experimental therapeutics for high-grade astrocytomas

Since TRPV1 activation led to cell death and resulted in longer survival of mice implanted with GL261 wildtype cells in comparison to TRPV1 knockdown cells, I wanted to investigate whether glioma cell death can be induced by application of arvanil, a synthetic, non-pungent vanilloid, which is able to pass the blood-brain-barrier and can therefore be administered intraperitoneally [Szallasi and Di Marzo, 2000; Veldhuis et al., 2003].

First, I used the organotypic brain slice model and injected fluorescently labeled high-grade astrocytoma cells (GL261-GFP). The medium was supplemented with arvanil (50 nM), temozolomide (200 µM, a conventional treatment of grade IV astrocytoma) or vehicle (DMSO) as control (Fig. 4.23 A, B). The tumor size was investigated after five days ($n = 3$).

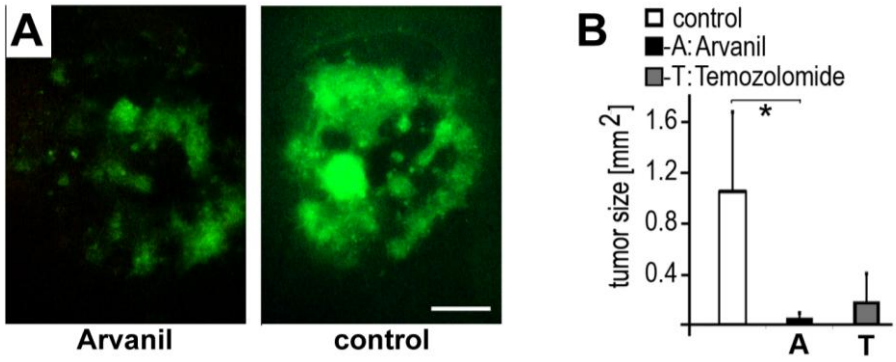

Fig. 4.23 Arvanil treatment leads to reduced sizes of experimental high-grade astrocytomas

GFP-expressing mouse high-grade astrocytoma cells (GL261) are implanted into organotypic brain slice cultures and treated after 24 hours with 50 nM arvanil (-A-) or left untreated (control) (A). Quantification of tumor sizes is done at day five after tumor inoculation (B). Values are compared to a conventional treatment of GBMs, temozolomide (-T-). Scale bar: 300 µm (A); Statistical significance shown: * for $p < 0.05$, test.

Arvanil led to a significant decrease in tumor size compared to control (0.06 ± 0.04 mm^2; 1.05 ± 0.63 mm^2, respectively). The effect was stronger than the alkylating cytostatic drug temozolomide (0.18 ± 0.22 mm^2), which is a conventional treatment of grade IV astrocytoma (glioblastoma multiforme) (Fig. 4.23 A, B).

It has been shown before that microglia, the innate immune cells of the brain, comprise 30% of the glioma mass and are involved in tumor cell expansion [Watters et al., 2005]. To exclude an effect of the immune cells of the brain to the anti-tumorigenic action of arvanil, I used organotypic brain slices and depleted microglial cells using clodronate-filled liposomes [Markovic et al., 2005; Markovic et al., 2009]. PBS-filled liposomes served as control. The experiment was conducted as shown before, the slices were inoculated with mouse high-grade astrocytoma cells (GL261) and treated with arvanil (50 nM) or vehicle (DMSO) and tumor size was measured after five days (n = 3) (Fig. 4.24).

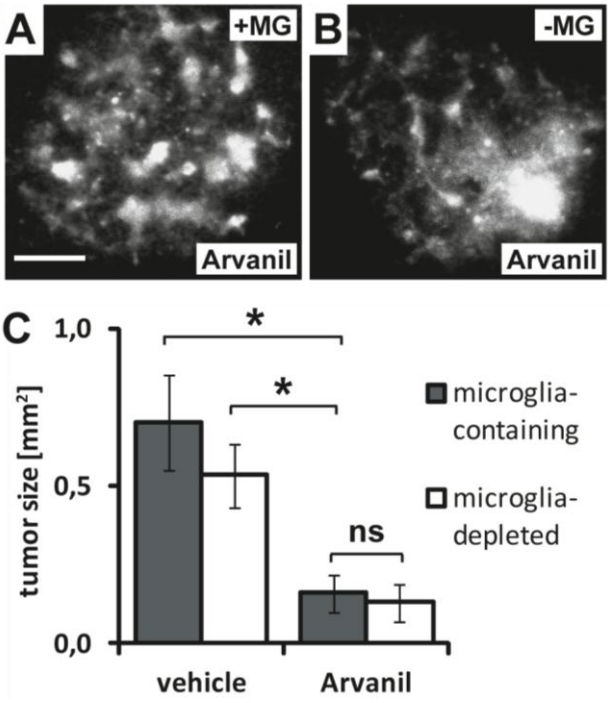

Fig. 4.24 Effect of arvanil on tumor growth is not microglia-dependent

GFP-expressing mouse high-grade-astrocytoma cells (GL621) are inocculated into organotypic brain slice cultures that are either microglia-containing (A) or depleted of microglia (B). One day later, the slices are treated with 50 nM arvanil or with vehicle (DMSO) as control. Tumor sizes are compared at day five after injection (C). Example pictures show microglia-containing (A) or microglia-depleted slices (B) treated with arvanil. Scale bar: 300 µm (A, B); Statistical significance shown: * for $p < 0.05$, t-test.

Tumor sizes in vehicle-treated organotypic brain slices were 0.70 ± 0.15 mm^2 for the microglia-containing and 0.53 ± 0.10 mm^2 for the microglia-depleted group. Arvanil treatment reduced the tumors to 0.16 ± 0.06 mm^2 (microglia-containing) and 0.13 ± 0.06 mm^2 (microglia-depleted). There was no difference in tumor size between microglia-depleted or microglia-containing slices treated with arvanil. So the activity of microglia is not required for the anti-tumorigenic effect.

After the in situ approach, arvanil was tested in a glioma survival study. Three different human primary GBM cells were injected into immune-deficient NOD/SCID mice, lacking the adoptive immune response ($n \geq 10$). After one week these mice got either four i.p.

injections of arvanil (1 µg / g body weight; green line) or vehicle only (blue line) (Fig. 4.25 A, B, D). Animals obtaining arvanil significantly outlived the control group. This survival study again shows that the immune system does not mediate the anti-tumorigenic effect of arvanil. Although all GBM cells reacted to arvanil treatment, there is heterogeneity between GBM cells as seen in clinical therapy as well. GBM1 and GBM3 (Fig. 4.25 A, D) responded better to arvanil than GBM2 (Fig. 4.25 B).

To investigate, whether the effect of arvanil is TRPV1-dependent, C57BL/6 wildtype mice were injected with GL261-TRPV1 wildtype or knockdown cells (Fig. 4.25 C) and treated with arvanil or vehicle ($n \geq 10$). Mice inoculated with GL261-TRPV1 knockdown cells did not show a beneficial effect after arvanil treatment as did mice bearing TRPV1 wildtype cell tumors, suggesting that arvanil acts via TRPV1 channels.

Additionally, temozolomide treatment was compared to arvanil (Fig. 4.25 D). These GBM cells were resistant to temozolomide treatment (100 µg/g, 5 daily injections [McConville et al., 2007]; red line), however arvanil increased survival significantly. The combination of temozolomide and arvanil (purple line) had the best effect in the survival study.

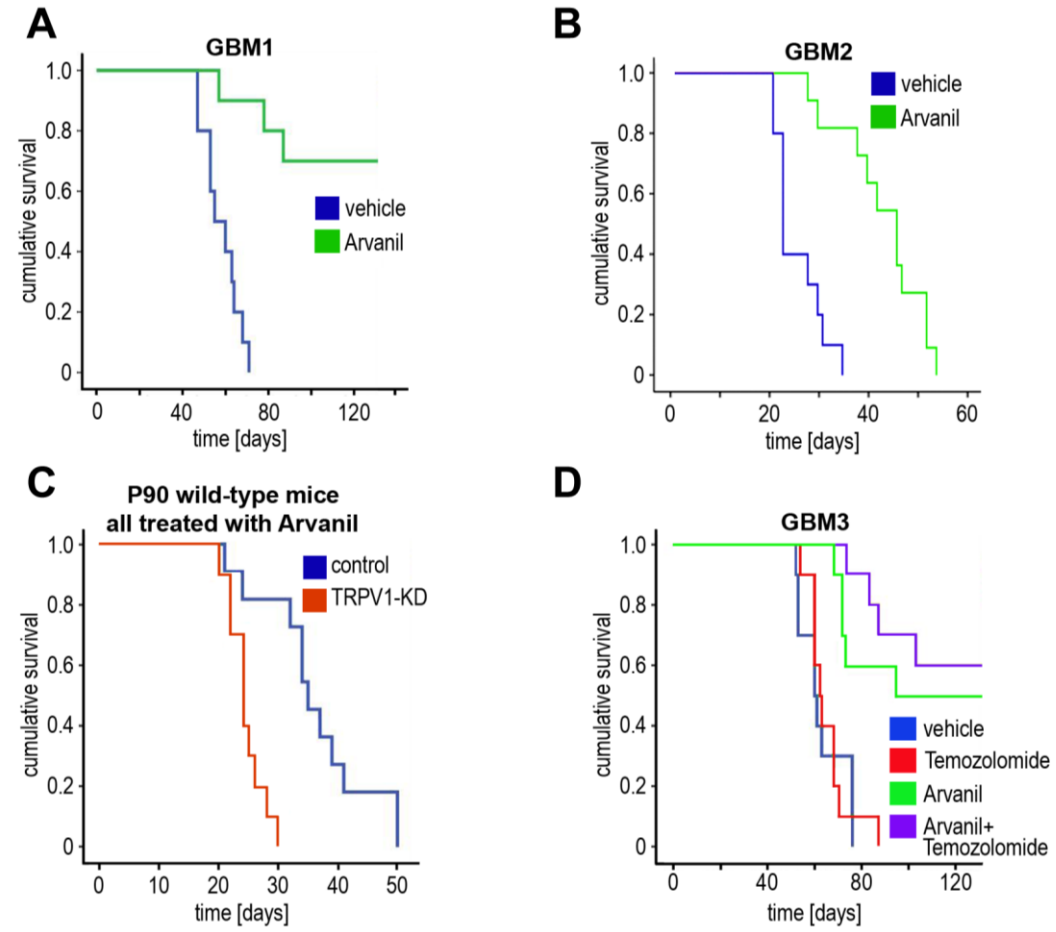

Fig. 4.25 The synthetic vanilloid arvanil has therapeutic effects on experimental high-grade astrocytomas

Immune-deficient NOD/SCID mice were implanted with primary huGBM cells (GBM1, GBM2). After established tumor growth, mice received either four i.p. injections of arvanil or vehicle only and survival times were analyzed (A, B). Arvanil significantly increases survival. Mice were inoculated with high-grade astrocytoma cells (GL261) expressing a scrambled shRNA (control) or a TRPV1 knockdown (TRPV1-KD) shRNA. After established tumor growth, mice received either four i.p. injections of arvanil or vehicle (C). Arvanil significantly improves survival only in animals receiving control GL261 cells. The effect of arvanil on tumor survival is tested against temozolomide in (D). Immune-deficient NOD/SCID mice were implanted with primary huGBM cells. After established tumor growth, mice received either four i.p. injections of arvanil, temozolomide, temozolomide together with arvanil or vehicle. Arvanil significantly improves survival while temozolomide alone is without effect in this tumor. Survival is statistically different with: $p < 0.001$.

In summary, NPCs release vanilloids, which act as endogenous paracrine tumor suppressors.

5. Discussion

5.1. The vanilloid receptor TRPV1 modulates neural precursor cell functions

5.1.1. Neural precursor cells continuously release anandamide

It is reported that anandamide is released from CNS neurons upon depolarization of the cell membrane and acts as auto- or paracrine signaling molecule [Di Marzo et al., 1994]. Anandamide has effects on memory processes, e.g. on long term potentiation (LTP) [Terranova et al., 1995] and forgetting [Terranova et al., 1996].

This work demonstrates that anandamide is also released from neural stem and precursor cells (NPCs) together with N-palmitoyl-ethanolamide (PEA) and N-oleoyl-ethanolamide (OEA), which exert anandamide function through TRPV1 channels [Ho and Gardiner, 2009]. It is shown in this study as a biological proof, that anandamide from NPCs can activate TRPV1 channels in TRPV1 expressing dorsal root ganglia neurons (DRGs).

In previous studies, anandamide function on NPCs is restricted to actions via cannabinoid receptors [Rueda et al., 2002; Aguado et al., 2005; Aguado et al., 2006; Soltys et al., 2010]. The fact that anandamide can act as a dual agonist on TRPV1 channels has not been addressed so far in the NPC context.

5.1.2. NPCs express functional TRPV1 channels

The expression and function of TRPV1 is well established and characterized in the dorsal root, trigeminal and nodose ganglia [Szallasi et al., 1995; Caterina et al., 1997; Tominaga et al., 1998; Davis et al., 2000; Caterina and Julius, 2001; Tominaga and Tominaga, 2005; Siemens et al., 2006; Dhaka et al., 2009]. However, also the presence in the brain is proven in neurons, astrocytes and pericytes by various studies for example by hybridization studies in adult rats and mice or human postmortem tissue on mRNA level (e.g. hypothalamus, hippocampus, basal ganglia and cerebral cortex) [Sasamura et al.,

1998; Mezey et al., 2000; Sanchez et al., 2001b] and partly also by immunohistochemistry [Mezey et al., 2000; Liapi and Wood, 2005; Toth et al., 2005; Cristino et al., 2006]. Furthermore, in radioligand binding studies, the specific TRPV1 agonist resiniferatoxin binds to membranes obtained from various CNS areas from rats and humans [Acs et al., 1996; Roberts et al., 2004]. However, the functions of the now well established expression of TRPV1 in the brain are discussed controversially.

Here, I report that TRPV1 is expressed in the stem cell niches of the brain by NPCs *in vitro* and *in vivo*. In addition, I demonstrate that not only interneurons in the CA1 stratum radiatum of the hippocampus [Gibson et al., 2008], but also Parvalbumin$^+$ interneurons express TRPV1 in the dentate gyrus *in vivo*. However, I did not find immunolabeling of granule cells in the molecular layer of the dentate gyrus as shown before [Cristino et al., 2006; Chavez et al., 2010]. Furthermore, my stainings affirm the presence of TRPV1 in the brain for example in the cortex and striatum (not shown) in accordance with previous work [Mezey et al., 2000; Liapi and Wood, 2005; Toth et al., 2005; Cristino et al., 2006].

Moreover, functional TRPV1 expression in NPCs is shown in this study. The receptor can be activated by application of 1 µM capsaicin to NPC cultures, the specific agonist on TRPV1 channels. Furthermore, I show that NPCs continuously release anandamide in high concentrations. Anandamide is a low intrinsic efficacy TRPV1 agonist that behaves as a partial agonist in tissues with a low receptor reserve, whereas in tissues with high receptor reserve and in circumstances associated with certain disease states, it behaves as a full agonist (for review see [Ross, 2003]). Calcium signals in response to capsaicin application from NPCs are smaller compared to DRGs. Thus, I assume a lower receptor expression in NPCs. In this situation higher anandamide concentrations would be required to activate TRPV1. These high concentrations could be established by inhibition of anandamide breakdown or a high synthesis rate, which would result in sufficient anandamide concentrations to activate TRPV1. Furthermore, also activation of TRPV1 results in an increased anandamide synthesis.

This study shows that NPCs do not only express TRPV1 *in vitro*, but also *in vivo* when neurogenesis is triggered. Here, I can demonstrate for the first time the expression in Nestin$^+$ NPCs during postnatal neurogenesis in SVZ and SGZ. After postnatal day 21 however, I could not detect TRPV1 expression in NPCs anymore. Only after physiological stimulation of adult hippocampal neurogenesis by a spatial learning task (Morris water maze, MWM), TRPV1 expression is restored in Dcx$^+$ NPCs. Performance in MWM is closely associated with hippocampal neurogenesis [Kempermann, 2002], particularly the reversal part of the task [Garthe et al., 2009; Wolf et al., 2009].

Evidence for functional activation of TRPV1 on neurons in the CNS by anandamide is found in the hippocampus. Al-Hayani et al. showed by extracellular recordings in the rat hippocampal CA1 region that anandamide activates TRPV1 on mature neurons, which could be mimicked by TRPV1 agonists and inhibited by TRPV1 antagonists [Al-Hayani et al., 2001]. TRPV1 is also involved in hypokinetic effects of anandamide, presumably related to a decrease in nigrostriatal dopaminergic activity [de Lago et al., 2004].

5.1.3. Loss of TRPV1 in postnatal NPCs changes their properties

The freshly isolated NPCs from both stem cell niches are cultured as neurospheres. Here, I report that the knockout of TRPV1 expression results in a significant increase in postnatally proliferating cells from both stem cell niches compared to wildtype controls. However, clonal efficiency analysis shows that the sphere formation capacity, i.e. the stemness of the cells, remains unchanged as shown by limiting dilution assay [Singh et al., 2003]. The increase in proliferation upon TRPV1 knockout is also present *in vivo* as investigated in this study during postnatal neurogenesis. Furthermore, under mild differentiating conditions *in vitro*, i.e. growth factor withdrawal and 0.1 % FCS addition, I demonstrate that TRPV1 knockout NPCs keep expressing stem cell genes as Nestin or

Sox2, while the expression of differentiation markers for astrocytes (GFAP, S100b) and neurons (beta3-tubulin) is reduced.

There is a close interplay between the endovanilloid and the endocannabinoid systems in the brain. Previous studies show that cannabinoids regulate neurogenesis via CB1 receptors [Rueda et al., 2002] and NPCs express the components of the cannabinoid system [Aguado et al., 2005; Arevalo-Martin et al., 2007; Oudin et al., 2011]. Endocannabinoids can be produced and degraded by NPCs, which I can confirm in this study as well. However, the endocannabinoid anandamide can activate TRPV1 channels as well. So far only CB1 contribution to proliferation, neurosphere generation and differentiation has been investigated. Upon CB1 knockout, adult NPC proliferation is decreased in both stem cell niches, the SVZ and the dentate gyrus [Jin et al., 2004; Aguado et al., 2005]. Jin et al. further show that the CB1 receptor antagonist drugs SR141716A (rimonabant) and AM251 increase neurogenesis in both wildtype and CB1 receptor knockout mice. They suggest the involvement of another player e.g. TRPV1, since the neurogenesis-promoting effect of rimonabant is lost in TRPV1 knockout mice [Jin et al., 2004]. They show that the number of $BrdU^+$ cells is increased in the dentate gyrus in adult TRPV1 knockout mice, but not in the SVZ. However, their experimental protocol does not allow the discrimination between NPC proliferation and survival, which is problematic since it is known that both can increase or decrease depending on how the treatment affects NPCs [Kempermann et al., 2004a; Kempermann et al., 2004b; Bruel-Jungerman et al., 2007]. Furthermore, the application of the dual antagonist rimonabant [Pegorini et al., 2006; Gibson et al., 2008] makes it difficult to separate CB1- and TRPV1-dependent effects. Here, I now clearly show that TRPV1 knockout mice exhibit an increased proliferation in the SVZ as well as SGZ when neurogenesis is triggered. In addition, I use the specific agonist of TRPV1, capsaicin, for channel activation in *in vitro* experiments.

Furthermore, neurosphere generation and self-renewal is negatively affected in CB1 knockouts [Aguado et al., 2005]. The expression of CB1 receptors is developmentally regulated [Jin et al., 2004; Aguado et al., 2005; Berghuis et al., 2005; Aguado et al., 2006]. The effect of CB1 receptor stimulation seems to vary, as pharmacological stimulation of CB1 results in neurogenesis [Jiang et al., 2005], but higher amounts of locally generated anandamide in FAAH knockout animals lead to an induction of astrogliogenesis [Aguado et al., 2006].

Furthermore, also pathological situations result in modulations of neurogenesis via the endocannabinoid / -vanilloid system. It is shown that the synthetic cannabinoid HU-210 induces anxiolytic and antidepressant effects, possibly by affecting neurogenesis [Jiang et al., 2005]. Since neurogenic activity in the stem cell niches correlates reversely with aging, a lower brain repair is shown in pathological situations [Lie et al., 2004]. Additionally, without the presence of CB1 receptors on NPCs in CB1 knockouts, these mice develop cognitive impairments [Bilkei-Gorzo et al., 2005].

CB1 expression in NPCs is not restricted to rodents, but it is also shown that the hNSC1 embryonic human neural stem cell line expresses CB1 *in vitro* [Rueda et al., 2002; Palazuelos et al., 2006]. *In vivo*, the expression is shown on a subpopulation of the human subependymal layer in the adult brain [Curtis et al., 2006].

This study suggests that TRPV1 could be a modulator of neurogenesis during postnatal development and whenever it is re-stimulated above baseline for example by spatial learning. It could be involved when NPCs stop proliferating and start differentiating in the stem cell niche, as I see higher proliferation and less differentiation in TRPV1 knockout cultures. These data confirm the link between TRPV1 and control of proliferation which was found in a previous study in epidermal skin cells [Bode et al., 2009]. Their work shows that TRPV1 down-regulates the expression of the pro-proliferative epidermal growth factor receptor (EGFR). Furthermore, the activation of TRPV1 induces a G_0/G_1 cell cycle arrest in low-grade urothelial cancer cells [Amantini et al., 2009].

Since the environment in the stem cells niche is restrictive, the proliferative effect of the endocannabinoid / endovanilloid system in NPCs may result in astrogliogenesis and/or neurogenesis depending on the intensity of stimulation or the (patho-)physiological context.

In conclusion, TRPV1 knockout mice have a larger stem cell pool available. This can result in an increase in synaptic connections but can also lead to miswiring. New neurons need to develop, migrate and integrate correctly to be beneficial. This is not always the case, as shown in animal models of temporal lobe epilepsy [Parent et al., 2006].

5.1.4. Physiological stimulation of adult neurogenesis is modulated by TRPV1 channels

Since TRPV1 effects postnatal neurogenesis, the spatial learning ability of TRPV1 wildtype and knockout mice is assessed in this study using Morris water maze (MWM). This is closely associated with hippocampal neurogenesis [Kempermann, 2002], particularly to the reversal performance [Garthe et al., 2009; Wolf et al., 2009]. Here, I report that during acquisition, both wildtype and knockout mice learn to reach the platform. However, knockout mice show a steeper learning curve which represents faster task acquisition. The probe trial assesses the success of learning and reference memory [Morris et al., 1982; Wolfer et al., 1997]. Knockout mice are significantly more effective in discriminating the previously trained zone as they re-enter the former platform zone significantly more often than wildtype mice. In the reversal, the mice have to be cognitive flexible to re-learn the new location of the hidden platform. Interestingly, knockout mice persist longer in searching in the previous platform quadrant, indicating a lower cognitive flexibility and incapacity to adapt to the new situation. However, as already shown during acquisition, after an initial lower performance, knockout mice acquire the new task faster as seen in a steeper learning curve. Usually, learning curves are steeper in the acquisition phase than in the reversal, since the animals know already the visual

cues and that the escape from the pool is associated with finding the platform [Terry, 2009]. However, TRPV1 knockout mice show the same slope for both phases, indicating again a faster task acquisition. It is shown that loss of TRPV1 in rats leads to defects in both long term potentiation (LTP) as well as long term depression (LTD), mechanisms associated with learning and memory [Gibson et al., 2008]. LTD is blocked when TRPV1 is antagonized and could be induced by application of the specific agonist capsaicin. The reduction of LTD in absence of TRPV1 function can be confirmed by my MWM data. In the reversal task, where the paradigm shifts and the animals need to forget the old position of the platform and need to re-learn a new position, I can show that TRPV1 knockout mice have a higher perseverance for the old platform area, which could be indicative not only for neurogenic cell-based memory dysfunctions, but also for LTD impairments. Furthermore, I marked NPCs dividing during the water maze experiment by BrdU and the survival of those cells is assessed four weeks later. Here again, TRPV1 knockout animals show higher numbers of $BrdU^+$ cells in the dentate gyrus after performing the spatial learning task, which is associated with the hippocampus. The differentiation stages are not affected.

However, I cannot clearly discriminate neurogenesis-driven changes in behavior from the impact of synaptic plasticity on MWM performance. I therefore propose that TRPV1 expression on NPCs modulates spatial memory performance in conjunction with the known impact on LTP and LTD via TRPV1 on interneurons in the hippocampus.

Furthermore, this study shows that TRPV1 knockout mice follow a different strategy while executing the task. As seen from day one to day two of training, they reduce their swim speed and increase their immobility time to orient in the pool. Since this strategy proved to be successful for the escape from the pool, they kept it throughout the whole experiment.

The analysis of search strategies is used to analyze the performance of animals in behavioral tasks [Sutherland et al., 1982; Wolfer and Lipp, 2000; Grootendorst et al.,

2001; Graziano et al., 2003; Lang et al., 2003; Janus, 2004]. However, the reason for strategic differences is so far unknown. The investigation of the cholinergic system reveals a change in strategy in initial hidden platform searching in MWM upon blockade of muscarinic acetylcholine receptors [Whishaw and Petrie, 1988; Whishaw, 1989]. The investigation of search strategies is not only important in animals for the understanding of the mechanisms involved. A recent study shows the search strategy classification in a virtual human water maze analogue as well [Schoenfeld et al., 2010].

In conclusion, I can show that TRPV1 expression in the stem cell niches is important when neurogenesis is active. This is shown during postnatal neurogenesis as well as after physiological stimulation of neurogenesis by a spatial learning task (MWM). Since TRPV1 expression is flexible and regulated by growth factors (e.g. NGF and GDNF) [Amaya et al., 2004], a differential regulation of expression is likely as it occurs during inflammation [Ji et al., 2002; Amaya et al., 2004]. This would explain the different expression patterns of TRPV1 in the brain in the literature. These studies are hardly comparable, using not only diverse methods of detection but also different ages and species. If TRPV1 is strictly developmentally regulated, this leads to confusing conclusions about the presence or absence of TRPV1 in the brain. Furthermore, some studies suggest an expression *in vitro*, but so far no *in vivo* data are shown. Also, the use of reporter systems did not overcome the difficulties of TRPV1 detection, amongst others due to the sensitivity of the reporter.

5.1.5. Clinical relevance of TRPV1 in the brain

TRPV1 channels are a new target for pain relief either by agonist-induced desensitization of the channel or by TRPV1 antagonism. Moreover, preclinical data hint to a broader spectrum of application for example for migraine, cough, pancreatitis, urinary incontinence

and inflammatory bowel disease (see review by [Szallasi et al., 2006; Szallasi et al., 2007]).

However, TRPV1 antagonists produced severe unexpected side effects in clinical trials e.g. hyperthermia and an increase in the heat threshold of the patients.

The investigation of TRPV1 expression in the brain is very important since it was recently shown that the anti-obesity drug rimonabant (also known as SR141716A), which is thought to act via a CB1-dependant mechanism, acts on TRPV1 channels as well, thereby depressing brain synapses [Pegorini et al., 2006; Gibson et al., 2008]. The blockades of both receptors lead to depression, anxiety and suicidal thoughts. Rimonabant was approved and in clinical use as an anti-obesity drug [Tucci et al., 2006; Padwal and Majumdar, 2007; Van Gaal et al., 2008], but is now withdrawn from the market.

TRPV1 functions in the brain may help to understand the devastating side effects of drugs like rimonabant, but may also open new drug targets for neurological diseases, since it has been shown that activation of TRPV1 is neuroprotective against *in vivo* excitotoxicity [Skaper et al., 1996; Shen and Thayer, 1998; Nagayama et al., 1999; Veldhuis et al., 2003; Pegorini et al., 2005; Pegorini et al., 2006]. The endocannabinoid system as well as the hippocampus are related to different neurological disorders like depression [Lafourcade et al., 2011], schizophrenia [Giuffrida et al., 2004] or Alzheimer's disease [Ramirez et al., 2005].

TRPV1 is also investigated in acute stress conditions, since stress intensifies neuropsychiatric and cognitive disorders. The study shows anti-stress effects of TRPV1 channels on synaptic plasticity and spatial memory [Li et al., 2008]. It is suggested that TRPV1 facilitates LTP and suppresses LTD, which is consistent with the changes of LTP and LTD in TRPV1 knockout mice [Marsch et al., 2007; Gibson et al., 2008]. Dysfunctions in synaptic plasticity contribute for example to Alzheimer's or Parkinson's disease [Brun et al., 2001].

Endogenously generated endocannabinoids / -vanilloids like anandamide accumulate during neurodegeneration [Hansen et al., 2001]. Anandamide is a dual agonist on TRPV1 [Zygmunt et al., 1999] and CB1 [Devane et al., 1992] receptors and the receptors are co-expressed in different brain areas including the hippocampus which is associated with different neurological disorders. However, TRPV1 action seems to be differentially regulated since a high concentration of agonists leads to cell death in mesencephalic [Kim et al., 2005] and hippocampal neurons [Cernak et al., 2004]. This resulted in speculations whether TRPV1 could be involved in neuropathologies e.g. Parkinson's disease, Alzheimer's disease and schizophrenia (for review see [Starowicz et al., 2008; Cortright and Szallasi, 2009]).

Another role for TRPV1 is the neuroimmunological regulation as seen in type-1 autoimmune diabetes (reviewed in [Suri and Szallasi, 2008]) and possibly in other autoimmune diseases for example multiple sclerosis. This might be involved in neuroinflammatory processes associated with Alzheimer's disease [Yamamoto et al., 2007].

Thus, the contribution of the endocannabinoid / endovanilloid system in NPCs in development and adult neurogenesis as well as after brain injury and the interplay with other signaling pathways need to be further investigated. The understanding of the processes might open new perspectives for the treatment of neural disorders while respecting the delicate balance of this system to maintain brain homeostasis as the basis of brain plasticity.

5.2. Neural precursor cells induce cell-death of high-grade astrocytomas via stimulation of TRPV1

5.2.1. Human primary NPCs and human primary glioblastoma cells express TRPV1

The second part of my study shows for the first time that TRPV1 is not only expressed in primary mouse NPCs, but also in primary human NPCs. Furthermore TRPV1 expression is investigated in the glioma pathology context. Therefore, primary human GBM cells (huGBMs) are analyzed for TRPV1 expression. Here as well, I can detect TRPV1 expression. This is in agreement with two previous studies reporting TRPV1 in human glioma cell lines and tissue [Contassot et al., 2004; Amantini et al., 2007]. I can show that the expression of the receptor is lower in NPCs than in huGBMs. Furthermore, huGBMs show a variation in receptor expression. This heterogeneity in expression is a therapeutic challenge which causes many problems in clinical approaches.

5.2.2. NPC-released TRPV1-agonists induce glioma cell death

As shown in the first part of the study, NPCs release fatty-acid ethanolamides like anandamide or PEA and OEA. To test whether released substances from NPCs can act on glioma cells, I treated huGBMs with human NPC-conditioned medium (huNPC-CM). This application results in a significant reduction of huGBM cell numbers. The signaling pathway that is activated by this exposure is investigated further. I show that upon stimulation with huNPC-CM, there is an increase in cell death of huGBM cells. This effect is observed in all three primary huGBM cells, however also here there is heterogeneity as shown in slightly different kinetics and time courses. The cell death is blocked by application of the specific TRPV1 antagonist capsazepine, showing a TRPV1-dependent cell death mechanism.

It has been shown that endogenous as well as exogenous neural precursor cells show tropism for brain tumors [Aboody et al., 2000; Glass et al., 2005; Assanah et al., 2006; Walzlein et al., 2008; Assanah et al., 2009]. This study suggests that after homing to the brain tumor, they release endovanilloids, which induces glioma cell death via TRPV1.

5.2.3. NPC-released TRPV1-agonists induce endoplasmic reticulum-stress

Due to the diversity of cell death mechanisms described in cancer cells, I study the impact of endovanilloids on the cell death of HG-astrocytomas.

HuGBM cells show an increase in ER size upon huNPC-CM stimulation, which is reduced by application of the specific TRPV1 antagonist CZP comparable to values of cells receiving normal NB/B-27 medium. This shows that ER stress upon huNPC-CM stimulation is TRPV1-dependent, which is in agreement with previous reports indicating that synthetic anandamide induces HG-astrocytoma apoptotic cell death [Maccarrone et al., 2000] and neuronal death via the ER-stress pathway [Pasquariello et al., 2009]. Also in pancreatic and lung cancer, it is shown that cannabinoids induce apoptosis via endoplasmic reticulum stress-related genes [Carracedo et al., 2006a; Thomas et al., 2012].

5.2.4. NPC-mediated tumor suppression is restricted to the young brain

It has previously been shown, that the number of endogenous NPCs cumulating at gliomas depends on age. This reflects the reduction of neurogenic activity in the stem cell niches with increasing age [Corotto et al., 1993; Seki and Arai, 1995; Kuhn et al., 1996; Tropepe et al., 1997; Walzlein et al., 2008]. Therefore, only in the young brain, there are sufficient numbers of NPCs that can migrate to the glioma and execute its endovanilloid

mediated anti-tumorigenic effect. This may be correlated with the age-related increase in glioblastomas [Ohgaki and Kleihues, 2005; Ohgaki and Kleihues, 2007].

This study shows that the loss of TRPV1 on glioma cells results in a significantly increased tumor size as compared to control glioma cells in young mice. However, in old mice the presence or absence of TRPV1 did not result in differences in glioma size. This is due to the decline in stem cell activity, which could be overcome by co-implanting exogenous NPCs together with glioma cells. To underline this finding, cyclin D2 (cdk2) knockout mice are used here, which have reduced neurogenesis *per se* [Kowalczyk et al., 2004; Walzlein et al., 2008]. Those animals show larger tumors than wildtype mice. These data show that both components, the neurogenesis, i.e. NPCs releasing endovanilloids, and the TRPV1 channel triggering cell death of the glioma cells, must be present to reduce tumor size. So younger mice have the advantage of an intrinsic protective mechanism against HG-astrocytomas, which is dependent on endovanilloid signaling.

5.2.5. Anti-tumoral activity of cannabinoids on gliomas

Cannabinoids, for example delta9-tetrahydrocannabinol (THC) are in clinical use as palliatives to alleviate side effects of chemotherapy e.g. nausea, vomiting and pain [Sallan et al., 1975; Tramer et al., 2001]. But they have also anti-tumorigenic properties in different cancers for example gliomas, lymphomas, prostate, pancreatic, skin, breast and lung cancer [Blazquez et al., 2006; Carracedo et al., 2006a; Carracedo et al., 2006b; Gustafsson et al., 2006; Ligresti et al., 2006; Sarfaraz et al., 2006]. These anti-tumorigenic actions are modulated by different signaling pathways to inhibit cell growth and induce cell death mostly via apoptosis. *In vitro* experiments show that cannabinoids lead to cell death via apoptosis in rat C6 glioma cells [Sanchez et al., 1998]. But also *in vivo*, the same effect could be shown in Wistar rats inoculated with C6 gliomas leading to an increased survival of cannabinoid-treated animals [Galve-Roperh et al., 2000; Sanchez et al.,

2001a]. However, it is also shown that these effects are dose-dependent since low doses of cannabinoid agonists can also stimulate tumor cell growth [Preet et al., 2008]. In glioblastoma multiforme, cannabinoid receptor agonists showed anti-tumorigenic effects via the accumulation of ceramide and activation of the extracellular signal-regulated kinases 1/2 (ERK1/2)-pathway [Galve-Roperh et al., 2000; Gomez del Pulgar et al., 2002b]. Also induction of pro-apoptotic signaling via activation of Bad protein is shown [Ellert-Miklaszewska et al., 2005]. Cannabinoids can exert anti-tumorigenic actions via a diversity of mechanisms: 1) they induce cell death via apoptosis [Guzman, 2003] or autophagy [Salazar et al., 2009], 2) they inhibit the migration of glioma cells [Vaccani et al., 2005] and 3) they inhibit tumor angiogenesis and metastasis [Blazquez et al., 2003]. Cannabinoid receptor agonists are also tested in clinical trials. In a small group of patients with recurrent glioblastoma multiforme, the safety profile of THC is accessed in a phase I clinical trial. THC application leads to anti-proliferative actions on tumor cells without showing psychoactive effects, which THC also exerts via CB1 receptors in the brain [Guzman et al., 2006]. Furthermore, cannabinoids are tested in clinical trials in combination with current standard therapies [Torres et al., 2011]. Due to the abuse potential of psychoactive drugs, a non-psychoactive alternative, cannabidiol, was tested on human glioma cells, which led to caspase activation and oxidative stress [Massi et al., 2006].

However, the cell death effects of cannabinoids seem to be selective for transformed cells [Guzman, 2003], since it is reported that cannabinoids protect physiological astrocytes [Gomez Del Pulgar et al., 2002a], oligodendrocytes [Molina-Holgado et al., 2002] and neurons [Mechoulam et al., 2002; Torres et al., 2011] from apoptosis via CB1 receptors and the phosphatidylinositol 3-kinases / Akt kinase (PI3K/Akt) -pathway. Yet, also neurotoxic effects are observed in culture [Chan et al., 1998; Downer et al., 2003]. The different outcomes of cannabinoid action on transformed and physiological cells might be due to different signaling pathways involved depending on the state of the cells.

Unwanted psychotropic effects of cannabinoids limit their potential as anti-tumorigenic agents. But, since those effects are largely mediated by CB1 receptors in the brain, the potential of CB2 receptor agonists is evaluated. It is shown that activation of CB2 in gliomas [Sanchez et al., 2001a] and skin cancer [Casanova et al., 2003] leads to a decrease in tumor size. The disadvantage of CB2 agonists though, is the limited expression of CB2 in human GBMs and glioma cell lines [Sanchez et al., 2001a; Cudaback et al., 2010]. Furthermore, it is also shown that CB2 agonists can impair the anti-tumor immunity [Zhu et al., 2000].

Therefore, the search for other non-psychoactive, non-CB receptor-based mechanisms is needed. It is shown that cannabidiol, which probably acts via a novel cannabinoid receptor named GPR55 [Ryberg et al., 2007] inhibits glioma cell growth *in vitro* and *in vivo* [Jacobsson et al., 2000; Massi et al., 2004]. Cannabinoids can also act via TRPV1 channels, which can result in pro-apoptotic actions in gliomas [Jacobsson et al., 2000; Maccarrone et al., 2000].

5.2.6. The role of TRPV1 in tumor biology

Since the family of transient receptor potential (TRP) channels are calcium channels, they modulate intracellular calcium concentrations, which is important for cell proliferation as well as cell death. The expression of TRP channels is altered during tumor growth and metastasis [Gkika and Prevarskaya, 2009]. In 1998 it was shown that C6 rat glioma cells respond to vanilloids [Biro et al., 1998]. Furthermore, TRPV1 expression is up-regulated in the ER-membrane in gliomas [Contassot et al., 2004]. Increased TRPV1 expression is also associated with other types of cancer for example pancreatic cancer [Hartel et al., 2006], bladder carcinomas [Lazzeri et al., 2005], prostate cancer [Sanchez et al., 2005] and colon cancer [Domotor et al., 2005]. However, also under physiological conditions TRPV1 is expressed in the urothelium of the bladder [Daly et al., 2007]. The expression of TRPV1 during cancer progression seems to be regulated as well. It is shown for

cancerous urothelium that TRPV1 expression decreases with aggressiveness of the tumor [Lazzeri et al., 2005]. The antagonization or lack of TRPV1 expression results in an increase in skin carcinogenesis through epidermal growth factor receptor / Akt kinase (EGFR/Akt) signaling [Li et al., 2011].

Furthermore, it is suggested that TRPV1 may be an oncogene, however the expression varies between cancer types and progression stages [Gkika and Prevarskaya, 2009].

5.2.7. Synthetic vanilloids are promising experimental therapeutics for high-grade astrocytomas

This study shows that TRPV1 activation by endovanilloids leads to glioma cell death and results in longer survival of mice. However, since transplantation of NPCs is problematic due the risks of *de novo* tumor formation [Amariglio et al., 2009], the application of an exogenous vanilloid, arvanil, is tested here. Arvanil is a synthetic, non-pungent vanilloid, which is able to pass the blood-brain-barrier and can therefore be administered intraperitoneally [Szallasi and Di Marzo, 2000; Veldhuis et al., 2003]. This study shows that arvanil leads to a significant decrease in tumor size compared to controls in an *ex vivo* organotypic brain slice model as well as in an *in vivo* survival study. The effect is stronger than temozolomide [Newlands et al., 1997], which is a conventional treatment of grade IV astrocytomas (glioblastoma multiforme). Although all GBM cells reacted to arvanil treatment, there is heterogeneity between GBM cells as seen in clinical therapy as well. Furthermore, there is a fraction of gliomas which is resistant to temozolomide treatment [Bobola et al., 1996]. But also in a glioma in this study which is resistant to temozolomide treatment, arvanil increases survival significantly, suggesting that synthetic vanilloid compounds may have clinical potential for brain tumor treatment.

The activation of TRPV1 via the synthetic vanilloid arvanil shows anti-tumorigenic actions but is also proven to be neuroprotective by attenuating excitotoxic brain injury [Veldhuis et al., 2003].

5.2.8. Challenges of anti-tumorigenic therapies

GBMs show a high heterogeneity between and within tumors [Maher et al., 2001]. These changes are investigated intensively [Maher et al., 2001; Merlo, 2003; Mischel et al., 2003]. There is a high diversity of molecular mechanisms leading to GBMs. One of those is the overexpression of EGFR or of a constitutively active truncated form [Maher et al., 2001]. It has been shown that cannabinoids can decrease EGFR signaling in prostate [Mimeault et al., 2003] and skin cancer [Casanova et al., 2003]. Furthermore, it is reported that TRPV1 channels down-regulate EGFR expression [Bode et al., 2009]. TRPV1 activation could be useful in patients with changes in EGFR signaling. Due to the tumor's high resistance to current therapies, new approaches should be tested in combination with standard treatments. It is already reported to be beneficial, to use cannabinoid drugs that induce cell death via ceramide accumulation as combination therapy [Radin, 2003; Torres et al., 2011]. Nevertheless, also the resistance of glioma cells to cannabinoid-induced apoptosis is shown, most probably due to the heterogeneity of expression profiles of cannabinoid receptors [Galve-Roperh et al., 2000; De Jesus et al., 2010]. Though, cannabinoids e.g. anandamide can also act via TRPV1 channels and induce glioma cell death via TRPV1-dependent apoptosis [Contassot et al., 2004; Amantini et al., 2007]. Furthermore the resistance to cannabinoid-induced cell death might be due to the inhibition of the ER stress pathway in those cells [Velasco et al., 2007]. As I could show in the present study, vanilloids can activate the ER stress pathway in human GBM cells, which could be used to neutralize this resistance and enhance the response to anti-tumorigenic treatments.

Novel approaches will lead to individualized therapies for patients depending on the molecular and cellular mechanism underlying their GBM formation (reviewed in [Bleeker et al., 2012]). The selective targeting of subpopulations in a tumor using combined approaches will result in a more efficient therapy for patients.

6. Summary

The transient receptor potential vanilloid type 1 (TRPV1) has a well investigated role in pain signal detection and transduction. There are multiple clinical studies trying TRPV1 agonists to desensitize or antagonists to block the receptor for pain relief. The presence of TRPV1 in the brain is now well established but the functions remain mostly unclear. Due to this fact and to avoid unnecessary side effects of drug application, the expression and role of TRPV1 needs to be further studied.

Since the discovery of neurogenesis in the brain in 1965 by Altman and Das, many endogenous and environmental influencing factors have been identified. In the recent years, the endovanilloid system has come into focus as a novel intrinsic modulator system of neurogenesis.

Here, I have identified a previously unknown function of TRPV1 in the central nervous system. I show that TRPV1 is expressed in the stem cell niches in neural precursor cells (NPCs) *in vitro* and *in vivo*, when neurogenesis is triggered. Loss of the receptor in TRPV1 knockout mice leads to an increase in proliferation in the stem cell niches and in cultured NPCs. Functionality of the receptor is further shown by calcium imaging in NPC cultures. After differentiation, TRPV1 knockout NPCs show an increased expression of stem cell genes and a reduced expression of differentiation markers. In conclusion, TRPV1 knockout animals have a larger stem cell pool available.

The hippocampus-dependent performance in the Morris water maze task reveals phenotype differences between TRPV1 wildtype and knockout mice. TRPV1 knockout animals show a faster task acquisition and better reference memory. However, they show a lower cognitive flexibility. Also, the search strategy differs from wildtype mice.

In conclusion, I can show that TRPV1 expression in the stem cell niches is important to control proliferation when neurogenesis is active. This is demonstrated during postnatal

neurogenesis as well as after physiological stimulation of neurogenesis by a spatial learning task (Morris water maze).

NPCs are also involved in pathological contexts. They migrate to astrocytomas of high histopathological grade (high-grade astrocytomas) and reduce glioma expansion, thereby prolonging survival. However, the anti-tumorigenic response of NPCs is lost with aging and primary high grade-astrocytomas are largely restricted to older patients and are almost invariably fatal despite multimodal therapy. In a second approach, the anti-tumorigenic action of NPCs should be investigated.

Here, I show that the young brain has an endogenous defense mechanism against high-grade astrocytomas. The present study is the first to identify NPCs as a cellular source for tumor suppressive fatty-acid ethanolamides that have agonistic activity on TRPV1 channels. TRPV1 expression is higher in human primary high-grade astrocytoma cells than in human NPCs. Activation of TRPV1 leads to an increase in cytotoxicity and endoplasmic reticulum (ER) size in human glioma cells, indicating cell death via the ER-stress pathway. The NPC-induced cell death is TRPV1-dependent *in vitro* and *in vivo* since TRPV1 knockdown or selective TRPV1 antagonists neutralize the cell death-promoting effect. NPC-mediated tumor suppression can be mimicked in the old brain by systemic administration of the synthetic vanilloid arvanil as shown by prolonged survival, indicating that TRPV1 agonists hold potential as new high-grade astrocytoma therapeutics.

7. Zusammenfassung

Teile der Schmerzsignal-Erkennung und -Weiterleitung finden unter Beteiligung des „transient receptor potential vanilloid Typ 1“ (TRPV1)-Kanals statt. Es gibt mehrere klinische Studien, in denen TRPV1-Agonisten eingesetzt werden, um den Rezeptor zu desensibilisieren. Aber auch Antagonisten werden verwendet, um den Rezeptor zu blockieren und Schmerzlinderung zu erwirken. Die Expression von TRPV1 im Gehirn ist ebenfalls etabliert, aber die Funktionen sind größtenteils unverstanden. Aufgrund dieser Tatsache und um unnötige Nebenwirkungen von Medikamenten zu vermeiden, müssen die Expression und Funktion von TRPV1 im Gehirn weiter untersucht werden.

Seit der Entdeckung der Neurogenese im Gehirn im Jahr 1965 von Altman und Das, wurden viele endogene und exogene Faktoren identifiziert, die den Prozess beeinflussen. In den letzten Jahren rückte das Endovanilloid-System, zu dem der TRPV1-Kanal gehört, als ein neuer endogener Modulator der Neurogenese in den Fokus der Aufmerksamkeit.
In meiner Arbeit habe ich eine bisher unbekannte Funktion von TRPV1 im zentralen Nervensystem identifiziert. Ich zeige, dass TRPV1 in den Stammzellnischen in neuralen Vorläuferzellen (NPCs) *in vitro* und *in vivo* exprimiert ist, wenn die Neurogenese physiologisch aktiviert wird. Der Verlust des Rezeptors in TRPV1-Knockout-Mäusen führt zu einer Erhöhung der Proliferation in den Stammzellnischen und in kultivierten NPCs. Die Funktionalität des Rezeptors habe ich durch Kalzium-Imaging in NPC-Kulturen gezeigt. Unter Differenzierungsbedingungen weisen TRPV1-Knockout-NPCs eine erhöhte Expression von Stammzellgenen und eine reduzierte Expression von Differenzierungsmarkern auf. TRPV1-Knockout-Tieren steht daher ein größerer Stammzell-Pool zur Verfügung. Bei einem Test für räumliches Lernen, welcher Hippokampus-abhängig ist, zeigen sich Unterschiede zwischen TRPV1-Wildtyp und -Knockout-Mäusen. TRPV1-Knockout-Tiere erlernen die Aufgabe schneller und haben ein besseres Bezugsgedächtnis. Allerdings zeigen sie eine geringere kognitive Flexibilität. Weiterhin gibt es Unterschiede in der angewandten Suchstrategie.

Zusammenfassend kann ich sagen, dass TRPV1-Expression in den Stammzellnischen wichtig ist, um die Proliferation zu steuern wenn die Neurogenese aktiv ist. Dies kann ich während der postnatalen Neurogenese sowie nach physiologischer Stimulation der Neurogenese durch eine räumliche Lernaufgabe (Morris-Wasserlabyrinth) zeigen.

NPCs sind aber auch an pathologischen Zusammenhängen beteiligt. Sie migrieren zu Astrozytomen mit hohem histopathologischem Grad, reduzieren die Expansion dieses Glioms und erhöhen somit die Überlebenszeit. Allerdings geht die anti-tumorigene Wirkung der NPCs mit zunehmendem Lebensalter verloren. Primäre hochgradige Astrozytome sind weitgehend mit einem höheren Lebensalter des Patienten assoziiert und enden trotz einer multimodalen Therapie fast ausnahmslos tödlich. In einem zweiten Ansatz sollte daher die anti-tumorigene Wirkung von NPCs untersucht werden.
In meiner Arbeit zeige ich, dass das junge Gehirn über einen endogenen Abwehrmechanismus gegen hochgradige Astrozytome verfügt. Die vorliegende Studie ist die erste, die NPCs als zelluläre Quelle für tumorsuppressive Fettsäure-Ethanolamide identifiziert, die agonistische Wirkung an TRPV1-Kanälen haben. Die TRPV1-Expression in humanen primären hochgradigen Astrozytomzellen ist höher als in humanen NPCs. Eine Aktivierung von TRPV1 führt zu einer Erhöhung der Zytotoxizität sowie einer Vergrößerung des endoplasmatischen Retikulums (ER) in humanen Gliomzellen, welches auf Zelltod über den ER-Stress-Weg hindeutet. Der NPC-induzierte Zelltod ist *in vitro* und *in vivo* TRPV1-abhängig, da TRPV1-Knockdown oder selektive TRPV1-Antagonisten die Zelltod-fördernde Wirkung neutralisieren können. Weiterhin kann die NPC-vermittelte Tumorsuppression im alten Gehirn durch systemische Verabreichung des synthetischen Vanilloids Arvanil nachgeahmt werden und die Überlebenszeit verlängern, was darauf hindeutet, dass TRPV1-Agonisten therapeutisches Potential als neue Therapeutika gegen hochgradige Astrozytome besitzen.

8. References

Aboody, K.S., Brown, A., Rainov, N.G., Bower, K.A., Liu, S., Yang, W., Small, J.E., Herrlinger, U., Ourednik, V., Black, P.M. (2000). Neural stem cells display extensive tropism for pathology in adult brain: evidence from intracranial gliomas. *Proc Natl Acad Sci U S A* 97, 12846-12851.

Abrous, D.N., Koehl, M.and Le Moal, M. (2005). Adult neurogenesis: from precursors to network and physiology. *Physiological reviews* 85, 523-569.

Acs, G., Palkovits, M.and Blumberg, P.M. (1996). Specific binding of [3H]resiniferatoxin by human and rat preoptic area, locus ceruleus, medial hypothalamus, reticular formation and ventral thalamus membrane preparations. *Life Sci* 59, 1899-1908.

Aguado, T., Monory, K., Palazuelos, J., Stella, N., Cravatt, B., Lutz, B., Marsicano, G., Kokaia, Z., Guzman, M.and Galve-Roperh, I. (2005). The endocannabinoid system drives neural progenitor proliferation. *FASEB J* 19, 1704-1706.

Aguado, T., Palazuelos, J., Monory, K., Stella, N., Cravatt, B., Lutz, B., Marsicano, G., Kokaia, Z., Guzman, M.and Galve-Roperh, I. (2006). The endocannabinoid system promotes astroglial differentiation by acting on neural progenitor cells. *J Neurosci* 26, 1551-1561.

Aimone, J.B., Deng, W.and Gage, F.H. (2011). Resolving new memories: a critical look at the dentate gyrus, adult neurogenesis, and pattern separation. *Neuron* 70, 589-596.

Al-Hayani, A., Wease, K.N., Ross, R.A., Pertwee, R.G.and Davies, S.N. (2001). The endogenous cannabinoid anandamide activates vanilloid receptors in the rat hippocampal slice. *Neuropharmacology* 41, 1000-1005.

Altman, J. (1969). Autoradiographic and histological studies of postnatal neurogenesis. IV. Cell proliferation and migration in the anterior forebrain, with special reference to persisting neurogenesis in the olfactory bulb. *J Comp Neurol* 137, 433-457.

Altman, J.and Das, G.D. (1965). Autoradiographic and histological evidence of postnatal hippocampal neurogenesis in rats. *J Comp Neurol* 124, 319-335.

Altman, J.and Das, G.D. (1967). Postnatal neurogenesis in the guinea-pig. *Nature* 214, 1098-1101.

Alvarez-Buylla, A.and Lim, D.A. (2004). For the long run: maintaining germinal niches in the adult brain. *Neuron* 41, 683-686.

Amantini, C., Ballarini, P., Caprodossi, S., Nabissi, M., Morelli, M.B., Lucciarini, R., Cardarelli, M.A., Mammana, G.and Santoni, G. (2009). Triggering of transient receptor potential vanilloid type 1 (TRPV1) by capsaicin induces Fas/CD95-mediated apoptosis of urothelial cancer cells in an ATM-dependent manner. *Carcinogenesis* 30, 1320-1329.

Amantini, C., Mosca, M., Nabissi, M., Lucciarini, R., Caprodossi, S., Arcella, A., Giangaspero, F.and Santoni, G. (2007). Capsaicin-induced apoptosis of glioma cells is mediated by TRPV1 vanilloid receptor and requires p38 MAPK activation. *Journal of neurochemistry* 102, 977-990.

Amariglio, N., Hirshberg, A., Scheithauer, B.W., Cohen, Y., Loewenthal, R., Trakhtenbrot, L., Paz, N., Koren-Michowitz, M., Waldman, D., Leider-Trejo, L. (2009). Donor-derived brain tumor following neural stem cell transplantation in an ataxia telangiectasia patient. *PLoS Med* 6, e1000029.

Amaya, F., Shimosato, G., Nagano, M., Ueda, M., Hashimoto, S., Tanaka, Y., Suzuki, H.and Tanaka, M. (2004). NGF and GDNF differentially regulate TRPV1 expression that contributes to development of inflammatory thermal hyperalgesia. *Eur J Neurosci* 20, 2303-2310.

Arevalo-Martin, A., Garcia-Ovejero, D., Rubio-Araiz, A., Gomez, O., Molina-Holgado, F.and Molina-Holgado, E. (2007). Cannabinoids modulate Olig2 and polysialylated neural cell adhesion molecule expression in the subventricular zone of post-natal rats through cannabinoid receptor 1 and cannabinoid receptor 2. *Eur J Neurosci* 26, 1548-1559.

Arvidsson, A., Collin, T., Kirik, D., Kokaia, Z.and Lindvall, O. (2002). Neuronal replacement from endogenous precursors in the adult brain after stroke. *Nat Med* 8, 963-970.

Arvidsson, A., Kokaia, Z.and Lindvall, O. (2001). N-methyl-D-aspartate receptor-mediated increase of neurogenesis in adult rat dentate gyrus following stroke. *Eur J Neurosci* 14, 10-18.

Assanah, M., Lochhead, R., Ogden, A., Bruce, J., Goldman, J.and Canoll, P. (2006). Glial progenitors in adult white matter are driven to form malignant gliomas by platelet-derived growth factor-expressing retroviruses. *J Neurosci* 26, 6781-6790.

Assanah, M.C., Bruce, J.N., Suzuki, S.O., Chen, A., Goldman, J.E.and Canoll, P. (2009). PDGF stimulates the massive expansion of glial progenitors in the neonatal forebrain. *Glia* 57, 1835-1847.

Bai, F., Bergeron, M.and Nelson, D.L. (2003). Chronic AMPA receptor potentiator (LY451646) treatment increases cell proliferation in adult rat hippocampus. *Neuropharmacology* 44, 1013-1021.

Bari, M., Tedesco, M., Battista, N., Pasquariello, N., Pucci, M., Gasperi, V., Scaldaferri, M.L., Farini, D., De Felici, M.and Maccarrone, M. (2011). Characterization of the endocannabinoid system in mouse embryonic stem cells. *Stem Cells Dev* 20, 139-147.

Bayer, S.A. (1983). 3H-thymidine-radiographic studies of neurogenesis in the rat olfactory bulb. *Exp Brain Res* 50, 329-340.

Berghuis, P., Dobszay, M.B., Wang, X., Spano, S., Ledda, F., Sousa, K.M., Schulte, G., Ernfors, P., Mackie, K., Paratcha, G. (2005). Endocannabinoids regulate interneuron migration and morphogenesis by transactivating the TrkB receptor. *Proc Natl Acad Sci U S A* 102, 19115-19120.

Bick-Sander, A., Steiner, B., Wolf, S.A., Babu, H.and Kempermann, G. (2006). Running in pregnancy transiently increases postnatal hippocampal neurogenesis in the offspring. *Proc Natl Acad Sci U S A* 103, 3852-3857.

Bilkei-Gorzo, A., Racz, I., Valverde, O., Otto, M., Michel, K., Sastre, M.and Zimmer, A. (2005). Early age-related cognitive impairment in mice lacking cannabinoid CB1 receptors. *Proc Natl Acad Sci U S A* 102, 15670-15675.

Birder, L.A., Kanai, A.J., de Groat, W.C., Kiss, S., Nealen, M.L., Burke, N.E., Dineley, K.E., Watkins, S., Reynolds, I.J.and Caterina, M.J. (2001). Vanilloid receptor expression suggests a sensory role for urinary bladder epithelial cells. *Proc Natl Acad Sci U S A* 98, 13396-13401.

Birder, L.A., Nakamura, Y., Kiss, S., Nealen, M.L., Barrick, S., Kanai, A.J., Wang, E., Ruiz, G., De Groat, W.C., Apodaca, G. (2002). Altered urinary bladder function in mice lacking the vanilloid receptor TRPV1. *Nat Neurosci* 5, 856-860.

Biro, T., Brodie, C., Modarres, S., Lewin, N.E., Acs, P.and Blumberg, P.M. (1998). Specific vanilloid responses in C6 rat glioma cells. *Brain Res Mol Brain Res* 56, 89-98.

Bisogno, T., Maurelli, S., Melck, D., De Petrocellis, L.and Di Marzo, V. (1997). Biosynthesis, uptake, and degradation of anandamide and palmitoylethanolamide in leukocytes. *J Biol Chem* 272, 3315-3323.

Blazquez, C., Carracedo, A., Barrado, L., Real, P.J., Fernandez-Luna, J.L., Velasco, G., Malumbres, M.and Guzman, M. (2006). Cannabinoid receptors as novel targets for the treatment of melanoma. *FASEB J* 20, 2633-2635.

Blazquez, C., Casanova, M.L., Planas, A., Gomez Del Pulgar, T., Villanueva, C., Fernandez-Acenero, M.J., Aragones, J., Huffman, J.W., Jorcano, J.L.and Guzman, M. (2003). Inhibition of tumor angiogenesis by cannabinoids. *FASEB J* 17, 529-531.

Bleeker, F.E., Molenaar, R.J.and Leenstra, S. (2012). Recent advances in the molecular understanding of glioblastoma. *J Neurooncol*.

Bobola, M.S., Tseng, S.H., Blank, A., Berger, M.S.and Silber, J.R. (1996). Role of O6-methylguanine-DNA methyltransferase in resistance of human brain tumor cell lines to the clinically relevant methylating agents temozolomide and streptozotocin. *Clin Cancer Res* 2, 735-741.

Bode, A.M., Cho, Y.Y., Zheng, D., Zhu, F., Ericson, M.E., Ma, W.Y., Yao, K.and Dong, Z. (2009). Transient receptor potential type vanilloid 1 suppresses skin carcinogenesis. *Cancer Res* 69, 905-913.

Brezun, J.M.and Daszuta, A. (2000). Serotonin may stimulate granule cell proliferation in the adult hippocampus, as observed in rats grafted with foetal raphe neurons. *Eur J Neurosci* 12, 391-396.

Bruehlmeier, M., Roelcke, U., Blauenstein, P., Missimer, J., Schubiger, P.A., Locher, J.T., Pellikka, R.and Ametamey, S.M. (2003). Measurement of the extracellular space in brain tumors using 76Br-bromide and PET. *Journal of nuclear medicine : official publication, Society of Nuclear Medicine* 44, 1210-1218.

Bruel-Jungerman, E., Rampon, C.and Laroche, S. (2007). Adult hippocampal neurogenesis, synaptic plasticity and memory: facts and hypotheses. *Reviews in the neurosciences* 18, 93-114.

Brun, V.H., Ytterbo, K., Morris, R.G., Moser, M.B.and Moser, E.I. (2001). Retrograde amnesia for spatial memory induced by NMDA receptor-mediated long-term potentiation. *J Neurosci* 21, 356-362.

Cameron, H.A., McEwen, B.S.and Gould, E. (1995). Regulation of adult neurogenesis by excitatory input and NMDA receptor activation in the dentate gyrus. *J Neurosci* 15, 4687-4692.

Cameron, H.A., Woolley, C.S., McEwen, B.S.and Gould, E. (1993). Differentiation of newly born neurons and glia in the dentate gyrus of the adult rat. *Neuroscience* 56, 337-344.

Carracedo, A., Gironella, M., Lorente, M., Garcia, S., Guzman, M., Velasco, G.and Iovanna, J.L. (2006a). Cannabinoids induce apoptosis of pancreatic tumor cells via endoplasmic reticulum stress-related genes. *Cancer Res* 66, 6748-6755.

Carracedo, A., Lorente, M., Egia, A., Blazquez, C., Garcia, S., Giroux, V., Malicet, C., Villuendas, R., Gironella, M., Gonzalez-Feria, L. (2006b). The stress-regulated protein p8 mediates cannabinoid-induced apoptosis of tumor cells. *Cancer cell* 9, 301-312.

Casanova, M.L., Blazquez, C., Martinez-Palacio, J., Villanueva, C., Fernandez-Acenero, M.J., Huffman, J.W., Jorcano, J.L.and Guzman, M. (2003). Inhibition of skin tumor growth and angiogenesis in vivo by activation of cannabinoid receptors. *J Clin Invest* 111, 43-50.

Caterina, M.J. (2003). Vanilloid receptors take a TRP beyond the sensory afferent. *Pain* 105, 5-9.

Caterina, M.J.and Julius, D. (2001). The vanilloid receptor: a molecular gateway to the pain pathway. *Annu Rev Neurosci* 24, 487-517.

Caterina, M.J., Leffler, A., Malmberg, A.B., Martin, W.J., Trafton, J., Petersen-Zeitz, K.R., Koltzenburg, M., Basbaum, A.I.and Julius, D. (2000). Impaired nociception and pain sensation in mice lacking the capsaicin receptor. *Science* 288, 306-313.

Caterina, M.J., Schumacher, M.A., Tominaga, M., Rosen, T.A., Levine, J.D.and Julius, D. (1997). The capsaicin receptor: a heat-activated ion channel in the pain pathway. *Nature* 389, 816-824.

Cavanaugh, D.J., Chesler, A.T., Jackson, A.C., Sigal, Y.M., Yamanaka, H., Grant, R., O'Donnell, D., Nicoll, R.A., Shah, N.M., Julius, D. (2011). Trpv1 reporter mice reveal highly restricted brain distribution and functional expression in arteriolar smooth muscle cells. *J Neurosci* 31, 5067-5077.

Cernak, I., Vink, R., Natale, J., Stoica, B., Lea, P.M.t., Movsesyan, V., Ahmed, F., Knoblach, S.M., Fricke, S.T.and Faden, A.I. (2004). The "dark side" of endocannabinoids: a neurotoxic role for anandamide. *Journal of cerebral blood flow and metabolism : official journal of the International Society of Cerebral Blood Flow and Metabolism* 24, 564-578.

Chan, G.C., Hinds, T.R., Impey, S.and Storm, D.R. (1998). Hippocampal neurotoxicity of Delta9-tetrahydrocannabinol. *J Neurosci* 18, 5322-5332.

Chavez, A.E., Chiu, C.Q.and Castillo, P.E. (2010). TRPV1 activation by endogenous anandamide triggers postsynaptic long-term depression in dentate gyrus. *Nat Neurosci* 13, 1511-1518.

Chen, C.W., Lee, S.T., Wu, W.T., Fu, W.M., Ho, F.M.and Lin, W.W. (2003). Signal transduction for inhibition of inducible nitric oxide synthase and cyclooxygenase-2 induction by capsaicin and related analogs in macrophages. *Br J Pharmacol* 140, 1077-1087.

Chen, Y., Willcockson, H.H.and Valtschanoff, J.G. (2009). Influence of the vanilloid receptor TRPV1 on the activation of spinal cord glia in mouse models of pain. *Experimental neurology* 220, 383-390.

Chirasani, S.R., Sternjak, A., Wend, P., Momma, S., Campos, B., Herrmann, I.M., Graf, D., Mitsiadis, T., Herold-Mende, C., Besser, D. (2010). Bone morphogenetic protein-7 release from endogenous neural precursor cells suppresses the tumourigenicity of stem-like glioblastoma cells. *Brain* 133, 1961-1972.

Chuang, H.H., Prescott, E.D., Kong, H., Shields, S., Jordt, S.E., Basbaum, A.I., Chao, M.V.and Julius, D. (2001). Bradykinin and nerve growth factor release the capsaicin receptor from PtdIns(4,5)P2-mediated inhibition. *Nature* 411, 957-962.

Contassot, E., Wilmotte, R., Tenan, M., Belkouch, M.C., Schnuriger, V., de Tribolet, N., Burkhardt, K.and Dietrich, P.Y. (2004). Arachidonylethanolamide induces apoptosis of human glioma cells through vanilloid receptor-1. *Journal of neuropathology and experimental neurology* 63, 956-963.

Corotto, F.S., Henegar, J.A.and Maruniak, J.A. (1993). Neurogenesis persists in the subependymal layer of the adult mouse brain. *Neurosci Lett* 149, 111-114.

Cortright, D.N.and Szallasi, A. (2009). TRP channels and pain. *Curr Pharm Des* 15, 1736-1749.

Cristino, L., de Petrocellis, L., Pryce, G., Baker, D., Guglielmotti, V.and Di Marzo, V. (2006). Immunohistochemical localization of cannabinoid type 1 and vanilloid transient receptor potential vanilloid type 1 receptors in the mouse brain. *Neuroscience* 139, 1405-1415.

Cudaback, E., Marrs, W., Moeller, T.and Stella, N. (2010). The expression level of CB1 and CB2 receptors determines their efficacy at inducing apoptosis in astrocytomas. *PLoS One* 5, e8702.

Cullen, B.R. (2006). Enhancing and confirming the specificity of RNAi experiments. *Nat Methods* 3, 677-681.

Curtis, M.A., Faull, R.L.and Glass, M. (2006). A novel population of progenitor cells expressing cannabinoid receptors in the subependymal layer of the adult normal and Huntington's disease human brain. *J Chem Neuroanat* 31, 210-215.

Daly, D., Rong, W., Chess-Williams, R., Chapple, C.and Grundy, D. (2007). Bladder afferent sensitivity in wild-type and TRPV1 knockout mice. *J Physiol* 583, 663-674.

Darsalia, V., Heldmann, U., Lindvall, O.and Kokaia, Z. (2005). Stroke-induced neurogenesis in aged brain. *Stroke* 36, 1790-1795.

Dash, P.K., Mach, S.A.and Moore, A.N. (2001). Enhanced neurogenesis in the rodent hippocampus following traumatic brain injury. *Journal of neuroscience research* 63, 313-319.

Davis, J.B., Gray, J., Gunthorpe, M.J., Hatcher, J.P., Davey, P.T., Overend, P., Harries, M.H., Latcham, J., Clapham, C., Atkinson, K. (2000). Vanilloid receptor-1 is essential for inflammatory thermal hyperalgesia. *Nature* 405, 183-187.

de Godoy, L.M., Olsen, J.V., Cox, J., Nielsen, M.L., Hubner, N.C., Frohlich, F., Walther, T.C.and Mann, M. (2008). Comprehensive mass-spectrometry-based proteome quantification of haploid versus diploid yeast. *Nature* 455, 1251-1254.

De Jesus, M.L., Hostalot, C., Garibi, J.M., Salles, J., Meana, J.J.and Callado, L.F. (2010). Opposite changes in cannabinoid CB1 and CB2 receptor expression in human gliomas. *Neurochem Int* 56, 829-833.

de Lago, E., de Miguel, R., Lastres-Becker, I., Ramos, J.A.and Fernandez-Ruiz, J. (2004). Involvement of vanilloid-like receptors in the effects of anandamide on motor behavior and nigrostriatal dopaminergic activity: in vivo and in vitro evidence. *Brain Res* 1007, 152-159.

DeAngelis, L.M. (2001). Brain tumors. *N Engl J Med* 344, 114-123.

Denda, M., Fuziwara, S., Inoue, K., Denda, S., Akamatsu, H., Tomitaka, A.and Matsunaga, K. (2001). Immunoreactivity of VR1 on epidermal keratinocyte of human skin. *Biochem Biophys Res Commun* 285, 1250-1252.

Deng, W., Aimone, J.B.and Gage, F.H. (2010). New neurons and new memories: how does adult hippocampal neurogenesis affect learning and memory? *Nat Rev Neurosci* 11, 339-350.

Derbenev, A.V., Monroe, M.J., Glatzer, N.R.and Smith, B.N. (2006). Vanilloid-mediated heterosynaptic facilitation of inhibitory synaptic input to neurons of the rat dorsal motor nucleus of the vagus. *J Neurosci* 26, 9666-9672.

Devane, W.A., Breuer, A., Sheskin, T., Jarbe, T.U., Eisen, M.S.and Mechoulam, R. (1992). A novel probe for the cannabinoid receptor. *J Med Chem* 35, 2065-2069.

Dhaka, A., Uzzell, V., Dubin, A.E., Mathur, J., Petrus, M., Bandell, M.and Patapoutian, A. (2009). TRPV1 is activated by both acidic and basic pH. *J Neurosci* 29, 153-158.

Di Marzo, V., Bisogno, T.and De Petrocellis, L. (2001). Anandamide: some like it hot. *Trends Pharmacol Sci* 22, 346-349.

Di Marzo, V., Fontana, A., Cadas, H., Schinelli, S., Cimino, G., Schwartz, J.C.and Piomelli, D. (1994). Formation and inactivation of endogenous cannabinoid anandamide in central neurons. *Nature* 372, 686-691.

Docherty, R.J., Yeats, J.C., Bevan, S.and Boddeke, H.W. (1996). Inhibition of calcineurin inhibits the desensitization of capsaicin-evoked currents in cultured dorsal root ganglion neurones from adult rats. *Pflugers Arch* 431, 828-837.

Doetsch, F., Garcia-Verdugo, J.M.and Alvarez-Buylla, A. (1997). Cellular composition and three-dimensional organization of the subventricular germinal zone in the adult mammalian brain. *J Neurosci* 17, 5046-5061.

Domotor, A., Peidl, Z., Vincze, A., Hunyady, B., Szolcsanyi, J., Kereskay, L., Szekeres, G.and Mozsik, G. (2005). Immunohistochemical distribution of vanilloid receptor, calcitonin-gene related peptide and substance P in gastrointestinal mucosa of patients with different gastrointestinal disorders. *Inflammopharmacology* 13, 161-177.

Downer, E.J., Fogarty, M.P.and Campbell, V.A. (2003). Tetrahydrocannabinol-induced neurotoxicity depends on CB1 receptor-mediated c-Jun N-terminal kinase activation in cultured cortical neurons. *Br J Pharmacol* 140, 547-557.

Ellert-Miklaszewska, A., Kaminska, B.and Konarska, L. (2005). Cannabinoids down-regulate PI3K/Akt and Erk signalling pathways and activate proapoptotic function of Bad protein. *Cellular signalling* 17, 25-37.

Eriksson, P.S., Perfilieva, E., Bjork-Eriksson, T., Alborn, A.M., Nordborg, C., Peterson, D.A.and Gage, F.H. (1998). Neurogenesis in the adult human hippocampus. *Nat Med* 4, 1313-1317.

Fabel, K., Wolf, S.A., Ehninger, D., Babu, H., Leal-Galicia, P.and Kempermann, G. (2009). Additive effects of physical exercise and environmental enrichment on adult hippocampal neurogenesis in mice. *Front Neurosci* 3, 50.

Fischbach, T., Greffrath, W., Nawrath, H.and Treede, R.D. (2007). Effects of anandamide and noxious heat on intracellular calcium concentration in nociceptive drg neurons of rats. *J Neurophysiol* 98, 929-938.

Fogaça, M.V., Aguiar, D.C., Moreira, F.A.and Guimarães, F.S. (2012). The endocannabinoid and endovanilloid systems interact in the rat prelimbic medial prefrontal cortex to control anxiety-like behavior. *Neuropharmacology*.

Freund, T.F., Katona, I.and Piomelli, D. (2003). Role of endogenous cannabinoids in synaptic signaling. *Physiological reviews* 83, 1017-1066.

Friese, M.A., Steinle, A.and Weller, M. (2004). The innate immune response in the central nervous system and its role in glioma immune surveillance. *Onkologie* 27, 487-491.

Gage, F.H. (2000). Mammalian neural stem cells. *Science* 287, 1433-1438.

Galoyan, S.M., Petruska, J.C.and Mendell, L.M. (2003). Mechanisms of sensitization of the response of single dorsal root ganglion cells from adult rat to noxious heat. *Eur J Neurosci* 18, 535-541.

Galve-Roperh, I., Aguado, T., Rueda, D., Velasco, G.and Guzman, M. (2006). Endocannabinoids: a new family of lipid mediators involved in the regulation of neural cell development. *Curr Pharm Des* 12, 2319-2325.

Galve-Roperh, I., Sanchez, C., Cortes, M.L., Gomez del Pulgar, T., Izquierdo, M.and Guzman, M. (2000). Anti-tumoral action of cannabinoids: involvement of sustained ceramide accumulation and extracellular signal-regulated kinase activation. *Nat Med* 6, 313-319.

Garcia-Sanz, N., Fernandez-Carvajal, A., Morenilla-Palao, C., Planells-Cases, R., Fajardo-Sanchez, E., Fernandez-Ballester, G.and Ferrer-Montiel, A. (2004). Identification of a tetramerization domain in the C terminus of the vanilloid receptor. *J Neurosci* 24, 5307-5314.

Garthe, A., Behr, J.and Kempermann, G. (2009). Adult-generated hippocampal neurons allow the flexible use of spatially precise learning strategies. *PLoS One* 4, e5464.

Gibson, H.E., Edwards, J.G., Page, R.S., Van Hook, M.J.and Kauer, J.A. (2008). TRPV1 channels mediate long-term depression at synapses on hippocampal interneurons. *Neuron* 57, 746-759.

Giuffrida, A., Leweke, F.M., Gerth, C.W., Schreiber, D., Koethe, D., Faulhaber, J., Klosterkotter, J.and Piomelli, D. (2004). Cerebrospinal anandamide levels are elevated in acute schizophrenia and are inversely correlated with psychotic symptoms. *Neuropsychopharmacology* 29, 2108-2114.

Gkika, D.and Prevarskaya, N. (2009). Molecular mechanisms of TRP regulation in tumor growth and metastasis. *Biochimica et biophysica acta* 1793, 953-958.

Glass, R., Synowitz, M., Kronenberg, G., Walzlein, J.H., Markovic, D.S., Wang, L.P., Gast, D., Kiwit, J., Kempermann, G.and Kettenmann, H. (2005). Glioblastoma-induced attraction of endogenous neural precursor cells is associated with improved survival. *J Neurosci* 25, 2637-2646.

Goadsby, P.J. (2007). Emerging therapies for migraine. *Nat Clin Pract Neurol* 3, 610-619.

Goldman, S.A., Nedergaard, M., Crystal, R.G., Fraser, R.A., Goodman, R., Harrison-Restelli, C., Jiang, J., Keyoung, H.M., Leventhal, C., Pincus, D.W. (1997). Neural precursors and neuronal production in the adult mammalian forebrain. *Ann N Y Acad Sci* 835, 30-55.

Gomez Del Pulgar, T., De Ceballos, M.L., Guzman, M.and Velasco, G. (2002a). Cannabinoids protect astrocytes from ceramide-induced apoptosis through the phosphatidylinositol 3-kinase/protein kinase B pathway. *J Biol Chem* 277, 36527-36533.

Gomez del Pulgar, T., Velasco, G., Sanchez, C., Haro, A.and Guzman, M. (2002b). De novo-synthesized ceramide is involved in cannabinoid-induced apoptosis. *Biochem J* 363, 183-188.

Gould, E.and Gross, C.G. (2002). Neurogenesis in adult mammals: some progress and problems. *J Neurosci* 22, 619-623.

Gould, E., Vail, N., Wagers, M.and Gross, C.G. (2001). Adult-generated hippocampal and neocortical neurons in macaques have a transient existence. *Proc Natl Acad Sci U S A* 98, 10910-10917.

Graziano, A., Petrosini, L.and Bartoletti, A. (2003). Automatic recognition of explorative strategies in the Morris water maze. *Journal of neuroscience methods* 130, 33-44.

Grootendorst, J., de Kloet, E.R., Dalm, S.and Oitzl, M.S. (2001). Reversal of cognitive deficit of apolipoprotein E knockout mice after repeated exposure to a common environmental experience. *Neuroscience* 108, 237-247.

Grueter, B.A., Brasnjo, G.and Malenka, R.C. (2010). Postsynaptic TRPV1 triggers cell type-specific long-term depression in the nucleus accumbens. *Nat Neurosci* 13, 1519-1525.

Grunweller, A., Wyszko, E., Bieber, B., Jahnel, R., Erdmann, V.A.and Kurreck, J. (2003). Comparison of different antisense strategies in mammalian cells using locked nucleic acids, 2'-O-methyl RNA, phosphorothioates and small interfering RNA. *Nucleic Acids Res* 31, 3185-3193.

Gustafsson, K., Christensson, B., Sander, B.and Flygare, J. (2006). Cannabinoid receptor-mediated apoptosis induced by R(+)-methanandamide and Win55,212-2 is associated with ceramide accumulation and p38 activation in mantle cell lymphoma. *Mol Pharmacol* 70, 1612-1620.

Guzman, M. (2003). Cannabinoids: potential anticancer agents. *Nat Rev Cancer* 3, 745-755.

Guzman, M., Duarte, M.J., Blazquez, C., Ravina, J., Rosa, M.C., Galve-Roperh, I., Sanchez, C., Velasco, G.and Gonzalez-Feria, L. (2006). A pilot clinical study of Delta9-tetrahydrocannabinol in patients with recurrent glioblastoma multiforme. *Br J Cancer* 95, 197-203.

Hallbergson, A.F., Gnatenco, C.and Peterson, D.A. (2003). Neurogenesis and brain injury: managing a renewable resource for repair. *J Clin Invest* 112, 1128-1133.

Hansen, H.H., Schmid, P.C., Bittigau, P., Lastres-Becker, I., Berrendero, F., Manzanares, J., Ikonomidou, C., Schmid, H.H., Fernandez-Ruiz, J.J.and Hansen, H.S. (2001). Anandamide, but not 2-arachidonoylglycerol, accumulates during in vivo neurodegeneration. *Journal of neurochemistry* 78, 1415-1427.

Hardman, H.F., Domino, E.F.and Seevers, M.H. (1971). General pharmacological actions of some synthetic tetrahydrocannabinol derivatives. *Pharmacol Rev* 23, 295-315.

Hartel, M., di Mola, F.F., Selvaggi, F., Mascetta, G., Wente, M.N., Felix, K., Giese, N.A., Hinz, U., Di Sebastiano, P., Buchler, M.W. (2006). Vanilloids in pancreatic cancer: potential for chemotherapy and pain management. *Gut* 55, 519-528.

Heiner, I., Eisfeld, J., Halaszovich, C.R., Wehage, E., Jungling, E., Zitt, C.and Luckhoff, A. (2003). Expression profile of the transient receptor potential (TRP) family in neutrophil granulocytes: evidence for currents through long TRP channel 2 induced by ADP-ribose and NAD. *Biochem J* 371, 1045-1053.

Ho, W.S.and Gardiner, S.M. (2009). Acute hypertension reveals depressor and vasodilator effects of cannabinoids in conscious rats. *Br J Pharmacol* 156, 94-104.

Hong, S., Fan, J., Kemmerer, E.S., Evans, S., Li, Y.and Wiley, J.W. (2009). Reciprocal changes in vanilloid (TRPV1) and endocannabinoid (CB1) receptors contribute to visceral hyperalgesia in the water avoidance stressed rat. *Gut* 58, 202-210.

Huang, S.M., Bisogno, T., Trevisani, M., Al-Hayani, A., De Petrocellis, L., Fezza, F., Tognetto, M., Petros, T.J., Krey, J.F., Chu, C.J. (2002). An endogenous capsaicin-like substance with high potency at recombinant and native vanilloid VR1 receptors. *Proc Natl Acad Sci U S A* 99, 8400-8405.

Inoue, K., Koizumi, S., Fuziwara, S., Denda, S.and Denda, M. (2002). Functional vanilloid receptors in cultured normal human epidermal keratinocytes. *Biochem Biophys Res Commun* 291, 124-129.

Ishii, I.and Chun, J. (2002). Anandamide-induced neuroblastoma cell rounding via the CB1 cannabinoid receptors. *Neuroreport* 13, 593-596.

Jacobsson, S.O., Rongard, E., Stridh, M., Tiger, G.and Fowler, C.J. (2000). Serum-dependent effects of tamoxifen and cannabinoids upon C6 glioma cell viability. *Biochem Pharmacol* 60, 1807-1813.

Janus, C. (2004). Search strategies used by APP transgenic mice during navigation in the Morris water maze. *Learn Mem* 11, 337-346.

Jara-Oseguera, A., Simon, S.A.and Rosenbaum, T. (2008). TRPV1: on the road to pain relief. *Curr Mol Pharmacol* 1, 255-269.

Jessberger, S., Toni, N., Clemenson, G.D., Jr., Ray, J.and Gage, F.H. (2008). Directed differentiation of hippocampal stem/progenitor cells in the adult brain. *Nat Neurosci* 11, 888-893.

Ji, R.R., Samad, T.A., Jin, S.X., Schmoll, R.and Woolf, C.J. (2002). p38 MAPK activation by NGF in primary sensory neurons after inflammation increases TRPV1 levels and maintains heat hyperalgesia. *Neuron* 36, 57-68.

Jiang, W., Zhang, Y., Xiao, L., Van Cleemput, J., Ji, S.P., Bai, G.and Zhang, X. (2005). Cannabinoids promote embryonic and adult hippocampus neurogenesis and produce anxiolytic- and antidepressant-like effects. *J Clin Invest* 115, 3104-3116.

Jin, K., Sun, Y., Xie, L., Peel, A., Mao, X.O., Batteur, S.and Greenberg, D.A. (2003). Directed migration of neuronal precursors into the ischemic cerebral cortex and striatum. *Mol Cell Neurosci* 24, 171-189.

Jin, K., Xie, L., Kim, S.H., Parmentier-Batteur, S., Sun, Y., Mao, X.O., Childs, J.and Greenberg, D.A. (2004). Defective adult neurogenesis in CB1 cannabinoid receptor knockout mice. *Mol Pharmacol* 66, 204-208.

Jones, B.J.and Roberts, D.J. (1968). The quantiative measurement of motor inco-ordination in naive mice using an acelerating rotarod. *The Journal of pharmacy and pharmacology* 20, 302-304.

Kaplan, M.S. (1985). Formation and turnover of neurons in young and senescent animals: an electronmicroscopic and morphometric analysis. *Ann N Y Acad Sci* 457, 173-192.

Kaplan, M.S.and Bell, D.H. (1983). Neuronal proliferation in the 9-month-old rodent-radioautographic study of granule cells in the hippocampus. *Exp Brain Res* 52, 1-5.

Kaplan, M.S.and Bell, D.H. (1984). Mitotic neuroblasts in the 9-day-old and 11-month-old rodent hippocampus. *J Neurosci* 4, 1429-1441.

Kaplan, M.S.and Hinds, J.W. (1977). Neurogenesis in the adult rat: electron microscopic analysis of light radioautographs. *Science* 197, 1092-1094.

Karasu, T., Marczylo, T.H., Maccarrone, M.and Konje, J.C. (2011). The role of sex steroid hormones, cytokines and the endocannabinoid system in female fertility. *Hum Reprod Update* 17, 347-361.

Kempermann, G. (2002). Regulation of adult hippocampal neurogenesis - implications for novel theories of major depression. *Bipolar Disord* 4, 17-33.

Kempermann, G., ed. (2006). Adult Neurogenesis. Stem Cells and Neuronal Development in the Adult Brain (Oxford University Press).

Kempermann, G., Jessberger, S., Steiner, B.and Kronenberg, G. (2004a). Milestones of neuronal development in the adult hippocampus. *Trends Neurosci* 27, 447-452.

Kempermann, G., Kuhn, H.G.and Gage, F.H. (1997). More hippocampal neurons in adult mice living in an enriched environment. *Nature* 386, 493-495.

Kempermann, G., Wiskott, L.and Gage, F.H. (2004b). Functional significance of adult neurogenesis. *Curr Opin Neurobiol* 14, 186-191.

Kim, D.and Thayer, S.A. (2001). Cannabinoids inhibit the formation of new synapses between hippocampal neurons in culture. *J Neurosci* 21, RC146.

Kim, S.R., Kim, S.U., Oh, U.and Jin, B.K. (2006). Transient receptor potential vanilloid subtype 1 mediates microglial cell death in vivo and in vitro via Ca2+-mediated mitochondrial damage and cytochrome c release. *J Immunol* 177, 4322-4329.

Kim, S.R., Lee, D.Y., Chung, E.S., Oh, U.T., Kim, S.U.and Jin, B.K. (2005). Transient receptor potential vanilloid subtype 1 mediates cell death of mesencephalic dopaminergic neurons in vivo and in vitro. *J Neurosci* 25, 662-671.

Kishi, K. (1987). Golgi studies on the development of granule cells of the rat olfactory bulb with reference to migration in the subependymal layer. *J Comp Neurol* 258, 112-124.

Kleihues, P., Burger, P.C.and Scheithauer, B.W. (1993). The new WHO classification of brain tumours. *Brain Pathol* 3, 255-268.

Kornack, D.R.and Rakic, P. (1999). Continuation of neurogenesis in the hippocampus of the adult macaque monkey. *Proc Natl Acad Sci U S A* 96, 5768-5773.

Kornack, D.R.and Rakic, P. (2001a). Cell proliferation without neurogenesis in adult primate neocortex. *Science* 294, 2127-2130.

Kornack, D.R.and Rakic, P. (2001b). The generation, migration, and differentiation of olfactory neurons in the adult primate brain. *Proc Natl Acad Sci U S A* 98, 4752-4757.

Kowalczyk, A., Filipkowski, R.K., Rylski, M., Wilczynski, G.M., Konopacki, F.A., Jaworski, J., Ciemerych, M.A., Sicinski, P.and Kaczmarek, L. (2004). The critical role of cyclin D2 in adult neurogenesis. *J Cell Biol* 167, 209-213.

Kronenberg, G., Bick-Sander, A., Bunk, E., Wolf, C., Ehninger, D.and Kempermann, G. (2006). Physical exercise prevents age-related decline in precursor cell activity in the mouse dentate gyrus. *Neurobiol Aging* 27, 1505-1513.

Kuhn, H.G., Dickinson-Anson, H.and Gage, F.H. (1996). Neurogenesis in the dentate gyrus of the adult rat: age-related decrease of neuronal progenitor proliferation. *J Neurosci* 16, 2027-2033.

Lafourcade, M., Larrieu, T., Mato, S., Duffaud, A., Sepers, M., Matias, I., De Smedt-Peyrusse, V., Labrousse, V.F., Bretillon, L., Matute, C. (2011). Nutritional omega-3 deficiency abolishes endocannabinoid-mediated neuronal functions. *Nat Neurosci* 14, 345-350.

Lang, U.E., Lang, F., Richter, K., Vallon, V., Lipp, H.P., Schnermann, J.and Wolfer, D.P. (2003). Emotional instability but intact spatial cognition in adenosine receptor 1 knock out mice. *Behav Brain Res* 145, 179-188.

Lazzeri, M., Vannucchi, M.G., Spinelli, M., Bizzoco, E., Beneforti, P., Turini, D.and Faussone-Pellegrini, M.S. (2005). Transient receptor potential vanilloid type 1 (TRPV1) expression changes from normal urothelium to transitional cell carcinoma of human bladder. *Eur Urol* 48, 691-698.

Lazzeri, M., Vannucchi, M.G., Zardo, C., Spinelli, M., Beneforti, P., Turini, D.and Faussone-Pellegrini, M.S. (2004). Immunohistochemical evidence of vanilloid receptor 1 in normal human urinary bladder. *Eur Urol* 46, 792-798.

Leonelli, M., Graciano, M.F.and Britto, L.R. (2011). TRP channels, omega-3 fatty acids, and oxidative stress in neurodegeneration: from the cell membrane to intracellular cross-links. *Braz J Med Biol Res* 44, 1088-1096.

Lerner, M. (1963). Marihuana: Tetrahydrocannabinol and Related Compounds. *Science* 140, 175-176.

Li, D.P., Chen, S.R.and Pan, H.L. (2004). VR1 receptor activation induces glutamate release and postsynaptic firing in the paraventricular nucleus. *J Neurophysiol* 92, 1807-1816.

Li, H.B., Mao, R.R., Zhang, J.C., Yang, Y., Cao, J.and Xu, L. (2008). Antistress effect of TRPV1 channel on synaptic plasticity and spatial memory. *Biological psychiatry* 64, 286-292.

Li, S., Bode, A.M., Zhu, F., Liu, K., Zhang, J., Kim, M.O., Reddy, K., Zykova, T., Ma, W.Y., Carper, A.L. (2011). TRPV1-antagonist AMG9810 promotes mouse skin tumorigenesis through EGFR/Akt signaling. *Carcinogenesis* 32, 779-785.

Liapi, A.and Wood, J.N. (2005). Extensive co-localization and heteromultimer formation of the vanilloid receptor-like protein TRPV2 and the capsaicin receptor TRPV1 in the adult rat cerebral cortex. *Eur J Neurosci* 22, 825-834.

Lie, D.C., Song, H., Colamarino, S.A., Ming, G.L.and Gage, F.H. (2004). Neurogenesis in the adult brain: new strategies for central nervous system diseases. *Annu Rev Pharmacol Toxicol* 44, 399-421.

Ligresti, A., Moriello, A.S., Starowicz, K., Matias, I., Pisanti, S., De Petrocellis, L., Laezza, C., Portella, G., Bifulco, M.and Di Marzo, V. (2006). Antitumor activity of plant cannabinoids with emphasis on the effect of cannabidiol on human breast carcinoma. *The Journal of pharmacology and experimental therapeutics* 318, 1375-1387.

Liu, X.S., Chopp, M., Zhang, X.G., Zhang, R.L., Buller, B., Hozeska-Solgot, A., Gregg, S.R.and Zhang, Z.G. (2009). Gene profiles and electrophysiology of doublecortin-expressing cells in the subventricular zone after ischemic stroke. *Journal of cerebral blood flow and metabolism : official journal of the International Society of Cerebral Blood Flow and Metabolism* 29, 297-307.

Lois, C.and Alvarez-Buylla, A. (1994). Long-distance neuronal migration in the adult mammalian brain. *Science* 264, 1145-1148.

Louis, D.N., Ohgaki, H., Wiestler, O.D., Cavenee, W.K., Burger, P.C., Jouvet, A., Scheithauer, B.W.and Kleihues, P. (2007). The 2007 WHO classification of tumours of the central nervous system. *Acta Neuropathol* 114, 97-109.

Lu, D., Mahmood, A., Zhang, R.and Copp, M. (2003a). Upregulation of neurogenesis and reduction in functional deficits following administration of DEtA/NONOate, a nitric oxide donor, after traumatic brain injury in rats. *Journal of neurosurgery* 99, 351-361.

Lu, L., Bao, G., Chen, H., Xia, P., Fan, X., Zhang, J., Pei, G.and Ma, L. (2003b). Modification of hippocampal neurogenesis and neuroplasticity by social environments. *Experimental neurology* 183, 600-609.

Luskin, M.B. (1993). Restricted proliferation and migration of postnatally generated neurons derived from the forebrain subventricular zone. *Neuron* 11, 173-189.

Maccarrone, M., Lorenzon, T., Bari, M., Melino, G.and Finazzi-Agro, A. (2000). Anandamide induces apoptosis in human cells via vanilloid receptors. Evidence for a protective role of cannabinoid receptors. *J Biol Chem* 275, 31938-31945.

Maccarrone, M., Rossi, S., Bari, M., De Chiara, V., Fezza, F., Musella, A., Gasperi, V., Prosperetti, C., Bernardi, G., Finazzi-Agro, A. (2008). Anandamide inhibits metabolism and physiological actions of 2-arachidonoylglycerol in the striatum. *Nat Neurosci* 11, 152-159.

Maher, E.A., Furnari, F.B., Bachoo, R.M., Rowitch, D.H., Louis, D.N., Cavenee, W.K.and DePinho, R.A. (2001). Malignant glioma: genetics and biology of a grave matter. *Genes Dev* 15, 1311-1333.

Maione, S., Starowicz, K., Palazzo, E., Rossi, F.and Marzo, V.D. (2006). The endocannabinoid and endovanilloid systems and their interactions in neuropathic pain. *Drug Development Research* Volume 67, 287–415.

Malberg, J.E., Eisch, A.J., Nestler, E.J.and Duman, R.S. (2000). Chronic antidepressant treatment increases neurogenesis in adult rat hippocampus. *J Neurosci* 20, 9104-9110.

Marinelli, S., Di Marzo, V., Berretta, N., Matias, I., Maccarrone, M., Bernardi, G.and Mercuri, N.B. (2003). Presynaptic facilitation of glutamatergic synapses to dopaminergic neurons of the rat substantia nigra by endogenous stimulation of vanilloid receptors. *J Neurosci* 23, 3136-3144.

Markakis, E.A.and Gage, F.H. (1999). Adult-generated neurons in the dentate gyrus send axonal projections to field CA3 and are surrounded by synaptic vesicles. *J Comp Neurol* 406, 449-460.

Markovic, D.S., Glass, R., Synowitz, M., Rooijen, N.and Kettenmann, H. (2005). Microglia stimulate the invasiveness of glioma cells by increasing the activity of metalloprotease-2. *Journal of neuropathology and experimental neurology* 64, 754-762.

Markovic, D.S., Vinnakota, K., Chirasani, S., Synowitz, M., Raguet, H., Stock, K., Sliwa, M., Lehmann, S., Kalin, R., van Rooijen, N. (2009). Gliomas induce and exploit microglial MT1-MMP expression for tumor expansion. *Proc Natl Acad Sci U S A* 106, 12530-12535.

Marsch, R., Foeller, E., Rammes, G., Bunck, M., Kossl, M., Holsboer, F., Zieglgansberger, W., Landgraf, R., Lutz, B.and Wotjak, C.T. (2007). Reduced anxiety, conditioned fear, and hippocampal long-term potentiation in transient receptor potential vanilloid type 1 receptor-deficient mice. *J Neurosci* 27, 832-839.

Marsicano, G., Wotjak, C.T., Azad, S.C., Bisogno, T., Rammes, G., Cascio, M.G., Hermann, H., Tang, J., Hofmann, C., Zieglgansberger, W. (2002). The endogenous cannabinoid system controls extinction of aversive memories. *Nature* 418, 530-534.

Massi, P., Vaccani, A., Bianchessi, S., Costa, B., Macchi, P.and Parolaro, D. (2006). The non-psychoactive cannabidiol triggers caspase activation and oxidative stress in human glioma cells. *Cellular and molecular life sciences : CMLS* 63, 2057-2066.

Massi, P., Vaccani, A., Ceruti, S., Colombo, A., Abbracchio, M.P.and Parolaro, D. (2004). Antitumor effects of cannabidiol, a nonpsychoactive cannabinoid, on human glioma cell lines. *The Journal of pharmacology and experimental therapeutics* 308, 838-845.

Matta, J.A.and Ahern, G.P. (2007). Voltage is a partial activator of rat thermosensitive TRP channels. *J Physiol* 585, 469-482.

McConville, P., Hambardzumyan, D., Moody, J.B., Leopold, W.R., Kreger, A.R., Woolliscroft, M.J., Rehemtulla, A., Ross, B.D.and Holland, E.C. (2007). Magnetic resonance imaging determination of tumor grade and early response to temozolomide in a genetically engineered mouse model of glioma. *Clin Cancer Res* 13, 2897-2904.

Mechoulam, R., Spatz, M.and Shohami, E. (2002). Endocannabinoids and neuroprotection. *Science's STKE : signal transduction knowledge environment* 2002, re5.

Merlo, A. (2003). Genes and pathways driving glioblastomas in humans and murine disease models. *Neurosurg Rev* 26, 145-158.

Mezey, E., Toth, Z.E., Cortright, D.N., Arzubi, M.K., Krause, J.E., Elde, R., Guo, A., Blumberg, P.M.and Szallasi, A. (2000). Distribution of mRNA for vanilloid receptor subtype 1 (VR1), and VR1-like immunoreactivity, in the central nervous system of the rat and human. *Proc Natl Acad Sci U S A* 97, 3655-3660.

Michael, G.J.and Priestley, J.V. (1999). Differential expression of the mRNA for the vanilloid receptor subtype 1 in cells of the adult rat dorsal root and nodose ganglia and its downregulation by axotomy. *J Neurosci* 19, 1844-1854.

Mimeault, M., Pommery, N., Wattez, N., Bailly, C.and Henichart, J.P. (2003). Anti-proliferative and apoptotic effects of anandamide in human prostatic cancer cell lines: implication of epidermal growth factor receptor down-regulation and ceramide production. *Prostate* 56, 1-12.

Mirescu, C., Peters, J.D.and Gould, E. (2004). Early life experience alters response of adult neurogenesis to stress. *Nat Neurosci* 7, 841-846.

Mischel, P.S., Shai, R., Shi, T., Horvath, S., Lu, K.V., Choe, G., Seligson, D., Kremen, T.J., Palotie, A., Liau, L.M. (2003). Identification of molecular subtypes of glioblastoma by gene expression profiling. *Oncogene* 22, 2361-2373.

Molina-Holgado, E., Vela, J.M., Arevalo-Martin, A., Almazan, G., Molina-Holgado, F., Borrell, J.and Guaza, C. (2002). Cannabinoids promote oligodendrocyte progenitor survival: involvement of cannabinoid receptors and phosphatidylinositol-3 kinase/Akt signaling. *J Neurosci* 22, 9742-9753.

Montell, C. (2005). The TRP superfamily of cation channels. *Science's STKE : signal transduction knowledge environment* 2005, re3.

Moreira, F.A.and Wotjak, C.T. (2010). Cannabinoids and anxiety. *Curr Top Behav Neurosci* 2, 429-450.

Mori, F., Ribolsi, M., Kusayanagi, H., Monteleone, F., Mantovani, V., Buttari, F., Marasco, E., Bernardi, G., Maccarrone, M.and Centonze, D. (2012). TRPV1 Channels Regulate Cortical Excitability in Humans. *J Neurosci* 32, 873-879.

Moriyama, T., Higashi, T., Togashi, K., Iida, T., Segi, E., Sugimoto, Y., Tominaga, T., Narumiya, S.and Tominaga, M. (2005). Sensitization of TRPV1 by EP1 and IP reveals peripheral nociceptive mechanism of prostaglandins. *Mol Pain* 1, 3.

Morris, R.G., Garrud, P., Rawlins, J.N.and O'Keefe, J. (1982). Place navigation impaired in rats with hippocampal lesions. *Nature* 297, 681-683.

Munson, A.E., Harris, L.S., Friedman, M.A., Dewey, W.L.and Carchman, R.A. (1975). Antineoplastic activity of cannabinoids. *J Natl Cancer Inst* 55, 597-602.

Musella, A., De Chiara, V., Rossi, S., Prosperetti, C., Bernardi, G., Maccarrone, M.and Centonze, D. (2009). TRPV1 channels facilitate glutamate transmission in the striatum. *Mol Cell Neurosci* 40, 89-97.

Nagayama, T., Sinor, A.D., Simon, R.P., Chen, J., Graham, S.H., Jin, K.and Greenberg, D.A. (1999). Cannabinoids and neuroprotection in global and focal cerebral ischemia and in neuronal cultures. *J Neurosci* 19, 2987-2995.

Nagy, I., Santha, P., Jancso, G.and Urban, L. (2004). The role of the vanilloid (capsaicin) receptor (TRPV1) in physiology and pathology. *Eur J Pharmacol* 500, 351-369.

Newlands, E.S., Stevens, M.F., Wedge, S.R., Wheelhouse, R.T.and Brock, C. (1997). Temozolomide: a review of its discovery, chemical properties, pre-clinical development and clinical trials. *Cancer Treat Rev* 23, 35-61.

Nixon, K.and Crews, F.T. (2002). Binge ethanol exposure decreases neurogenesis in adult rat hippocampus. *Journal of neurochemistry* 83, 1087-1093.

Ohgaki, H. (2009). Epidemiology of brain tumors. *Methods Mol Biol* 472, 323-342.

Ohgaki, H.and Kleihues, P. (2005). Epidemiology and etiology of gliomas. *Acta Neuropathol* 109, 93-108.

Ohgaki, H.and Kleihues, P. (2007). Genetic pathways to primary and secondary glioblastoma. *Am J Pathol* 170, 1445-1453.

Oudin, M.J., Gajendra, S., Williams, G., Hobbs, C., Lalli, G.and Doherty, P. (2011). Endocannabinoids regulate the migration of subventricular zone-derived neuroblasts in the postnatal brain. *J Neurosci* 31, 4000-4011.

Padwal, R.S.and Majumdar, S.R. (2007). Drug treatments for obesity: orlistat, sibutramine, and rimonabant. *Lancet* 369, 71-77.

Palazuelos, J., Aguado, T., Egia, A., Mechoulam, R., Guzman, M.and Galve-Roperh, I. (2006). Non-psychoactive CB2 cannabinoid agonists stimulate neural progenitor proliferation. *FASEB J* 20, 2405-2407.

Parent, J.M. (2002). The role of seizure-induced neurogenesis in epileptogenesis and brain repair. *Epilepsy Res* 50, 179-189.

Parent, J.M., Elliott, R.C., Pleasure, S.J., Barbaro, N.M.and Lowenstein, D.H. (2006). Aberrant seizure-induced neurogenesis in experimental temporal lobe epilepsy. *Ann Neurol* 59, 81-91.

Parent, J.M., Vexler, Z.S., Gong, C., Derugin, N.and Ferriero, D.M. (2002). Rat forebrain neurogenesis and striatal neuron replacement after focal stroke. *Ann Neurol* 52, 802-813.

Parent, J.M., Yu, T.W., Leibowitz, R.T., Geschwind, D.H., Sloviter, R.S.and Lowenstein, D.H. (1997). Dentate granule cell neurogenesis is increased by seizures and contributes to aberrant network reorganization in the adult rat hippocampus. *J Neurosci* 17, 3727-3738.

Pasquariello, N., Catanzaro, G., Marzano, V., Amadio, D., Barcaroli, D., Oddi, S., Federici, G., Urbani, A., Finazzi Agro, A.and Maccarrone, M. (2009). Characterization of the endocannabinoid system in human neuronal cells and proteomic analysis of anandamide-induced apoptosis. *J Biol Chem* 284, 29413-29426.

Pegorini, S., Braida, D., Verzoni, C., Guerini-Rocco, C., Consalez, G.G., Croci, L.and Sala, M. (2005). Capsaicin exhibits neuroprotective effects in a model of transient global cerebral ischemia in Mongolian gerbils. *Br J Pharmacol* 144, 727-735.

Pegorini, S., Zani, A., Braida, D., Guerini-Rocco, C.and Sala, M. (2006). Vanilloid VR1 receptor is involved in rimonabant-induced neuroprotection. *Br J Pharmacol* 147, 552-559.

Pham, K., Nacher, J., Hof, P.R.and McEwen, B.S. (2003). Repeated restraint stress suppresses neurogenesis and induces biphasic PSA-NCAM expression in the adult rat dentate gyrus. *Eur J Neurosci* 17, 879-886.

Piomelli, D. (2000). Pot of gold for glioma therapy. *Nat Med* 6, 255-256.

Preet, A., Ganju, R.K.and Groopman, J.E. (2008). Delta9-Tetrahydrocannabinol inhibits epithelial growth factor-induced lung cancer cell migration in vitro as well as its growth and metastasis in vivo. *Oncogene* 27, 339-346.

Premkumar, L.S. (2010). Targeting TRPV1 as an alternative approach to narcotic analgesics to treat chronic pain conditions. *AAPS J* 12, 361-370.

Radin, N.S. (2003). Designing anticancer drugs via the achilles heel: ceramide, allylic ketones, and mitochondria. *Bioorg Med Chem* 11, 2123-2142.

Ramirez, B.G., Blazquez, C., Gomez del Pulgar, T., Guzman, M.and de Ceballos, M.L. (2005). Prevention of Alzheimer's disease pathology by cannabinoids: neuroprotection mediated by blockade of microglial activation. *J Neurosci* 25, 1904-1913.

Ramsey, I.S., Delling, M.and Clapham, D.E. (2006). An introduction to TRP channels. *Annu Rev Physiol* 68, 619-647.

Rappsilber, J., Mann, M.and Ishihama, Y. (2007). Protocol for micro-purification, enrichment, pre-fractionation and storage of peptides for proteomics using StageTips. *Nat Protoc* 2, 1896-1906.

Razavi, R., Chan, Y., Afifiyan, F.N., Liu, X.J., Wan, X., Yantha, J., Tsui, H., Tang, L., Tsai, S., Santamaria, P. (2006). TRPV1+ sensory neurons control beta cell stress and islet inflammation in autoimmune diabetes. *Cell* 127, 1123-1135.

Reynolds, B.A.and Weiss, S. (1992). Generation of neurons and astrocytes from isolated cells of the adult mammalian central nervous system. *Science* 255, 1707-1710.

Rice, A.C., Khaldi, A., Harvey, H.B., Salman, N.J., White, F., Fillmore, H.and Bullock, M.R. (2003). Proliferation and neuronal differentiation of mitotically active cells following traumatic brain injury. *Experimental neurology* 183, 406-417.

Roberts, J.C., Davis, J.B.and Benham, C.D. (2004). [3H]Resiniferatoxin autoradiography in the CNS of wild-type and TRPV1 null mice defines TRPV1 (VR-1) protein distribution. *Brain Res* 995, 176-183.

Ross, R.A. (2003). Anandamide and vanilloid TRPV1 receptors. *Br J Pharmacol* 140, 790-801.

Rossi, F., Bellini, G., Luongo, L., Torella, M., Mancusi, S., De Petrocellis, L., Petrosino, S., Siniscalco, D., Orlando, P., Scafuro, M. (2011). The endovanilloid/endocannabinoid system: a new potential target for osteoporosis therapy. *Bone* 48, 997-1007.

Rowbotham, M.C., Nothaft, W., Duan, W.R., Wang, Y., Faltynek, C., McGaraughty, S., Chu, K.L.and Svensson, P. (2011). Oral and cutaneous thermosensory profile of selective TRPV1 inhibition by ABT-102 in a randomized healthy volunteer trial. *Pain* 152, 1192-1200.

Rueda, D., Navarro, B., Martinez-Serrano, A., Guzman, M.and Galve-Roperh, I. (2002). The endocannabinoid anandamide inhibits neuronal progenitor cell differentiation through attenuation of the Rap1/B-Raf/ERK pathway. *J Biol Chem* 277, 46645-46650.

Ryberg, E., Larsson, N., Sjogren, S., Hjorth, S., Hermansson, N.O., Leonova, J., Elebring, T., Nilsson, K., Drmota, T.and Greasley, P.J. (2007). The orphan receptor GPR55 is a novel cannabinoid receptor. *Br J Pharmacol* 152, 1092-1101.

Sahay, A., Scobie, K.N., Hill, A.S., O'Carroll, C.M., Kheirbek, M.A., Burghardt, N.S., Fenton, A.A., Dranovsky, A.and Hen, R. (2011). Increasing adult hippocampal neurogenesis is sufficient to improve pattern separation. *Nature* 472, 466-470.

Salazar, M., Carracedo, A., Salanueva, I.J., Hernandez-Tiedra, S., Lorente, M., Egia, A., Vazquez, P., Blazquez, C., Torres, S., Garcia, S. (2009). Cannabinoid action induces autophagy-mediated cell death through stimulation of ER stress in human glioma cells. *J Clin Invest* 119, 1359-1372.

Sallan, S.E., Zinberg, N.E.and Frei, E., 3rd (1975). Antiemetic effect of delta-9-tetrahydrocannabinol in patients receiving cancer chemotherapy. *N Engl J Med* 293, 795-797.

Sanai, N., Alvarez-Buylla, A.and Berger, M.S. (2005). Neural stem cells and the origin of gliomas. *N Engl J Med* 353, 811-822.

Sanchez, A.M., Martinez-Botas, J., Malagarie-Cazenave, S., Olea, N., Vara, D., Lasuncion, M.A.and Diaz-Laviada, I. (2008). Induction of the endoplasmic reticulum stress protein GADD153/CHOP by capsaicin in prostate PC-3 cells: a microarray study. *Biochem Biophys Res Commun* 372, 785-791.

Sanchez, C., de Ceballos, M.L., Gomez del Pulgar, T., Rueda, D., Corbacho, C., Velasco, G., Galve-Roperh, I., Huffman, J.W., Ramon y Cajal, S.and Guzman, M. (2001a). Inhibition of glioma growth in vivo by selective activation of the CB(2) cannabinoid receptor. *Cancer Res* 61, 5784-5789.

Sanchez, C., Galve-Roperh, I., Canova, C., Brachet, P.and Guzman, M. (1998). Delta9-tetrahydrocannabinol induces apoptosis in C6 glioma cells. *FEBS Lett* 436, 6-10.

Sanchez, J.F., Krause, J.E.and Cortright, D.N. (2001b). The distribution and regulation of vanilloid receptor VR1 and VR1 5' splice variant RNA expression in rat. *Neuroscience* 107, 373-381.

Sanchez, M.G., Sanchez, A.M., Collado, B., Malagarie-Cazenave, S., Olea, N., Carmena, M.J., Prieto, J.C.and Diaz-Laviada, I.I. (2005). Expression of the transient receptor potential vanilloid 1 (TRPV1) in LNCaP and PC-3 prostate cancer cells and in human prostate tissue. *Eur J Pharmacol* 515, 20-27.

Sappington, R.M.and Calkins, D.J. (2008). Contribution of TRPV1 to microglia-derived IL-6 and NFkappaB translocation with elevated hydrostatic pressure. *Invest Ophthalmol Vis Sci* 49, 3004-3017.

Sarfaraz, S., Afaq, F., Adhami, V.M., Malik, A.and Mukhtar, H. (2006). Cannabinoid receptor agonist-induced apoptosis of human prostate cancer cells LNCaP proceeds through sustained activation of ERK1/2 leading to G1 cell cycle arrest. *J Biol Chem* 281, 39480-39491.

Sasamura, T., Sasaki, M., Tohda, C.and Kuraishi, Y. (1998). Existence of capsaicin-sensitive glutamatergic terminals in rat hypothalamus. *Neuroreport* 9, 2045-2048.

Schoenfeld, R., Moenich, N., Mueller, F.J., Lehmann, W.and Leplow, B. (2010). Search strategies in a human water maze analogue analyzed with automatic classification methods. *Behav Brain Res* 208, 169-177.

Seki, T.and Arai, Y. (1993). Highly polysialylated neural cell adhesion molecule (NCAM-H) is expressed by newly generated granule cells in the dentate gyrus of the adult rat. *J Neurosci* 13, 2351-2358.

Seki, T.and Arai, Y. (1995). Age-related production of new granule cells in the adult dentate gyrus. *Neuroreport* 6, 2479-2482.

Shen, M.and Thayer, S.A. (1998). Cannabinoid receptor agonists protect cultured rat hippocampal neurons from excitotoxicity. *Mol Pharmacol* 54, 459-462.

Sicinski, P., Donaher, J.L., Geng, Y., Parker, S.B., Gardner, H., Park, M.Y., Robker, R.L., Richards, J.S., McGinnis, L.K., Biggers, J.D. (1996). Cyclin D2 is an FSH-responsive gene involved in gonadal cell proliferation and oncogenesis. *Nature* 384, 470-474.

Siemens, J., Zhou, S., Piskorowski, R., Nikai, T., Lumpkin, E.A., Basbaum, A.I., King, D.and Julius, D. (2006). Spider toxins activate the capsaicin receptor to produce inflammatory pain. *Nature* 444, 208-212.

Sikand, P.and Premkumar, L.S. (2007). Potentiation of glutamatergic synaptic transmission by protein kinase C-mediated sensitization of TRPV1 at the first sensory synapse. *J Physiol* 581, 631-647.

Singh, S.K., Clarke, I.D., Terasaki, M., Bonn, V.E., Hawkins, C., Squire, J.and Dirks, P.B. (2003). Identification of a cancer stem cell in human brain tumors. *Cancer Res* 63, 5821-5828.

Skaper, S.D., Buriani, A., Dal Toso, R., Petrelli, L., Romanello, S., Facci, L.and Leon, A. (1996). The ALIAmide palmitoylethanolamide and cannabinoids, but not anandamide, are protective in a delayed postglutamate paradigm of excitotoxic death in cerebellar granule neurons. *Proc Natl Acad Sci U S A* 93, 3984-3989.

Soltys, J., Yushak, M.and Mao-Draayer, Y. (2010). Regulation of neural progenitor cell fate by anandamide. *Biochem Biophys Res Commun* 400, 21-26.

Song, H.J., Stevens, C.F.and Gage, F.H. (2002). Neural stem cells from adult hippocampus develop essential properties of functional CNS neurons. *Nat Neurosci* 5, 438-445.

Staflin, K., Honeth, G., Kalliomaki, S., Kjellman, C., Edvardsen, K.and Lindvall, M. (2004). Neural progenitor cell lines inhibit rat tumor growth in vivo. *Cancer Res* 64, 5347-5354.

Staflin, K., Zuchner, T., Honeth, G., Darabi, A.and Lundberg, C. (2009). Identification of proteins involved in neural progenitor cell targeting of gliomas. *BMC Cancer* 9, 206.

Stander, S., Moormann, C., Schumacher, M., Buddenkotte, J., Artuc, M., Shpacovitch, V., Brzoska, T., Lippert, U., Henz, B.M., Luger, T.A. (2004). Expression of vanilloid receptor subtype 1 in cutaneous sensory nerve fibers, mast cells, and epithelial cells of appendage structures. *Exp Dermatol* 13, 129-139.

Stanfield, B.B.and Trice, J.E. (1988). Evidence that granule cells generated in the dentate gyrus of adult rats extend axonal projections. *Exp Brain Res* 72, 399-406.

Starowicz, K., Cristino, L.and Di Marzo, V. (2008). TRPV1 receptors in the central nervous system: potential for previously unforeseen therapeutic applications. *Curr Pharm Des* 14, 42-54.

Starowicz, K., Maione, S., Cristino, L., Palazzo, E., Marabese, I., Rossi, F., de Novellis, V.and Di Marzo, V. (2007). Tonic endovanilloid facilitation of glutamate release in brainstem descending antinociceptive pathways. *J Neurosci* 27, 13739-13749.

Steenland, H.W., Ko, S.W., Wu, L.J.and Zhuo, M. (2006). Hot receptors in the brain. *Mol Pain* 2, 34.

Stein, A.T., Ufret-Vincenty, C.A., Hua, L., Santana, L.F.and Gordon, S.E. (2006). Phosphoinositide 3-kinase binds to TRPV1 and mediates NGF-stimulated TRPV1 trafficking to the plasma membrane. *J Gen Physiol* 128, 509-522.

Stock, K., Nolden, L., Edenhofer, F., Quandel, T.and Brustle, O. (2010). Transcription factor-based modulation of neural stem cell differentiation using direct protein transduction. *Cellular and molecular life sciences : CMLS* 67, 2439-2449.

Strik, H.M., Marosi, C., Kaina, B.and Neyns, B. (2012). Temozolomide Dosing Regimens for Glioma Patients. *Curr Neurol Neurosci Rep*.

Stupp, R., Hegi, M.E., Mason, W.P., van den Bent, M.J., Taphoorn, M.J., Janzer, R.C., Ludwin, S.K., Allgeier, A., Fisher, B., Belanger, K. (2009). Effects of radiotherapy with concomitant and adjuvant temozolomide versus radiotherapy alone on survival in glioblastoma in a randomised phase III study: 5-year analysis of the EORTC-NCIC trial. *Lancet Oncol* 10, 459-466.

Stupp, R., Mason, W.P., van den Bent, M.J., Weller, M., Fisher, B., Taphoorn, M.J., Belanger, K., Brandes, A.A., Marosi, C., Bogdahn, U. (2005). Radiotherapy plus concomitant and adjuvant temozolomide for glioblastoma. *N Engl J Med* 352, 987-996.

Sturzebecher, A.S., Hu, J., Smith, E.S., Frahm, S., Santos-Torres, J., Kampfrath, B., Auer, S., Lewin, G.R.and Ibanez-Tallon, I. (2010). An in vivo tethered toxin approach for the cell-autonomous inactivation of voltage-gated sodium channel currents in nociceptors. *J Physiol* 588, 1695-1707.

Suri, A.and Szallasi, A. (2008). The emerging role of TRPV1 in diabetes and obesity. *Trends Pharmacol Sci* 29, 29-36.

Sutherland, R.J., Whishaw, I.Q.and Regehr, J.C. (1982). Cholinergic receptor blockade impairs spatial localization by use of distal cues in the rat. *Journal of comparative and physiological psychology* 96, 563-573.

Suzuki, T., Izumoto, S., Wada, K., Fujimoto, Y., Maruno, M., Yamasaki, M., Kanemura, Y., Shimazaki, T., Okano, H.and Yoshimine, T. (2005). Inhibition of glioma cell proliferation by neural stem cell factor. *J Neurooncol* 74, 233-239.

Szallasi, A.and Blumberg, P.M. (1999). Vanilloid (Capsaicin) receptors and mechanisms. *Pharmacol Rev* 51, 159-212.

Szallasi, A., Cortright, D.N., Blum, C.A.and Eid, S.R. (2007). The vanilloid receptor TRPV1: 10 years from channel cloning to antagonist proof-of-concept. *Nat Rev Drug Discov* 6, 357-372.

Szallasi, A., Cruz, F.and Geppetti, P. (2006). TRPV1: a therapeutic target for novel analgesic drugs? *Trends Mol Med* 12, 545-554.

Szallasi, A.and Di Marzo, V. (2000). New perspectives on enigmatic vanilloid receptors. *Trends Neurosci* 23, 491-497.

Szallasi, A., Nilsson, S., Farkas-Szallasi, T., Blumberg, P.M., Hokfelt, T.and Lundberg, J.M. (1995). Vanilloid (capsaicin) receptors in the rat: distribution in the brain, regional differences in the spinal cord, axonal transport to the periphery, and depletion by systemic vanilloid treatment. *Brain Res* 703, 175-183.

Terranova, J.P., Michaud, J.C., Le Fur, G.and Soubrie, P. (1995). Inhibition of long-term potentiation in rat hippocampal slices by anandamide and WIN55212-2: reversal by SR141716 A, a selective antagonist of CB1 cannabinoid receptors. *Naunyn Schmiedebergs Arch Pharmacol* 352, 576-579.

Terranova, J.P., Storme, J.J., Lafon, N., Perio, A., Rinaldi-Carmona, M., Le Fur, G.and Soubrie, P. (1996). Improvement of memory in rodents by the selective CB1 cannabinoid receptor antagonist, SR 141716. *Psychopharmacology (Berl)* 126, 165-172.

Terry, A.V., Jr. (2009). Spatial Navigation (Water Maze) Tasks.

Thomas, K.C., Roberts, J.K., Deering-Rice, C.E., Romero, E.G., Dull, R.O., Lee, J., Yost, G.S.and Reilly, C.A. (2012). Contributions of TRPV1, endovanilloids, and endoplasmic reticulum stress in lung cell death in vitro and lung injury. *American journal of physiology Lung cellular and molecular physiology* 302, L111-119.

Thomas, K.C., Sabnis, A.S., Johansen, M.E., Lanza, D.L., Moos, P.J., Yost, G.S.and Reilly, C.A. (2007). Transient receptor potential vanilloid 1 agonists cause endoplasmic reticulum stress and cell death in human lung cells. *The Journal of pharmacology and experimental therapeutics* 321, 830-838.

Tominaga, M.and Caterina, M.J. (2004). Thermosensation and pain. *J Neurobiol* 61, 3-12.

Tominaga, M., Caterina, M.J., Malmberg, A.B., Rosen, T.A., Gilbert, H., Skinner, K., Raumann, B.E., Basbaum, A.I.and Julius, D. (1998). The cloned capsaicin receptor integrates multiple pain-producing stimuli. *Neuron* 21, 531-543.

Tominaga, M.and Tominaga, T. (2005). Structure and function of TRPV1. *Pflugers Arch* 451, 143-150.

Torres, S., Lorente, M., Rodriguez-Fornes, F., Hernandez-Tiedra, S., Salazar, M., Garcia-Taboada, E., Barcia, J., Guzman, M.and Velasco, G. (2011). A combined preclinical therapy of cannabinoids and temozolomide against glioma. *Mol Cancer Ther* 10, 90-103.

Toth, A., Blumberg, P.M.and Boczan, J. (2009). Anandamide and the vanilloid receptor (TRPV1). *Vitam Horm* 81, 389-419.

Toth, A., Boczan, J., Kedei, N., Lizanecz, E., Bagi, Z., Papp, Z., Edes, I., Csiba, L.and Blumberg, P.M. (2005). Expression and distribution of vanilloid receptor 1 (TRPV1) in the adult rat brain. *Brain Res Mol Brain Res* 135, 162-168.

Tramer, M.R., Carroll, D., Campbell, F.A., Reynolds, D.J., Moore, R.A.and McQuay, H.J. (2001). Cannabinoids for control of chemotherapy induced nausea and vomiting: quantitative systematic review. *BMJ* 323, 16-21.

Tropepe, V., Craig, C.G., Morshead, C.M.and van der Kooy, D. (1997). Transforming growth factor-alpha null and senescent mice show decreased neural progenitor cell proliferation in the forebrain subependyma. *J Neurosci* 17, 7850-7859.

Tucci, S.A., Halford, J.C., Harrold, J.A.and Kirkham, T.C. (2006). Therapeutic potential of targeting the endocannabinoids: implications for the treatment of obesity, metabolic syndrome, drug abuse and smoking cessation. *Current medicinal chemistry* 13, 2669-2680.

Vaccani, A., Massi, P., Colombo, A., Rubino, T.and Parolaro, D. (2005). Cannabidiol inhibits human glioma cell migration through a cannabinoid receptor-independent mechanism. *Br J Pharmacol* 144, 1032-1036.

Van Gaal, L., Pi-Sunyer, X., Despres, J.P., McCarthy, C.and Scheen, A. (2008). Efficacy and safety of rimonabant for improvement of multiple cardiometabolic risk factors in overweight/obese patients: pooled 1-year data from the Rimonabant in Obesity (RIO) program. *Diabetes Care* 31 Suppl 2, S229-240.

van Praag, H., Kempermann, G.and Gage, F.H. (1999). Running increases cell proliferation and neurogenesis in the adult mouse dentate gyrus. *Nat Neurosci* 2, 266-270.

van Praag, H., Schinder, A.F., Christie, B.R., Toni, N., Palmer, T.D.and Gage, F.H. (2002). Functional neurogenesis in the adult hippocampus. *Nature* 415, 1030-1034.

Velasco, G., Carracedo, A., Blazquez, C., Lorente, M., Aguado, T., Haro, A., Sanchez, C., Galve-Roperh, I.and Guzman, M. (2007). Cannabinoids and gliomas. *Mol Neurobiol* 36, 60-67.

Veldhuis, W.B., van der Stelt, M., Wadman, M.W., van Zadelhoff, G., Maccarrone, M., Fezza, F., Veldink, G.A., Vliegenthart, J.F., Bar, P.R., Nicolay, K. (2003). Neuroprotection by the endogenous cannabinoid anandamide and arvanil against in vivo excitotoxicity in the rat: role of vanilloid receptors and lipoxygenases. *J Neurosci* 23, 4127-4133.

Voets, T., Droogmans, G., Wissenbach, U., Janssens, A., Flockerzi, V.and Nilius, B. (2004). The principle of temperature-dependent gating in cold- and heat-sensitive TRP channels. *Nature* 430, 748-754.

Walzlein, J.H., Synowitz, M., Engels, B., Markovic, D.S., Gabrusiewicz, K., Nikolaev, E., Yoshikawa, K., Kaminska, B., Kempermann, G., Uckert, W. (2008). The antitumorigenic response of neural precursors depends on subventricular proliferation and age. *Stem Cells* 26, 2945-2954.

Watters, J.J., Schartner, J.M.and Badie, B. (2005). Microglia function in brain tumors. *Journal of neuroscience research* 81, 447-455.

Whishaw, I.Q. (1989). Dissociating performance and learning deficits on spatial navigation tasks in rats subjected to cholinergic muscarinic blockade. *Brain research bulletin* 23, 347-358.

Whishaw, I.Q.and Petrie, B.F. (1988). Cholinergic blockade in the rat impairs strategy selection but not learning and retention of nonspatial visual discrimination problems in a swimming pool. *Behavioral neuroscience* 102, 662-677.

White, J.P., Cibelli, M., Rei Fidalgo, A., Paule, C.C., Noormohamed, F., Urban, L., Maze, M.and Nagy, I. (2010). Role of transient receptor potential and acid-sensing ion channels in peripheral inflammatory pain. *Anesthesiology* 112, 729-741.

Winston, J., Toma, H., Shenoy, M.and Pasricha, P.J. (2001). Nerve growth factor regulates VR-1 mRNA levels in cultures of adult dorsal root ganglion neurons. *Pain* 89, 181-186.

Wolf, S.A., Bick-Sander, A., Fabel, K., Leal-Galicia, P., Tauber, S., Ramirez-Rodriguez, G., Muller, A., Melnik, A., Waltinger, T.P., Ullrich, O. (2010). Cannabinoid receptor CB1 mediates baseline and activity-induced survival of new neurons in adult hippocampal neurogenesis. *Cell Commun Signal* 8, 12.

Wolf, S.A., Melnik, A.and Kempermann, G. (2011). Physical exercise increases adult neurogenesis and telomerase activity, and improves behavioral deficits in a mouse model of schizophrenia. *Brain Behav Immun* 25, 971-980.

Wolf, S.A., Steiner, B., Akpinarli, A., Kammertoens, T., Nassenstein, C., Braun, A., Blankenstein, T.and Kempermann, G. (2009). CD4-positive T lymphocytes provide a neuroimmunological link in the control of adult hippocampal neurogenesis. *J Immunol* 182, 3979-3984.

Wolfer, D.P.and Lipp, H.P. (2000). Dissecting the behaviour of transgenic mice: is it the mutation, the genetic background, or the environment? *Experimental physiology* 85, 627-634.

Wolfer, D.P., Muller, U., Stagliar, M.and Lipp, H.P. (1997). Assessing the effects of the 129/Sv genetic background on swimming navigation learning in transgenic mutants: a study using mice with a modified beta-amyloid precursor protein gene. *Brain Res* 771, 1-13.

Wong, G.Y.and Gavva, N.R. (2009). Therapeutic potential of vanilloid receptor TRPV1 agonists and antagonists as analgesics: Recent advances and setbacks. *Brain Res Rev* 60, 267-277.

Wu, X., Han, L., Zhang, X., Li, L., Jiang, C., Qiu, Y., Huang, R., Xie, B., Lin, Z., Ren, J. (2012). Alteration of endocannabinoid system in human gliomas. *Journal of neurochemistry* 120, 842-849.

Xing, J.and Li, J. (2007). TRPV1 receptor mediates glutamatergic synaptic input to dorsolateral periaqueductal gray (dl-PAG) neurons. *J Neurophysiol* 97, 503-511.

Yamaguchi, M., Saito, H., Suzuki, M.and Mori, K. (2000). Visualization of neurogenesis in the central nervous system using nestin promoter-GFP transgenic mice. *Neuroreport* 11, 1991-1996.

Yamamoto, S., Wajima, T., Hara, Y., Nishida, M.and Mori, Y. (2007). Transient receptor potential channels in Alzheimer's disease. *Biochimica et biophysica acta* 1772, 958-967.

Yang, K., Kumamoto, E., Furue, H.and Yoshimura, M. (1998). Capsaicin facilitates excitatory but not inhibitory synaptic transmission in substantia gelatinosa of the rat spinal cord. *Neurosci Lett* 255, 135-138.

Yiangou, Y., Facer, P., Dyer, N.H., Chan, C.L., Knowles, C., Williams, N.S.and Anand, P. (2001). Vanilloid receptor 1 immunoreactivity in inflamed human bowel. *Lancet* 357, 1338-1339.

Zhang, L.L., Yan Liu, D., Ma, L.Q., Luo, Z.D., Cao, T.B., Zhong, J., Yan, Z.C., Wang, L.J., Zhao, Z.G., Zhu, S.J. (2007). Activation of transient receptor potential vanilloid type-1 channel prevents adipogenesis and obesity. *Circ Res* 100, 1063-1070.

Zhang, R., Zhang, L., Zhang, Z., Wang, Y., Lu, M., Lapointe, M.and Chopp, M. (2001). A nitric oxide donor induces neurogenesis and reduces functional deficits after stroke in rats. *Ann Neurol* 50, 602-611.

Zhang, X., Huang, J.and McNaughton, P.A. (2005). NGF rapidly increases membrane expression of TRPV1 heat-gated ion channels. *EMBO J* 24, 4211-4223.

Zhou, D.and Song, Z.H. (2001). CB1 cannabinoid receptor-mediated neurite remodeling in mouse neuroblastoma N1E-115 cells. *Journal of neuroscience research* 65, 346-353.

Zhu, L.X., Sharma, S., Stolina, M., Gardner, B., Roth, M.D., Tashkin, D.P.and Dubinett, S.M. (2000). Delta-9-tetrahydrocannabinol inhibits antitumor immunity by a CB2 receptor-mediated, cytokine-dependent pathway. *J Immunol* 165, 373-380.

Zygmunt, P.M., Petersson, J., Andersson, D.A., Chuang, H., Sorgard, M., Di Marzo, V., Julius, D.and Hogestatt, E.D. (1999). Vanilloid receptors on sensory nerves mediate the vasodilator action of anandamide. *Nature* 400, 452-457.

9. Danksagung

Prof. Dr. Helmut Kettenmann möchte ich für die Bereitstellung dieses interessanten Themas, die Möglichkeit diese Arbeit in seinem Labor durchzuführen, sowie für die wertvolle Unterstützung herzlich danken.

Ein besonderer Dank gilt Dr. Susanne Wolf für die gute wissenschaftliche Betreuung und Unterstützung, sowie zahlreiche Anregungen und Diskussionen. Prof. Dr. Rainer Glaß danke ich ebenfalls für die Betreuung und für die Freiheiten zu eigenen Entscheidungen.

Dr. Susanne Wolf, Dr. Grietje Krabbe, Dr. Anika Langenfurth und Dr. Stephan Wierschke danke ich herzlich für die hilfsbereite Unterstützung beim Korrekturlesen.

Bei allen Mitarbeitern der Arbeitsgruppe „Zelluläre Neurowissenschaften“ möchte ich mich für die schöne Atmosphäre und für die Beantwortung all der kleinen und großen Fragen bedanken. Besonders Petya Georgieva, Dr. Grietje Krabbe, Dr. Anika Langenfurth, Julia Parnis, Nadine Richter und Katyayni Vinnakota haben meine Zeit hier positiv mitgestaltet.
Für exzellente technische Unterstützung möchte ich mich bei allen technischen Assistenten und vor allem bei Isabel Huber und Mareen Kamarys bedanken. Mein weiterer Dank gilt Birgit Jarchow für die Hilfe in allen administrativen Angelegenheiten.
Für die finanzielle Unterstützung danke ich der Helmholtz International Research School „Molecular Neurobiology“.

Vielen Dank an alle Freunde, die mich auf meinem bisherigen Weg begleitet haben.

Ein ganz besonderer Dank gilt meinen Eltern, Heidrun und Lothar Stock, sowie meinem Bruder Sebastian und meinem Freund Robert. Danke, dass ihr immer hinter mir gestanden habt und mich bei meinen Vorhaben unterstützt habt. Ohne euch wäre diese Arbeit nicht möglich gewesen. Daher ist diese Arbeit euch gewidmet. Danke.

10. Appendix

10.1. Curriculum vitae

Der Lebenslauf ist in der Online-Version aus Gründen des Datenschutzes nicht enthalten.

10.2. List of publications

Stock, K*; Kumar, J*; Synowitz, M* et al.; Di Marzo, V; Kettenmann, H*; Glass, R*

(* contributed equally)

'Neural precursor cells induce cell-death of high-grade astrocytomas via stimulation of TRPV1'

Nat Med. 2012; 18:1232-1238.

Stock, K; Nolden, L; Edenhofer, F; Quandel, T; Brüstle, O

'Transcription factor-based modulation of neural stem cell differentiation using direct protein transduction'

Cell Mol Life Sci. 2010; 67(14):2439-49.

Markovic, DS; Vinnakota, K; Chirasani, S; Synowitz, M; Raguet, H; Stock, K et al.; Glass, R; Kettenmann, H

'Gliomas induce and exploit microglial MT1-MMP expression for tumor expansion'

Proc Natl Acad Sci U S A. 2009;106(30):12530-5.

Stock, K*; Wolf, SA*; Garthe, A; Glass, R; Kettenmann, H (* contributed equally)

'The capsaicin receptor TRPV1 modulates neural precursor cell proliferation and mouse behavior'

in preparation

Langenfurth, A; Strotmann, J; Bautze, V; Stock, K; Kettenmann, H; Glass, R

'Reduced sensory input affects the olfactory bulb but not the supply of neural precursor cells from the subventricular zone'

in preparation

10.3. Meetings with talk or poster presentations

10.3.1. Conference abstracts - talks

Stock, K*; Kumar, J*; Synowitz, M; Matyash, V; Cristino, L; Di Marzo, V; Kettenmann, H*; Glass, R* (* contributed equally)

'Neural precursor cells induce glioma cell-death via stimulation of TRPV1'

Berlin Brain Days

Berlin, Germany; Dec 7-9, 2011

10.3.2. Selected conference abstracts - posters

Stock, K*; Kumar, J*; Synowitz, M; Matyash, V; Cristino, L; Di Marzo, V; Kettenmann, H*; Glass, R* (* contributed equally)

'Neural precursor cells induce glioma cell-death via stimulation of TRPV1'

SfN Neuroscience

Washington, DC, USA; Nov 12-16, 2011

Stock, K; Kettenmann, H; Glass, R

'Endovanilloids modulate adult neurogenesis'

Brain Tumor Meeting

Berlin, Germany; Jun 16-17, 2011

Stock, K; Kettenmann, H; Glass, R

'Endovanilloid Signaling In Adult Neural Precursor Cells'

Gordon Research Conference Cannabinoid Function in the CNS

Les Diablerets, Switzerland; May 22-27, 2011

Stock, K; Synowitz, M; Kettenmann, H; Glass, R

'BMP-7 release from endogenous NPCs attenuates self-renewal of glioma stem cells but not of untransformed NPCs'

Berlin Brain Days

Berlin, Germany; Nov 01-03, 2010

Stock, K; Chirasani, SR; Sternjak, A; Wend, P; Momma, S; Campos, B; Herrmann, IM; Herold-Mende, C; Besser, D; Synowitz, M; Kettenmann, H; Glass, R

'BMP-7 release from endogenous NPCs attenuates self-renewal of glioma stem cells but not of untransformed NPCs'

1st MDC/UCL Neuroscience Student Conference

Split, Croatia; Sep 16-19, 2010

Stock, K; Nolden, L; Edenhofer, F; Quandel, T; Brüstle, O

'Modulation of Neural Stem Cell Differentiation with a Recombinant Cell-Permeant Transcription Factor'

7th Forum Of European Neuroscience

Amsterdam, Netherlands; Jul 03-07, 2010

Stock, K; Raguet, H; Matyash, V; Glass, R; Kettenmann, H

'Microglia promote glioma cell invasion into brain tissue'

Berlin Brain Days

Berlin, Germany; Dec 09-11, 2009

Stock, K; Nolden, L; Edenhofer, F; Quandel, T; Brüstle, O

'Transcription factor-based instruction of an oligodendroglial fate using direct protein transduction'

9th European Meeting on Glial Cells in Health and Disease

Paris, France; Sep 8-12, 2009

11. Erklärung

„Ich, Kristin Stock, erkläre, dass ich die vorgelegte Dissertation mit dem Thema:

'New insights into TRPV1 function in the brain under physiological and pathological conditions'

selbst verfasst und keine anderen als die angegebenen Quellen und Hilfsmittel benutzt, ohne die (unzulässige) Hilfe Dritter verfasst und auch in Teilen keine Kopien anderer Arbeiten dargestellt habe."

Berlin, April 2012